Regulation and Function of Axonal Spheroids in the Peripheral Nervous System

Yu Yong

Zhuzhou, China.

B.S., Tongji University, 2016

A Dissertation presented to the Graduate Faculty of the University of Virginia in Candidacy for the Degree of Doctor of Philosophy

Department of Biology

University of Virginia

October, 2020

Abstract

Axons are the primary transmission cables of the nervous system. In response to injury, a process of axonal fragmentation, or Wallerian degeneration occurs, often resulting in loss of neural function. After axon fragmentation, the swift dismantling and clearance of injured axons contributes to the restoration of nerve function. Degeneration of axons is one of the earliest events associated with degenerative disorders such as Alzheimer's and Parkinson's disease. Despite the importance of persevering axons as therapeutic strategies, very little is known about the mechanisms underlying axon degeneration. Beyond pathological situations, axon degeneration is also an important aspect of nervous system refinement during development. Recent studies have revealed that the absence of sufficient neurotrophic signaling permits prodestructive cues originating from tumor necrosis factor receptor (TNFR) superfamily members, such as p75 neurotrophic receptor (p75NTR) and death receptor 6 (DR6), to promote axon degeneration in peripheral nervous system (PNS). Moreover, previous work in our lab has shown that loss of DR6 delays Wallerian degeneration. However, the relative contributions of p75NTR and DR6 specifically to latent and catastrophic phases of axon degeneration in distinct etiologies have largely been overlooked. The key pathways related to developmental and Wallerian degeneration are reviewed in Chapter 1 of this thesis.

To identify the hallmarks of axon degeneration in distinct etiologies, I firstly determined the morphological changes and calcium dynamics in axons after trophic deprivation or axotomy. Using an *in vitro* microfluidic culture system and live imaging, I found that after trophic deprivation or axotomy, intra-axonal calcium increases before catastrophic degeneration. This is accompanied by the formation of calcium-rich spheroids that grow and then rupture, releasing their contents (≤10 kDa) to the extracellular space while allowing an influx of extracellular

molecules into the intra-axonal space. Additionally, prodegenerative molecules (*e.g.,* calcium) released into the extracellular space are capable of hastening entry of latent phase into the catastrophic phase of axon degeneration. Further, I show that in response to trophic deprivation, p75NTR promotes spheroid formation, intra-axonal calcium rise, and membrane rupture in a Rho-dependent manner. In contrast, DR6 is required for transition into the catastrophic phase in response to conditioned media from degenerating axons but not for spheroid formation or rupture. This finding places p75NTR and DR6 upstream and downstream of spheroidal rupture, respectively. Furthermore, this work supports the existence of an interaxonal degenerative signal that promotes catastrophic degeneration. These findings are described in Chapter 2 (published on *J. Neuroscience*) and Chapter 3 (published on *Scientific Reports*). The methods and materials used for these analyses are listed in Chapter 5 (partially published on *Springer Protocols*).

In conclusion, this work established the notion that DR6 and p75NTR play separable but interactive roles in regulating axon degeneration. It also revealed regulatory pathways for the formation of functionally important axonal spheroids. However, several open questions remain to be addressed such as, the identity of prodegenerative cues released by spheroid rupture, the *in vivo* effects of axonal spheroids in progression of neurodegenerative diseases, and the non-cell autonomous interaction of DR6 and p75NTR in degeneration. As the universal hallmark of degeneration, axonal spheroids and their formation mechanisms are critical for investigating the pathology of neurodegenerative disorders. The significance and future directions are discussed in Chapter 4.

Acknowledgements

I would first like to thank my supervisor, Dr. Chris Deppmann, whose expertise was invaluable in providing scientific guidance, formulating research questions and methodology. Chris continually conveyed the enthusiasm and excitement for science and novel ideas, which gave me courage and inspirations to explore the unknown in neuroscience. He was very patient and generous whenever I needed advice and suggestions for my experiments, writing, presentations, and career establishment. Chris helped me immensely to grow not only as a scientist, but also as a person to achieve goals beyond my expectations during my grad school. As a teacher, Chris taught me how to be persistent and strategic in research. As a friend, he was always supportive and caring. Without this mentorship this dissertation would not have been possible.

I would like to thank my committee members. Dr. Barry Condron, who gave great advice and support in my project and career advancement. Dr. Sarah Kucenas, who was always available for insightful discussion about science and life being a woman scientist. Dr. Alev Erisir, for her help in electron microscopic experiments and support in my project. Dr. Xiaorong Liu, for her support as well as helping to shape my qualify presentation and scientific thinking.

I am very grateful to my colleagues in Deppmann lab and collaborators in the Biology department. I wish to thank Dr. John Campbell for his constructive advice and support in RNA sequencing experiments, especially during the COVID-19 pandemic. I also want to thank Dr. Ammasi Periasamy and staff in the Keck center for their help in confocal imaging. Dr. Tony Spano for being such a great biologist and a friend who always listened to my comments about graduate school life.

I want to express my gratitude to Austin Keeler who was always willing to discuss scientific questions with me and give great suggestions for my project. Sushanth Kumar for patiently spending his time to dissect and plate macrophages for me. Our previous lab member Kanchana Gamage who taught me every experiment about axon degeneration. I should also thank other lab members Shayla Clark, Brandon Podyma, Amrita Pathak, Vitaly Zimyanin, Ashley Mason and Amy van Deusen for making our laboratory such a friendly and supportive working environment. I am grateful for the undergraduate students Courtny Cushman and Kathryn Cheney, who were always the cheerleaders for every small advancement in my research. Many thanks to our lab manager Pam Neff for taking care of our orders and lab chores, allowing us to carry out experiments smoothly. It's my pleasure to work with such wonderful people and see the Deppmann lab core value in everyone.

I would also like to thank all my friends in many parts of the world and in Charlottesville for sharing, caring, and being supportive. They kept contact even though I had not seen them for years. Chatting online with them helped so much to highlight the colorful part of my life. My friends in Charlottesville, especially Lindsay Heckle, who kept our game night and movie night schedule going. Finally, I would like to thank my family for being there with me whenever I need anything. They support and love me without conditions.

Table of Contents

Chapter 1[1]

Introduction

The elimination of axons is both vital and deleterious during development and pathology, respectively (Luo and O'Leary, 2005). As neurons innervate their targets during development, they grow exuberant axon collaterals that are either retained or eliminated by degeneration (Neukomm and Freeman, 2014). In response to axon injury, a similar process of axonal fragmentation, or Wallerian degeneration (WD) occurs, often resulting in permanent loss of neural function (Vargas and Barres, 2007; Waller, 1851). Despite intense interest over the last several decades, very few common molecular pathways have been reported between different degenerative etiologies. Here, we review major molecular mechanisms and raise important yet unsolved questions in different degenerative etiologies, emphasizing the roles of calcium signaling, death receptors and axonal spheroids in axon degeneration.

Developmental axon degeneration

During development, innervating neurons compete for limiting quantities of target-derived survival promoting neurotrophic factors. Sympathetic and sensory axons that encounter sufficient nerve growth factor (NGF) survive and stabilize their axon collaterals, while those with low trophic signaling undergo death and degeneration. NGF promotes expression of its own receptor TrkA and depolarization in "strong" neurons, which secrete brain-derived neurotrophic factor (BDNF) and neurotrophin-4 (NT-4) to eliminate "weak" neighbors through p75 neurotrophin receptor

[1] Additional introductory material was published Y. Yong *et al.,* Glia signaling during neurological damage and disease. *eLS* (2017).

(p75NTR) (Deppmann et al., 2008; Singh and Miller, 2005; Singh et al., 2008). Moreover, lack of NGF-TrkA signaling permits the prodegenerative cues originating from death receptors, including tumor necrosis factor receptor 1a (TNFR1a), p75NTR and death receptor 6 (DR6), which have been implicated in developmental axon degeneration in the PNS (Barker et al., 2001; Olsen et al., 2014; Park et al., 2010; Wheeler et al., 2014).

The molecular mechanism regulating axon degeneration in development has been widely investigated (Fig.1). Global NGF deprivation on dissociated sympathetic neurons provides initial insights with *de novo* RNA and protein synthesis being required for active death programs (Freeman et al., 2004; Martin et al., 1988, 1992). Loss of NGF-TrkA signaling results in decreases in pro-survival PI3K-AKT (phosphoinositide 3-kinase-AKT/protein kinase B) and MAPK/ERK (mitogen-activated protein kinase/extracellular signal-regulated kinase) pathways, and leads to the activation of pro-death pathways involving DLK (dual leucine zipper kinase) and JNK (c-jun-N-terminal kinase) (Kristiansen and Ham, 2014). This results in the activation of transcriptional factors (*e.g.* Foxo3a, c-jun) that induce the pro-death BH3-only genes including Bim, Bmf, DP5/Hrk, and Puma, which together inhibit Bcl-2 family and promote activation of Bax (Geden and Deshmukh, 2016; Simon et al., 2016). Activated Bax then translocates to mitochondria, leading to release of cytochrome c (Cyt c) into the cytoplasm to drive activation of initiator caspase 9 (Casp9) and effector caspases 3 and 6 (Cusack et al., 2013; Simon et al., 2012). Unlike cellular apoptosis, apoptotic protease activating factor 1 (Apaf-1) is not required during axonal pruning induced by local NGF deprivation (Geden et al., 2019). As *in vivo* NGF signaling primarily occurs at the axon terminals and the signal is retrogradely transported to the cell body, NGF withdrawal from distal axons can drive degeneration via retrograde pro-apoptotic signaling as well as an anterograde degenerative program initiated by Puma in the cell body (Mok et al., 2009; Simon et al., 2016). Therefore, somatic integration of regressive and progressive signaling is crucial for selective axonal elimination during development (Maor-Nof et al., 2016). Recently, p75NTR has

been shown to mediate retrograde pro-apoptotic signaling in response to trophic deprivation or BDNF binding to p75NTR (Pathak et al., 2018). Whether and how p75NTR and other death receptors interact with retrograde and anterograde pro-degenerative signals in response to local NGF deprivation requires further investigation.

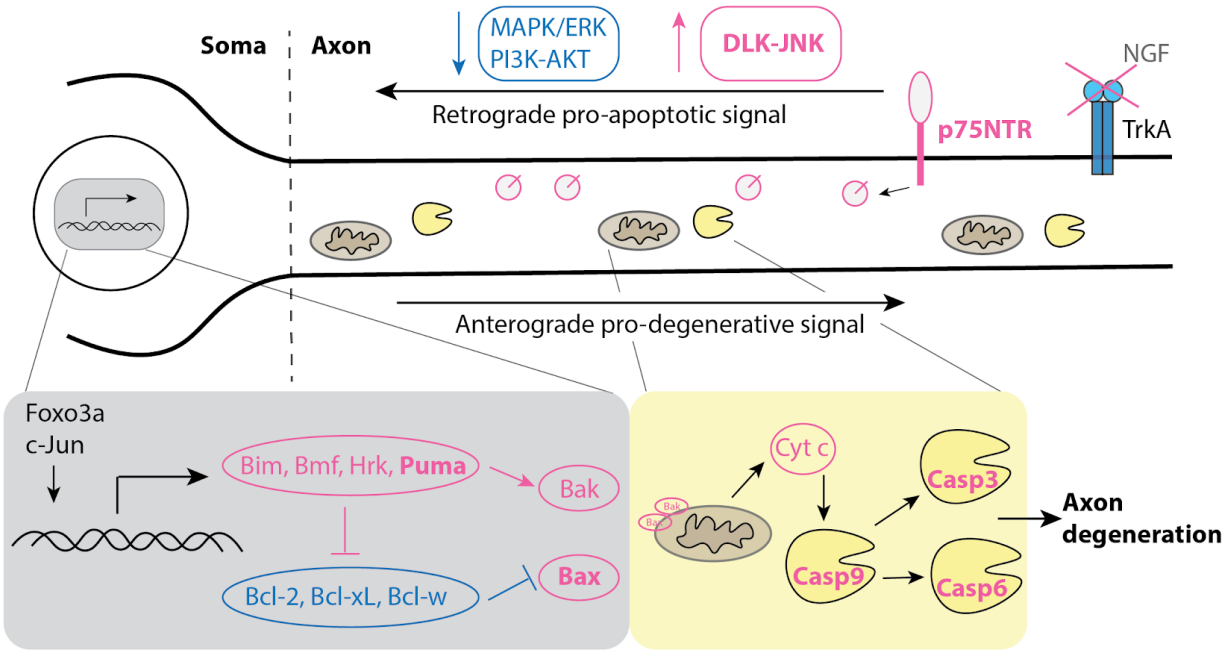

Figure 1: Developmental axon degeneration pathways

When neurons are deprived of NGF, the retrograde pro-apoptotic pathway initiated from p75NTR is activated, with decreased ERK and AKT signaling and increased DLK/JNK activity. The upregulation of transcriptional factors leads to increased expression of pro-death BH3-only genes (Bim, Bmf, Hrk, Puma) and inhibition of Bcl-2 family genes (Bcl-2, Bcl-xL, Bcl-w) in cell body. Puma induces anterograde pro-degenerative signaling by activating Bax, which promotes the release of Cyt c from mitochondria. Activation of downstream caspase cascade leads to axon degeneration.

Wallerian degeneration

Wallerian degeneration occurs after an axon is cut or crushed and entails the granular disintegration of the severed axon distal to the injury site (Waller, 1851). This degeneration process was originally characterized by breaking up of endoplasmic reticulum (ER), swelling and local accumulation of mitochondria and fragmentation of neurofilaments (Vial, 1958; deF. Webster, 1962). Careful microscopic analysis has revealed that the axon separated from the soma goes through a lag/latent phase where its overall morphology remains unchanged, followed by a execution/catastrophic phase where the axon begins to disassemble (Beirowski et al., 2005). However, the molecular pathways underlying these distinct phases of axon degeneration have long remained unknown and the implications of the phases as therapeutic targets for neurological disorders requires further investigation (Conforti et al., 2014).

WLD^S

Despite the importance of nutrients and extra-axonal support for long-term survival, injured axons are now thought to initiate self-destruction through a regulatable or active process that is distinct from apoptosis (Finn et al., 2000; Whitmore et al., 2003). This theory has come to light after the discovery of the *slow Wallerian degeneration* mutation mouse (*Wld*^{S}), in which distal axons survive ten times longer than normal in response to injury (Coleman et al., 1998; Lunn et al., 1989). The protective effect of *Wld*^{S} is conserved from insects to vertebrates and a variety of neurodegenerative diseases such as traumatic brain injury (TBI), multiple sclerosis (MS), Parkinson's disease (PD), glaucoma, Charcot-Marie-Tooth (CMT), and peripheral neuropathy (Krauss et al., 2020). Moreover, *Wld*^{S} has no effect on apoptotic death of the cell body, either in NGF-deprived sympathetic neuronal cultures or in axotomized motor neurons, indicating an axon-specific regulation (Adalbert et al., 2006; Deckwerth and Johnson, 1993; Hoopfer et al., 2006).

How does the *Wld*^{S} mutation protect axons from degeneration after injury? The Wld^S gene encodes an in-frame fusion protein comprised of full-length nicotinamide mononucleotide adenylyltransferase 1 (NMNAT1) and N-terminal 70 amino acids of E4-type ubiquitin ligase (Ube4b) (Coleman and Freeman, 2010; Conforti et al., 2000; Mack et al., 2001). As the NAD^+ biosynthetic enzyme, overexpression of Nmnat1 can protect severed axons from fragmentation but at levels significantly lower than Wld^S, suggesting that Nmnat1 is necessary but not sufficient for the severed axon-protecting activity of Wld^S (Conforti et al., 2007). Partial Ube4b sequence of Wld^s, on the other hand, lacks the ubiquitin ligase activity but shares protein binding activity (Laser et al., 2006). Importantly, the N-terminal 16 amino acids (N16) derived from Ube4b interacts with valosin containing protein (VCP) to potentially redistribute nuclear Nmnat1 activity to mitochondria or bring Nmnat1 together with VCP-associating proteins that mediate protective effects (Avery et al., 2009; Coleman and Freeman, 2010).

NMNAT

Nmnat enzymes are found in all organisms, catalyzing NAD^+ synthesis from adenosine triphosphate (ATP) and nicotinamide mononucleotide (NMN) that is converted from nicotinamide (NAM) by nicotinamide phosphoribosyltransferase (NAMPT) (Magni et al., 2004). The three mammalian isoforms have different subcellular localization: Nmnat1 is localized to the nucleus; Nmnat2 is found in the cytoplasm and trafficked anterogradely in the axoplasm; and Nmnat3 is mostly localized to mitochondria, allowing compartmentalization of NAD^+ metabolic pools for diverse cellular activities (Di Stefano and Conforti, 2013). Although overexpression of Nmnat1 fails to fully phenocopy *Wld*^{S} mutation, transgenic mice overexpressing NMNAT3 show delay of Wallerian degeneration similar to that in *Wld*^{S} mice, suggesting that localization of Nmnat is important for axonal survival (Avery et al., 2009; Yahata et al., 2009).

Unlike Nmnat1 and Nmnat3, endogenous Nmnat2 undergoes fast axonal transport and has a relatively short half-life due to proteasomal degradation. It's been shown that Nmnat2 is depleted in distal stumps of injured neurites, while exogenous Nmnat2 can protect injured neurites when expressed at high levels to overcome its short half-life (Gilley and Coleman, 2010). Several kinases including dual leucine zipper kinase (DLK) and leucine zipper bearing kinase (LZK) promote Nmnat2 turnover (Milde et al., 2013; Summers et al., 2018; Walker et al., 2017). The soluble, non-vesicular Nmnat2 is regulated by E3 ubiquitin ligase complex consisting of PAM/Highwire/Rpm1 (PHR1), S-phase kinase-associated protein 1 (SKP1) and F-box protein 45 (FBXO45) (Figley and DiAntonio, 2020; Summers et al., 2018; Xiong et al., 2012). Interestingly, removing sterile-α and Toll/interleukin 1 receptor (TIR) motif containing protein 1 (SARM1) in mice protects *Nmnat2* null axons without fully preserving NAD^+ levels after injury, indicating that Sarm1 acts downstream of Nmnat2 (Gilley et al., 2015). Moreover, Nmnat2 loss triggered by injury or disruption of mitochondrial membrane potential leads to the increase of substrate-to-product ratio (NMN/NAD^+), which might promote Sarm1 activation to execute downstream degeneration pathways (Di Stefano et al., 2015; Loreto et al., 2020; Zhao et al., 2019).

SARM1

SARM1 was first identified to be essential for axon degeneration after injury through genetic screens in Drosophila (Osterloh et al., 2012). Loss of Sarm1 has been shown to block Wallerian degeneration across species and protect axons from degeneration in various disease model, such as TBI, amyotrophic lateral sclerosis (ALS), optic nerve crush, chemotherapy-induced and diabetic peripheral neuropathy (Krauss et al., 2020; Llobet Rosell and Neukomm, 2019). Examining Sarm1 protein has revealed three functional domains: an N-terminal Heat/Armadillo (ARM) domain, important for autoinhibition; two central sterile α-motif (SAM) domains, responsible

for dimerization; and a C-terminal Toll-interleukin-1 receptor (TIR) domain in common with other Toll-like receptor (TLR) signaling molecule that possesses intrinsic NAD^+ cleavage activity to trigger axon degeneration (Essuman et al., 2017; Gerdts et al., 2013; Summers et al., 2016). In healthy axons, Sarm1 activity is autoinhibited by its N-terminal ARM domain, however, after injury this autoinhibition is released through an unknown mechanism to promote dimerization of SAM domains and degeneration via TIR domain-mediated NAD^+ destruction in response to injury (Gerdts et al., 2015, 2016)., The mechanism of Sarm1 activation during degeneration remains poorly understood.

Sarm1 has been considered to be the executioner and gatekeeper of commitment to Wallerian degeneration (Carty and Bowie, 2019). Supporting this notion, loss of Sarm1 protected axons more robustly than *Wld*^{S} mutation and rescues the ectopic degeneration observed in the *Nmant2*$^{-/-}$ neurons for the entire lifespan of the animals (Gilley et al., 2017). As the main factory for NAD^+ and ATP synthesis, mitochondrial respiration is crucial for axon survival and maintenance. Several studies indicate a mitochondrial-interacting sequence at the extreme N-terminus of Sarm1, which might tether Sarm1 to mitochondria during Wallerian degeneration (Kim et al., 2007; Panneerselvam et al., 2012). Furthermore, *Sarm1*$^{-/-}$ neurons were shown to prevent axonal degeneration caused by mitochondrial uncouplers, indicating that mitochondrial dysfunction could induce Sarm1 dependent axonal death (Summers et al., 2014). A recent study revealed that DLK activation and mitochondrial dysfunction independently decreased the levels of Nmnat2 and superior cervical ganglion 10 (SCG10), an axonal JNK substrate, resulting in Sarm1 dependent axon degeneration (Shin et al., 2012; Summers et al., 2020).

Other mediators

MAPK

The mitogen-activated protein kinase (MAPK) signaling pathway is involved in Wallerian degeneration. This cascade includes MKK4/7, MLK, DLK, JNK1/3 and SCG10 and represents the early degenerative response to axonal injury (Ehlers, 2004; Larhammar et al., 2017; Miller et al., 2009; Shin et al., 2012; Yang et al., 2015). Interestingly, JNK has been shown to phosphorylate Sarm1 to regulate NAD^+ cleavage during degeneration, while other studies indicate that phosphorylated JNK act at the downstream of Sarm1 activation to promote axon degeneration (Murata et al., 2018; Wang et al., 2018).

UPS and other proteases

Similar to NGF deprived neurons, inhibiting the ubiquitin proteasome system (UPS) by both pharmacological and genetic means can delay degeneration of transected axons (Zhai et al., 2003). An E3 ubiquitin ligase, zinc and ring finger 1 (ZNRF1) promotes Wallerian degeneration by targeting AKT to degrade, thereby increasing the non-phosphorylated active form of glycogen synthase kinase-3β (GSK3B) which phosphorylates collapsin response mediator protein 2 (CRMP2), which is required for microtubule reorganization in degenerating axons (Wakatsuki et al., 2011). Another family of calcium-dependent non-lysosomal protease, calpains and their endogenous inhibitors calpastatin have also been shown to regulate Walleian degeneration as a terminal event in axon death signaling (Glass et al., 2002; Ma et al., 2013). Moreover, CRMP4 functions in the distal axons where it facilitates Wallerian degeneration through calpain-dependent formation of harmful CRMP4 fragments (Girouard et al., 2020). As a “self-eating” process of the cell that sequesters misfolded proteins and dysfunctional organelles, autophagy and its related pathway has also been implicated in Wallerian degeneration. Vacuolar protein sorting 4 (Vps4), a component of endosomal sorting complexes required for transport (ESCRT) machinery, is shown to be rapidly depleted in injured mouse axons, inducing autophagic impediment and subsequent degeneration (Wang et al., 2019b).

Cytoskeletal modulation

As one of the characteristics of Wallerian degeneration, the mechanisms of cytoskeleton breakdown has been investigated. Rho activation was observed in the distal axons after injury, which triggered downstream Rho-kinase signaling to mediate actin polymerization (Yamagishi et al., 2005). Mammalian Sir2-related protein 2 (SIRT2), a NAD-dependent tubulin deacetylase, was also shown to regulate axon degeneration in response to injury. Decreased levels of SIRT2 and enhanced microtubule acetylation contribute to the resistance to axon degeneration in *Wld*^{S} mice (Suzuki and Koike, 2007). Genetic screen in drosophila has recently identified Axundead (Axed) as a mediator of axon death, acting downstream of Sarm1 on severed axons (Neukomm et al., 2017). However, the molecular mechanism of how Axed is activated after injury and its downstream targets remain unclear.

In summary, activation of UPS and MAPK signaling cascade triggered by injury leads to fast depletion of axonal Nmnat2 and NAD^+ pools, increasing the NMN/NAD^+ ratio to destructive threshold, which somehow activates Sarm1 to further facilitate NAD^+ loss. Mitochondrial dysfunction and coupled energy deficits, calpain activation, and other mediators promote cytoskeleton fragmentation and catastrophic axon degeneration (Fig.2) (Coleman and Höke, 2020; Ding and Hammarlund, 2019; Freeman, 2014).

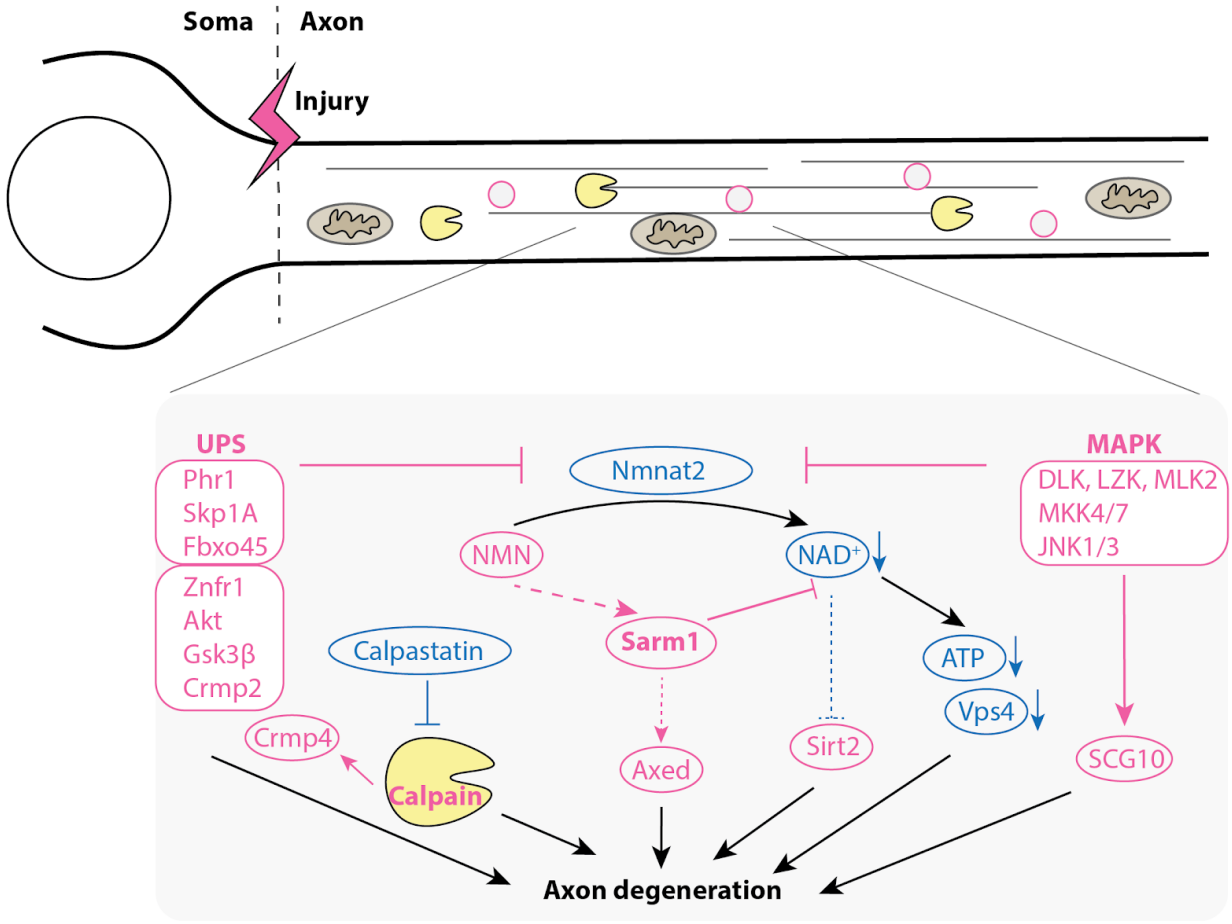

Figure 2: Wallerian degeneration pathways

In response to injury, activation of MAPK signaling cascade and UPS lead to Nmnat2 degradation, increase of NMN/NAD^+ ratio, and subsequent Sarm1 activation. Energy depletion along the axons and the cytoskeleton breakdown mediated by calpain, Axed, Sirt2, SCG10 and CRMP2/4 promote catastrophic axon degeneration.

Calcium signaling in axon degeneration

Neurons rapidly transfer electrochemical signals in a highly controlled spatiotemporal manner. As a major intracellular messenger, calcium mediates many fundamental functions of neurons, including neurite outgrowth, synaptic transmission, plasticity, neural survival and death. Disrupted calcium homeostasis and calcium regulating proteins are common features in aging and neurodegenerative diseases (Mattson, 2007; Müller et al., 2018). Perturbed axonal calcium due to calcium flux from outside the axon and lethal release of calcium from intracellular stores like ER and mitochondria can result in enhanced amyloid plaque formation, neurofibrillary degeneration, apoptosis, and PD pathogenesis (LaFerla, 2002; Stirling and Stys, 2010; Surmeier et al., 2017). In addition, studies have shown that mutations associated with aberrant regulation of calcium responsive proteins leads to neuropathy and CMT disease (Sun et al., 2019).

In vitro and *in vivo* calcium imaging have been used to investigate the relationship between intra-axonal calcium waves and the process of axon degeneration in both developmental and pathological conditions. Interestingly, compartmentalized calcium transients have been shown to act as temporal and spatial cues to trigger pruning (Kanamori et al., 2013). Moreover, the axonal calcium increase just prior to catastrophic degeneration, is thought to be a key instructive component of the degeneration program in response to injury (Adalbert et al., 2012; Vargas et al., 2015). Extracellular calcium influx has been considered as a major source for the pre-catastrophic axonal calcium wave since chelating extracellular calcium late in WD or after NGF deprivation delays fragmentation (Johnstone et al., 2019; Vargas et al., 2015). Blocking calcium-specific channels or their subunits, such as voltage-gated calcium channels (VGCCs) and sodium-calcium exchanger (NCX) has been shown to delay axonal degeneration in response to injury or oxidative stress and improve growth cone formation and axon regeneration (Barsukova et al., 2012;

Dombert et al., 2017; LoPachin and Lehning, 1997; Ribas et al., 2017; Tabata et al., 2018; Tedeschi et al., 2016). These studies suggest that calcium influx from the extracellular space via calcium channels and NCX reversal contribute to axon degeneration. However, the subtypes of calcium channels involved in the degeneration process may be dependent on neuronal types and the pathological insults. Despite a good amount of investigation implicating calcium channels in degeneration, a recent study has revealed a non-selective route for calcium entry across the axonal plasma membrane via nanoscale ruptures to drive axon degeneration in MS model (Witte et al., 2019). In addition to the current view of extracellular calcium influx in axon degeneration, ER and mitochondria-derived calcium can regulate degenerative program as well. Pharmacological depletion of ER calcium store, blockage of ryanodine and IP_3 receptors, disruption in mitochondrial permeability transition pore (mPTP), and inhibition of store-operated calcium entry (SOCE) have been shown to inhibit the loss of axonal function, cytoskeletal degradation, and secondary axonal degeneration (Orem et al., 2017, 2020; Staal et al., 2010; Tian et al., 2020a; Villegas et al., 2014). Taken together, both extracellular calcium and intracellular stores contribute to axon degeneration, while their spatial regulation and interaction at different stages of the degeneration program require further investigation.

Calcium signaling plays critical roles in axonal response to pathological insult, including the disruption of cell membrane and cytoskeleton, and induction of stress response. Rapid calcium increase after acute injury triggers the fusion of lipid membranes by mediating calcium binding proteins like synexin to repair torn or ruptured plasma membranes (McNeil and Kirchhausen, 2005; Papahadjopoulos et al., 1990). Calcium overload also activates kinases, phosphatases and proteases that cooperatively restructure microtubules and actin filaments (Girouard et al., 2018). Several studies have revealed that calcium-dependent calpain activation promotes cytoskeletal breakdown by cleaving spectrin near the plasma membrane (Czogalla and Sikorski, 2005; George et al., 1995). DLK signaling has also been shown to regulate axon regeneration in *c.elegans* by

calcium influx after injury (Yan and Jin, 2012). Blocking calcium channels could suppress the activation of JNK/c-Jun signaling to stabilize axons after optic nerve crush (Ribas and Lingor, 2016). Moreover, calcium dysregulation associated with ER and mitochondria triggers a series of cell stress pathways including mPTP opening and consequent disruption of ATP production which is also thought to promote axon degeneration (Lee et al., 2018; Malhotra and Kaufman, 2011). Interestingly, a recent study showed that incubation of HIV associated toxins result in delayed accumulation of intracellular calcium coupled with decreased rate of calcium clearance from neurons, focal swellings and impaired movement of mitochondria in neurites, which could be suppressed by application of p75NTR ligand (Meeker et al., 2016). This suggests that p75NTR may function upstream of calcium signaling to modulate neurodegeneration. How p75NTR and other death receptors might mediate calcium signaling in developmental and pathological axon degeneration remains unclear.

Death receptors in axon degeneration

Death receptors are the members of the tumor necrosis factor receptor (TNFR) superfamily whose cytoplasmic tail contains a conserved death domain (DD). In spite of their name, death receptors can trigger either cell death or survival. During development, death receptors and their ligands regulate neuronal expansion, growth, differentiation and regional pattern formation, important for brain development (Twohig et al., 2011). In neurodegenerative diseases, death receptor expression and signaling has been shown to mediate neuronal death, axon degeneration, excitotoxicity and inflammation (Haase et al., 2008). Adapter proteins, along with other binding partners, are recruited by means of DD interaction to transduce death receptor signals. For example, Fas, DR4, and DR5 primarily bind Fas-associated DD (FADD), while TNFR1, DR3 and DR6 primarily bind TNFR-associated DD (TRADD) to promote downstream signaling events (Mc Guire et al., 2011; Walczak, 2013). Despite a good amount of evidence suggesting the involvement of death receptors in apoptosis and necroptosis, axon-specific roles of these receptors during degeneration remain largely unexplored.

p75NTR

p75NTR is widely expressed in the developing nervous system, including sympathetic, sensory, and motor neurons, as well as glial cells. The expression of p75NTR is diminished in adulthood, but can be upregulated or re-expressed in response to injury or degenerative insult (Ibáñez and Simi, 2012; Zeng et al., 2011). Similar to other death receptors, extracellular structure of p75NTR highlighted by conserved cysteine-rich domains (CRDs) is responsible for binding to all the neurotrophins (NGF, BDNF, NT-3 and NT-4/5) and their pro-forms with similar affinity (Chao, 1994; Teng et al., 2010). Unlike other death receptors, p75NTR does not signal through the recruitment of adaptor proteins by its DD. Depending on the ligand and co-receptor, p75NTR can

initiate pro-survival and pro-apoptotic signals, regulate cell cycle entry, axonal elongation and synaptic transmission (Dechant and Barde, 2002; Meeker and Williams, 2015; Yamashita et al., 2005).

In the presence of NGF, p75NTR interacts with the TrkA receptor to promote sympathetic neuron survival through activating PI3K-AKT, Ras-MAPK and NF-kB pathways (Gentry et al., 2004). However, when sympathetic neurons are maintained with low quantities of NGF or KCl, BDNF can activate p75NTR and JNK pathway to cause neuronal apoptosis (Bamji et al., 1998). During developmental sympathetic axon competition, BDNF secreted from active axons drive activation of p75NTR on losing axons to cause degeneration (Singh et al., 2008). Moreover, p75NTR also modulates neural connectivity in the intact mature nervous system. Specifically, myelin triggers local axon degeneration by p75NTR-dependent sequestration of Rho guanine nucleotide dissociation inhibitor (Rho-GDI) and downstream activation of Rho and caspase-6 (Park et al., 2010). Importantly, p75NTR forms disulphide-linked dimers through the highly conserved Cys^{257} in its transmembrane domain. Upon neurotrophin binding, the close association of p75NTR DD is transiently disrupted by conformational change to allow binding of caspase recruitment domain (CARD) of RIP2 kinase for activation of the NF-kB pathway, competing with the binding of Rho-GDI for Rho activation (Lin et al., 2015; Tanaka et al., 2016; Vilar et al., 2009). This “snail tong” like conformational change of p75NTR provides a protein interaction interface for switching pathways involved in axon degeneration and elongation. Additionally, proteolysis of p75NTR in axons by the metalloprotease TNFα-converting enzyme (TACE, also known as ADAM17) and γ-secretase are required for generation of the intracellular domain (ICD) of p75NTR for retrograde degenerative signal in response to trophic deprivation or oxidative stress (Kraemer et al., 2014; Pathak et al., 2018).

Many studies have reported adult re-expression of p75NTR following injury and cellular stress. In AD models, small molecule p75NTR modulators have been shown to inhibit Aβ-induced neurite degeneration in the basal forebrain, hippocampus and cortex, and have been applied in phase 2 clinical trials for mild-moderate AD patients (Knowles et al., 2013; Simmons et al., 2014; Yang et al., 2008). Moreover, Aβ-induced tau hyperphosphorylation, synaptic disorder and neuronal loss were alleviated by genetic knockout of p75NTR, revealing the therapeutic potential of p75NTR in AD and other tauopathies (Shen et al., 2019). However, the molecular mechanisms that upregulate p75NTR during neural injury and neurodegeneration remain unclear (Ibáñez and Simi, 2012). Therefore, the specific roles of p75NTR in developmental and pathological axon degeneration requires further analysis.

DR6

Death receptor 6 (DR6) is a single pass transmembrane receptor, possesses four extracellular TNFR-like CRDs, a transmembrane domain and a cytoplasmic DD related to those of all known death receptors (Pan et al., 1998). DR6 is expressed in most human tissues and abundant transcript is detected in heart, brain, placenta, pancreas, thymus, lymph node and several non-lymphoid cancer cell lines (Pan et al., 1998). Studies have shown that DR6 associates with TRADD but not FADD to couple to downstream caspases to induce apoptosis and activation of NF-kB and JNK (Kasof et al., 2001; Pan et al., 1998).

DR6 did not receive much attention in the field of degeneration until the identification of APP as potential ligand for DR6 in axonal pruning. Trophic factor deprivation could trigger the β-secretase (BACE)-dependent shedding of surface APP, which binds DR6 and activates caspase 6 to promote axon degeneration (Nikolaev et al., 2009). However, further genetic and biochemical analysis revealed that although APP and DR6 work in the same pathway to control pruning, the

high-affinity binding to DR6 requires more C-terminal portion of the APP ectodomain, independent of BACE (Olsen et al., 2014). Structural analysis of DR6 indicated that unlike p75NTR, a positively charged surface patch on DR6 could interact with a negatively charged surface feature on the ligand responsible for the exclusive recognition, but the proposed model of the APP/DR6 complex did not obey the electrostatic surface binding mode between ligand and receptor (Kuester et al., 2011). Alternatively, a working model of APP-induced dimerization of DR6 was proposed whereby dimeric APP brings two DR6 molecules together to allow activation of downstream signaling associated with the DD (Xu et al., 2015). Given the link between APP, developmental axon pruning and AD, it's likely that DR6 contributes to neurodegeneration in AD and other axon degeneration paradigms. However, genetic deletion of DR6 failed to alter the formation of amyloid plaques, gliosis, synaptic loss, or cognitive behavioral deficits in AD mouse models (Kallop et al., 2014). In addition, APP cleavage, caspase 6 and DR6 activation are not involved in axonal degeneration induced by mechanical or toxic insults in sensory neuronal cultures and retinal ganglion cells (Fernandes et al., 2018; Vohra et al., 2010). However, DR6 and caspase 6 were shown to mediate axonal degeneration induced by the prion peptide in spinal cord neurons (Wang et al., 2015). Previous work in our lab also reported that DR6 is required for the activation of classic WD degeneration pathways (Gamage et al., 2017). Interestingly, in addition to the cell autonomous function of DR6 in axon degeneration, a recent study has revealed a non-cell autonomous function of DR6 in Schwann cell proliferation (Colombo et al., 2018). As a novel substrate for a disintegrin and metalloprotease 10 (ADAM10) and γ-secretase, neuronal DR6 was found to be cleaved and act *in trans* on Schwann cells to mediate their proliferation and myelination during development, independently of its cytoplasmic DD (Colombo et al., 2018). Given the diverse function of DR6 in degeneration, it's important to determine the specific mechanisms for DR6 activation in different cell types and degeneration models.

Stages of axon degeneration

Axon degeneration is an evolutionary conserved process that can be activated by different stimuli including trophic factor deprivation, mechanical damage, oxidative stress and toxic drug incubation. After injury, desomatized axons undergo three distinct stages of WD: 1. an acute local phase with degeneration proximal to lesion site (Kerschensteiner et al., 2005), 2. a latent phase, which lasts for 1-2 hours *in vitro* and up to 48 hours *in vivo*, and 3. a rapid and near synchronous "catastrophic"/execution phase, in which the cytoskeleton disintegrates (Beirowski et al., 2005; Rosenberg et al., 2012; Wang et al., 2012). Initial channel-mediated calcium influx of extracellular calcium is critical for triggering the acute axonal degeneration (Kerschensteiner et al., 2005; Wang et al., 2012). The local increase of the calcium close to the injury site promotes the re-seal of the membrane, which allows the distal axon to exhibit a period of structural quiescence and maintain physiological functions in latent phase (Eddleman et al., 1998; Ziv and Spira, 1995). In the catastrophic phase, molecules related to cytoskeleton breakdown, such as calpain, drive the final stage of axon disintegration (Ma et al., 2013; Salvadores et al., 2017). Degeneration induced by trophic deprivation consists of the final two stages but not the first. The degradation of calpastatin and activation of calpain have been implicated in the common downstream pathways shared by both developmental degeneration and WD (Yang et al., 2013). However, the vast majority of the molecular mechanisms mentioned above have not been assigned to particular phases of degeneration (*i.e.* latent versus catastrophic phase). Importantly, re-supplementation of NGF in previously trophically deprived axons in the early latent phase but not in the late catastrophic phase was able to reverse the degeneration progress, suggesting the existence of "point of no return" in axon and neuronal death (Deckwerth and Johnson, 1993). But the mechanisms that regulate the degeneration of axons transitioning from latent phase into catastrophic phase remain unclear. Interestingly, we observed axonal spheroid formation on

axons with morphologically intact cytoskeleton in both NGF deprived and injured neuronal cultures during the transition phase of degeneration (Fig.3). The regulation and function of the spheroids will be discussed in chapters 2 and 3 of this thesis.

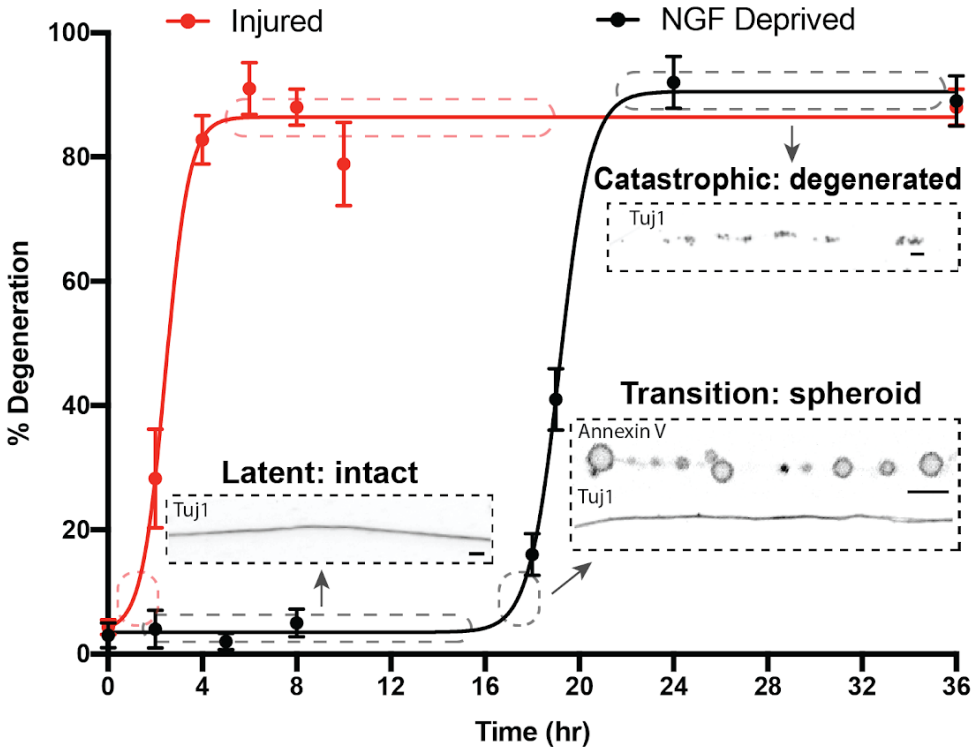

Figure 3: Stages and morphological hallmarks of degeneration in response to injury and NGF deprivation

Axons are intact and continuous during latent and transition phases, then fragmented in catastrophic phase, as indicated in Tuj1 (anti-βIII-tubulin) immunostained images. In the transition phase, axons develop spheroids with flipped phosphatidylserine on the outer surface of the membrane, indicated by Annexin V staining. Scale bar = 5μm.

Axonal spheroids

Many insults can trigger axon degeneration, often accompanied by the emergence of axonal spheroids. The formation of spheroid or process of beading was observed in spinal cord distal to a site of injury by Ramon y Cajal, who indicated that “the voluminous balls along the nerves were the seat of destructive process”, as they appeared earlier than nerve fragmentation (Ramón y Cajal, 1928). Similar to injury in the CNS, crushed peripheral nerve fibers swell, causing a beaded spherical morphology (Gershenbaum and Roisen, 1978). Axonal spheroids have also been observed in the aging brain (Bridge et al., 2009), TBI (Newell et al., 1999), and many neurodegenerative diseases including AD (Stokin et al., 2005), PD (Galvin et al., 1999), and ALS (Carpenter, 1968).

As the hallmark of axon pathology, it remains unclear whether spheroids in so many different neural disorders arise by a common mechanism. The slow Wallerian degeneration gene, *Wld*^{S}, inhibits axonal spheroid formation in injured CNS and PNS nerves, as well as disease model like gracile axonal dystrophy mice (Beirowski et al., 2005, 2010; Mi et al., 2005). The consistent suppression of spheroids in *Wld*^{S} mice reveals a mechanistic link for convergent axon degeneration mechanisms in diverse modules. Focal blockage of axonal transport often leads to accumulation of organelles and disorganized cytoskeleton in axonal varicosities. Importantly, axonal spheroids show accumulation of kinesin co-localized with highly phosphorylated neurofilaments in motor neuron disorder (Toyoshima et al., 1998) and APP in many CNS disorders (Coleman, 2005), indicating that failure of axonal transport may contribute to spheroid formation. However, early injury-induced spheroids in the optic nerve did not contain large accumulations of mitochondria that would have been expected if impaired mitochondrial transport caused focal dilation of the axons (Beirowski et al., 2010). These studies address the question

regarding whether axonal spheroids are a cause or consequence of impaired axonal transport, or both. Moreover, reactive oxygen species (ROS) triggered increase of axoplasmic calcium levels, accumulation of calcium channel and actin at the sites of spheroids (Barsukova et al., 2012), suggesting that rather than being a passive consequence of blocked axonal transport, axonal spheroids could be an active programmed response to damage.

Despite a good amount of morphological evidence about axonal spheroids in pathological condition, whether the axonal spheroid is an early or late event in degeneration remains unclear. The function of axonal spheroids in degeneration has been largely overlooked. Additionally, it is unknown whether the characteristics of axonal spheroids in disease stay the same in axon death during development. Molecular mechanisms governing formation of spheroids must be investigated for better understanding of degeneration and intervention of disease.

Chapter 2[2]

p75NTR and DR6 regulate distinct phases of axon degeneration demarcated by spheroid rupture

Authors

Yu Yong[1+], Kanchana Gamage[3,5+], Irene Cheng[1,2], Kelly Barford[2], Anthony Spano[1], Bettina Winckler[3], Christopher Deppmann[1,2,3,4*]

Author affiliations

[1]Department of Biology, University of Virginia, Charlottesville, VA, 22903, USA

[2] Neuroscience Graduate Program, University of Virginia, Charlottesville, VA, 22903, USA

[3]Department of Cell Biology, University of Virginia, Charlottesville, VA, 22903, USA

[4]Department of Biomedical Engineering, University of Virginia, Charlottesville, VA, 22903, USA

[5]Amgen, Massachusetts & Department of Stem Cell and Regenerative Biology, Harvard University, Cambridge, MA, 02138, USA

[+]Equal Contribution

Correspondence

*To whom correspondence should be sent:

Christopher D. Deppmann

Departments of Biology, Cell Biology, Neuroscience and Biomedical Engineering

[2] Y. Yong *et al.*, p75NTR and DR6 regulate distinct phases of axon degeneration demarcated by spheroid rupture. *J. Neurosci.* **39**, 9503–9520 (2019).

University of Virginia

Charlottesville, VA 22904-4328

email: deppmann@virginia.edu

Key words

Degeneration; DR6; p75NTR; pruning; spheroids

Significance statement

Developmental pruning shares several morphological similarities to both disease- and injury-induced degeneration, including spheroid formation. The function and underlying mechanisms governing axonal spheroid formation, however, remain unclear. In this study, we report that axons coordinate each other's degeneration during development via axonal spheroid rupture. Before irreversible breakdown of the axon in response to trophic withdrawal, p75 neurotrophic factor receptor-RhoA signaling governs the formation and growth of spheroids. These spheroids then rupture, allowing exchange of contents ≤10 kDa between the intracellular and extracellular space to drive death receptor 6 and calpain-dependent catastrophic degeneration. This finding informs not only our understanding of regressive events during development but may also provide a rationale for designing new treatments toward myriad neurodegenerative disorders.

Abstract

The regressive events associated with trophic deprivation are critical for sculpting a functional nervous system. After nerve growth factor withdrawal, sympathetic axons derived from male and female neonatal mice maintain their structural integrity for ~18 h (latent phase) followed by a rapid and near unison disassembly of axons over the next 3 h (catastrophic phase). Here we examine the molecular basis by which axons transition from latent to catastrophic phases of degeneration following trophic withdrawal. Before catastrophic degenera- tion, we observed an increase in intra-axonal calcium. This calcium flux is accompanied by p75 neurotrophic factor receptor-Rho-actin- dependent expansion of calcium-rich axonal spheroids that eventually rupture, releasing their contents to the extracellular space. Conditioned media derived from degenerating axons are capable of hastening transition into the catastrophic phase of degeneration. We also found that death receptor 6, but not p75 neurotrophic factor receptor, is required for transition into the catastrophic phase in response to conditioned media but not for the intra-axonal calcium flux, spheroid formation, or rupture that occur toward the end of latency. Our results support the existence of an interaxonal degenerative signal that promotes catastrophic degeneration among trophically deprived axons.

Introduction

Throughout nervous system development, axons, synapses and even entire neurons are initially overproduced and then refined through a period of organized culling (Hamburger and Oppenheim, 1990; Kantor and Kolodkin, 2003; Purves and Lichtman, 1980). Sympathetic neurons in the peripheral nervous system (PNS) rely on NGF-TrkA neurotrophic signaling to stabilize these components (Campenot, 1977; Gamage et al., 2017; Hendry and Campbell, 1976; Purves et al., 1988; Yan et al., 2010). The absence of sufficient neurotrophic signaling permits pro-destructive cues originating from tumor necrosis factor receptor superfamily (TNFRSF) members, such as p75 neurotrophin receptor (p75NTR), death receptor 6 (DR6) and tumor necrosis factor receptor 1a (TNFR1a), to promote regressive events like cell death, synapse restriction or axon degeneration in the PNS (Gamage et al., 2017; Nikolaev et al., 2009; Olsen et al., 2014; Singh et al., 2008; Wheeler et al., 2014). Axon degeneration is critical for proper nervous system wiring during development, but it's also a hallmark of several neural pathologies like Alzheimer's disease, amyotrophic lateral sclerosis (ALS), and injury (Saxena and Caroni, 2007). Both developmental and pathological degeneration occur in 2 phases: latent and catastrophic (Kristiansen and Ham, 2014; Wang et al., 2012).

During latent phase, axons are morphologically indistinguishable from those receiving trophic support (Deckwerth and Johnson, 1993). Re-addition of trophic factor or mild depolarization during the latent phase is capable of rescuing degeneration (Edwards et al., 1991). After latency, the catastrophic/ execution stage of degeneration occurs in a rapid and near synchronous manner. During this period, axonal transport ceases, axons develop swellings, neurofilaments become fragmented, the cytoskeleton disintegrates, and debris is removed by recruited phagocytes (Luo and O'Leary, 2005; Saxena and Caroni, 2007). Importantly, this stage of degeneration represents the point of no return where re-introduction of neurotrophic factors do

not rescue degeneration (Edwards et al., 1991). Although we and others have shown that in the absence of NGF-TrkA signaling, p75NTR and DR6 mediate axon degeneration (Bamji et al., 1998; Gamage et al., 2017; Nikolaev et al., 2009; Olsen et al., 2014; Singh et al., 2008), the relative contributions of p75NTR and DR6 specifically to latent and catastrophic phases of degeneration have largely been overlooked.

How do axons transition from latent to catastrophic phases? It was shown that calcium signaling in degenerating axons promote activation of calpain, the calcium sensitive protease required for the disassembly of cytoskeletal elements (Avery et al., 2012; George et al., 1995; Vargas et al., 2015). During development, it is thought that compartmentalized calcium transients act as temporal and spatial cues to trigger dendrite pruning (Kanamori et al., 2013). Moreover, it was recently shown that axoplasmic calcium increases before the emergence of gross morphological changes in NGF deprived DRG cultures (Johnstone et al., 2019), suggesting that intra-axonal calcium signaling could play a role in all phases of degeneration. However, whether death receptors act permissively to allow calcium dependent irreversible fragmentation in response to trophic withdrawal remains an open question.

In this study, we demonstrate that after trophic deprivation, intra-axonal calcium increases prior to catastrophic degeneration. This is accompanied by the formation of calcium-rich spheroids that grow and then rupture, releasing their contents (≤10 kDa) to the extracellular space while allowing an influx of extracellular molecules (*e.g.,* calcium) into the intra-axonal space. The pro-degenerative molecules released into the extracellular space are capable of hastening entry of trophically deprived axons into the catastrophic phase of degeneration. We show that p75NTR promotes spheroid formation, intra-axonal calcium rise, and membrane rupture in a Rho-dependent manner. In contrast, DR6 is not required for spheroid formation and rupture. Moreover,

DR6 is required to hasten entry into the catastrophic phase of degeneration in response to conditioned media from degenerating axons, whereas p75NTR is dispensable. Taken together, these data place p75NTR and DR6 upstream and downstream of spheroidal rupture, respectively. This is consistent with separable roles for these receptors in early and late phases of degeneration induced by trophic withdrawal.

Results

Intra-axonal calcium increases in trophic factor deprived axons and accumulates in spheroids prior to catastrophic degeneration

To study the kinetics of degeneration induced by trophic withdrawal, we cultured sympathetic neurons from P0-P2 mice in microfluidic devices, which separate soma and axons (Fig.1*A*). After establishment in 45ng/mL of NGF for 5-7 days *in vitro* (DIV), wild-type sympathetic neurons were globally or locally deprived of NGF with media containing anti-NGF function blocking antibody for indicated times. After global NGF deprivation, the majority of axons remain intact for roughly 18 hours as measured by microtubule integrity (β3-tubulin staining). This period of sustained axonal integrity is referred to as the latent phase of degeneration (Coleman, 2005). At the conclusion of the latent phase, the majority of axons rapidly degenerate from 4.4±1.5% to 90.4±2.2% of degeneration within 3 hours (Fig.1*B,C*). This is referred to as the catastrophic or execution phase of degeneration (Wang et al., 2012).

What are the molecular events that signal the transition from latent to catastrophic phase? Axonal calcium waves have been reported to be critical in promoting axon degeneration after axotomy (Vargas et al., 2015). Given the importance of the calcium dependent protease, calpain, in developmental axon degeneration, we speculated that calcium waves may occur at the transition between latent and catastrophic phases (Yang et al., 2013). We examined axonal calcium dynamics using Fluo4-AM imaging of axons that were withdrawn from NGF. Multiple small calcium peaks were detected during the first 12 hours, while the largest axoplasmic calcium flux that we observed occurred between 17-19 hours after global trophic withdrawal (Fig.1*D*), a time reflecting the transition window between latent and catastrophic phases (Fig.1*C*). Notably, axonal calcium increases up to 3 fold over baseline by 17hr50min after global NGF deprivation (Fig.1*F*).

After this initial increase, axonal calcium levels decrease approximately 1.5 fold. We hypothesize that axonal calcium increase may be a hallmark of the transition between latent and catastrophic degeneration phases.

In addition to axonal apoptosis induced by global NGF deprivation, pruning is critical for refinement of the nervous system during development. To examine whether axon pruning has similar calcium dynamics in relation to degeneration kinetics, we selectively deprived NGF in the axon compartment of sympathetic neurons grown in microfluidic devices (Fig.1*A*). The majority of axons remain intact until 46 hours after local NGF deprivation, indicating the delayed latent phase compared to global NGF deprivation, which is consistent with previous reports (Chen et al., 2012) (Fig.1*B,C*). Calcium levels in locally NGF deprived axons spiked prior to entry into the catastrophic phase of degeneration (Fig.1*D*). This relationship between calcium spike and catastrophic degeneration is similar to what we observed in neurons globally deprived of NGF, albeit with an overall delay in degeneration kinetics.

Upon closer inspection of calcium dynamics within the entire axon, we observed that much of this calcium is concentrated in nascent spheroids on NGF deprived axons (Fig.1*E*). The formation of axonal spheroids/beads has been observed in not only trophic withdrawal models of developmental degeneration but also in pathological scenarios (Beirowski et al., 2010; Griffiths et al., 1998; Mejia Maza et al., 2018; Probst et al., 2000; Takahashi et al., 1997). However, whether these beads/spheroids have a function as degeneration progresses remains an open question. Interestingly, after observing the initial formation of calcium rich spheroids, these structures increase in size from 4.1±0.5μm^2 to 19.6±2.7μm^2 (roughly 500%) within one hour (Fig.1*G*). In addition to the increase in average spheroid size, the number of spheroids increased from 1 to 13 per 100μm between 17 and 18 hours after trophic withdrawal (Fig.1*H*). Spheroidal calcium levels had a roughly 1.7 fold increase by 17 hours and 50 minutes after NGF deprivation (Fig.1*G*).

However, the spheroidal calcium levels varied depending on spheroid size. This value likely underestimates the increase in calcium since the spheroidal area measured increases with time. As such, we also normalized the areas used for the region of interest (ROI) to quantify the spheroidal calcium density and found the same trend (Fig.1*I*).

To determine whether intra-axonal calcium elevation is required for the formation of spheroids, we depleted axoplasmic calcium by BAPTA-AM and examined the morphological changes of NGF deprived axons by live imaging. We find that axons retain their capacity to form spheroids in the absence of intra-axonal calcium elevation (Fig.2*A,B*). These data indicate that while intra-axonal calcium flux may correlates with entry into the catastrophic phase of degeneration, it is not required for spheroid formation.

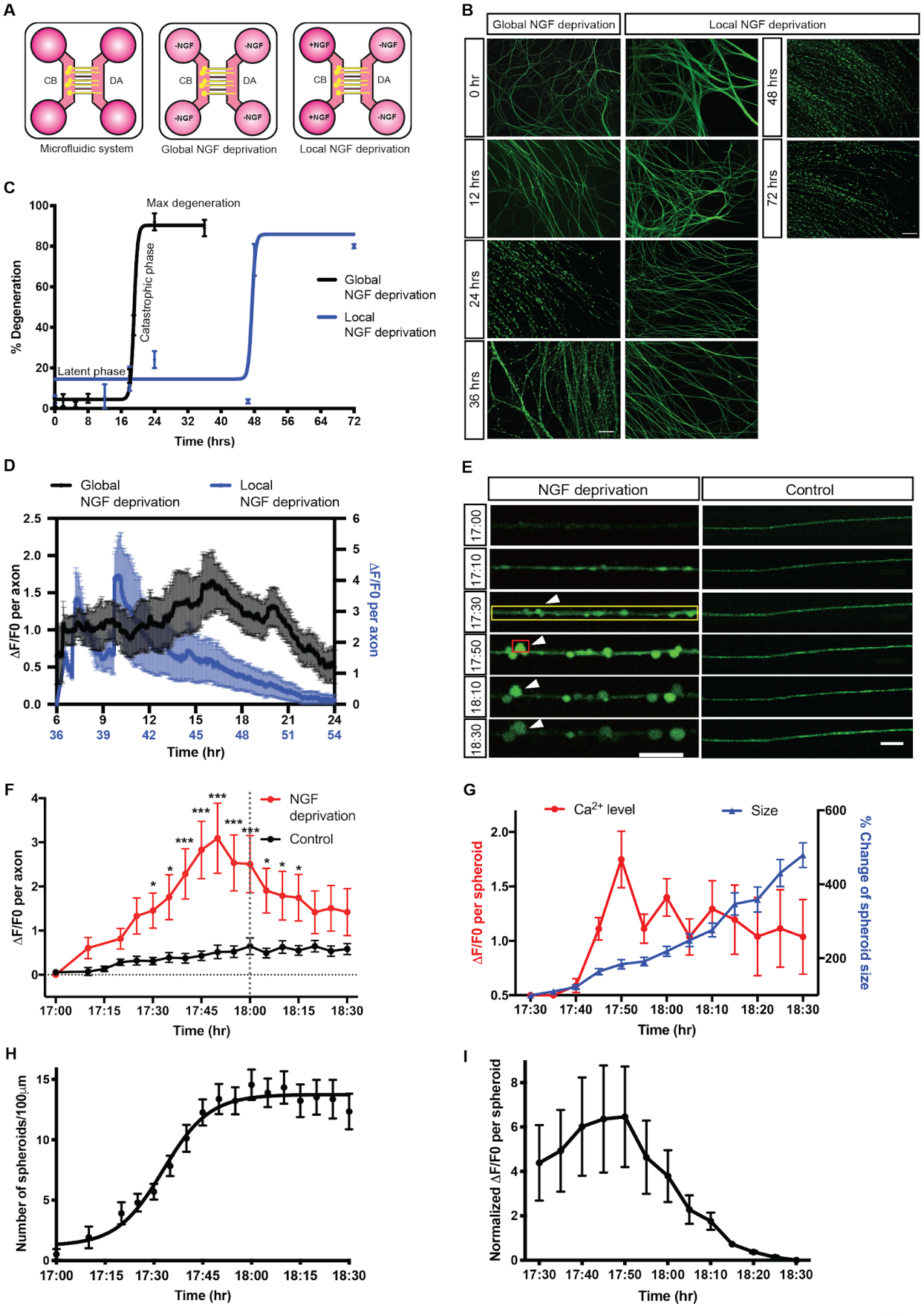
A
CB
DA
-NGF
+NGF
Microfluidic system
Global NGF deprivation
Local NGF deprivation
B
Global NGF deprivation
Local NGF deprivation
0 hr
12 hrs
24 hrs
36 hrs
48 hrs
72 hrs
C
Max degeneration
Catastrophic phase
Latent phase
% Degeneration
Time (hrs)
Global NGF deprivation
Local NGF deprivation
D
Global NGF deprivation
Local NGF deprivation
ΔF/F0 per axon
Time (hr)
E
NGF deprivation
Control
17:00
17:10
17:30
17:50
18:10
18:30
F
NGF deprivation
Control
ΔF/F0 per axon
Time (hr)
G
Ca2+ level
Size
ΔF/F0 per spheroid
% Change of spheroid size
Time (hr)
H
Number of spheroids/100μm
Time (hr)
I
Normalized ΔF/F0 per spheroid
Time (hr)

Figure 1: Axoplasmic calcium dynamics and formation of spheroids prior to catastrophic degeneration in response to NGF deprivation

A, Schematic representation of NGF deprivation paradigm in microfluidic devices. Cell bodies (CB) and distal axons (DA) are separated. For global NGF deprivation, sympathetic neurons were maintained in NGF-deficient media containing 1μg/mL anti-NGF antibody. For local NGF deprivation, sympathetic distal axons were maintained in 80μL per well of NGF-deficient media containing 1μg/mL anti-NGF antibody. Cell bodies were maintained in 150μL per well of media containing 45ng/mL NGF. ***B***, Representative images of β3-tubulin immuno-stained distal sympathetic axons before treatment (0hr), 12, 24, 36, 48 and 72 hours after global and local NGF deprivation. Scale bar = 50μm. ***C***, Degeneration time course after NGF deprivation. Latent and catastrophic phases of degeneration are noted. Nonlinear regression curve was drawn according to Hill equation. *n*=3 for each time point. ***D***, Normalized calcium fluorescence change of global (black, left y axis) and local (blue, right y axis) NGF deprived axons over time. Total number of *n*=6 (global NGF deprivation) and *n*=11 (local NGF deprivation) axons from 3 independent litters were quantified. ***E***, Fluo4-AM calcium imaging of sympathetic axons at the indicated times after global NGF deprivation. For the "NGF deprivation" condition, neurons were globally deprived of NGF for 17 hours, and then incubated with Fluo4-AM for calcium imaging. For the "Control" condition, no NGF deprivation was performed. Yellow box indicates the individual axon as a region of interest. Red box indicates axonal spheroid as a region of interest. White arrowheads indicate the formation and growth of spheroid. Scale bar = 10μm. ***F***, Calcium fluorescence change of control or NGF deprived axons over time. Grey vertical dotted line indicates the onset of catastrophic phase (18 hours after NGF deprivation). Black horizontal dotted line indicates the baseline without any calcium change. Total number of *n*=8 (NGF deprivation) and *n*=18 (control) of axons from 3 independent litters were quantified. ***G***, Calcium fluorescence and size change of axonal spheroid after 17 hours of global NGF deprivation. Total number of *n*=18 axonal spheroids from 3 independent litters were quantified. $p=0.0452$ (17:30), $p=0.0059$ (17:35), $p<0.0001$ (17:40,

17:45, 17:50, 17:55, 18:00), p=0.0037 (18:05), p=0.0380 (18:10), p=0.0293 (18:15), two-way ANOVA with Sidak's multiple comparisons test. ***H***, Quantification of axonal spheroid number per 100µm of axon at the indicated times after NGF deprivation. Nonlinear regression curve was drawn according to the Hill equation. Total number of n=11 axons from 3 independent litters were counted. ***I***, Quantification of normalized calcium fluorescence of axonal spheroids from 17.5 to 18.5 hours of global NGF deprivation. Individual axonal spheroids were quantified: n=18 spheroids from 3 independent replicates. Data are reported as mean±SEM, *p<0.05, ***p<0.0001.

Transcriptional induction of caspase activation is upstream of spheroid formation

Global NGF deprivation initiates apoptotic pathways to drive degeneration of axons and soma (Deckwerth and Johnson, 1993; Geden et al., 2019). Because caspases and calpain have been proposed to be involved in axon degeneration (Cusack et al., 2013; Ma et al., 2013; Simon et al., 2012, 2016; Yang et al., 2013), we next examined the requirement of these proteases in the formation of spheroids after NGF deprivation. Application of the pan-caspase inhibitor Z-VAD-FMK but not calpain inhibitor III blocked spheroid formation (Fig.2*A*). Less than two spheroids per 100μm of axons were observed in NGF deprived cultures treated with Z-VAD-FMK, while the numbers of spheroids reached 10.2±0.4 and 8.8±0.2 per 100μm after 19 hours of NGF deprivation in the DMSO and calpain inhibitor III treatments, respectively (Fig.2*B*). Taken together, these data indicate that caspase activation is upstream of spheroid formation occurring at the transition between latent and catastrophic phases.

It has been suggested that transcriptional upregulation of proapoptotic proteins (*e.g.* PUMA) are required for axon degeneration after trophic withdrawal (Maor-Nof et al., 2016; Simon et al., 2016). To determine whether inhibition of early prodegeneration transcriptional events could delay spheroid formation, we treated cell bodies with a transcription inhibitor, Actinomycin D, at the same time cells were deprived of NGF and examined spheroid formation between 17 and 19.5 hours after trophic withdrawal. Interestingly, Actinomycin D significantly diminished spheroid formation compared to the DMSO control (Fig.2*A,B*). Based on previous reports, we speculate that a transcriptional program induced by NGF withdrawal is permissive for the activation of caspase pathways, which in turn promotes spheroid formation (Maor-Nof et al., 2016; Simon et al., 2016).

Once cells become apoptotic, plasma membrane phosphatidylserine (PS) asymmetry is lost and membranes undergo blebbing. Importantly, PS enrichment on the outer leaflet of the plasma membrane is read as an 'eat-me' signal for phagocytes to aid apoptotic cell recognition and clearance (Poon et al., 2014; Zhang et al., 2018). After NGF deprivation, the formation of axonal spheroids were detected by live imaging. We next assessed PS exposure on the extracellular surface of axonal spheroids by Annexin V staining, which fluoresces upon binding to PS (Fig.2*C*, Movie 1,2). After 18 hours of NGF deprivation, about 60% of spheroids, but not the rest of the axon, are Annexin V-positive (Fig.2*D*), suggesting PS flipping to the outer leaflet on the spheroid membrane.

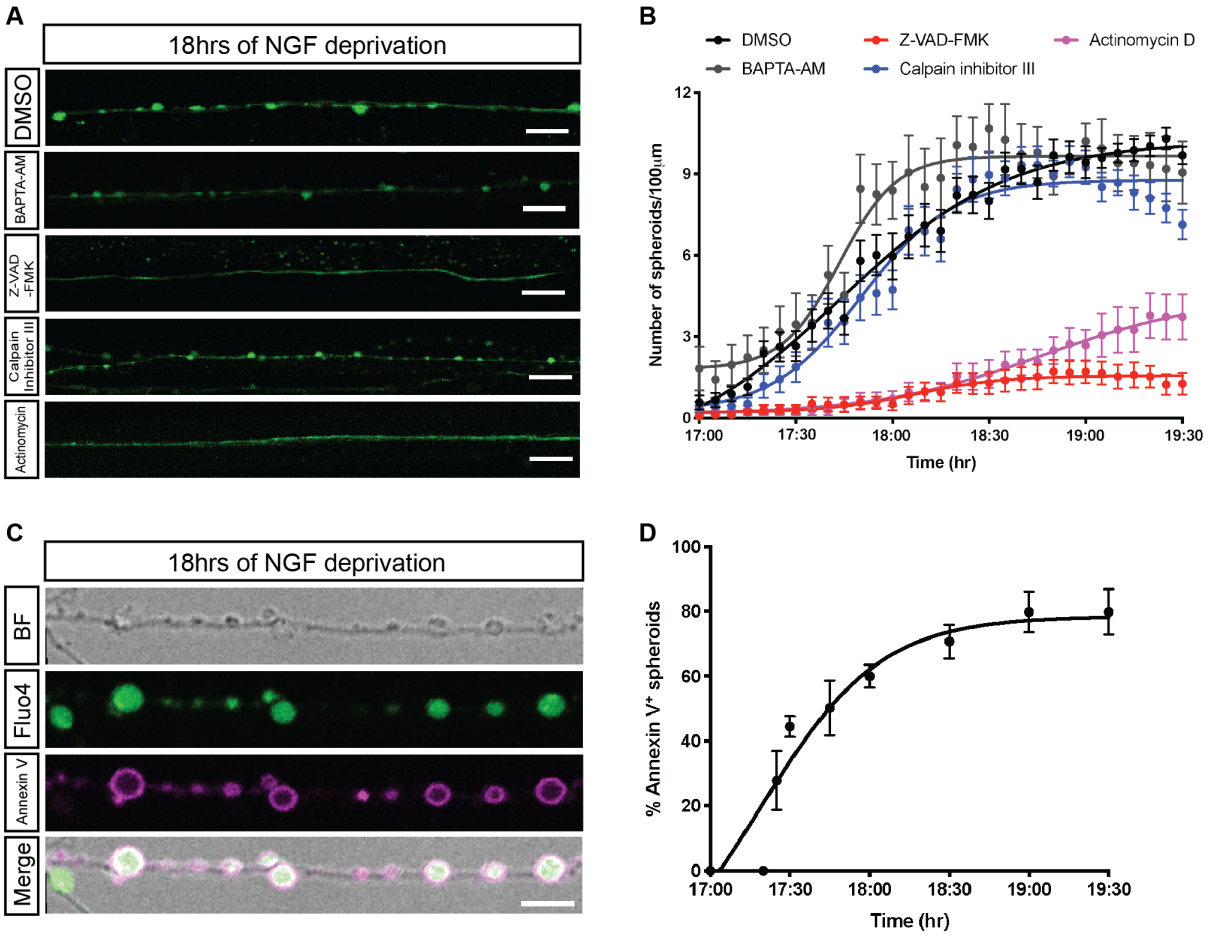

Figure 2: Transcription and caspase activation are required for formation of spheroids

A, ***B***, Fluo4-AM calcium imaging (***A***) and quantification of axonal spheroid number per 100µm of sympathetic axons (***B***) at the indicated times after NGF deprivation in the presence of DMSO, 10µM BAPTA-AM, 50µM V-ZAD-FMK, 20µM Calpain inhibitor III, and 1µg/mL Actinomycin, respectively. Scale bar = 10µm. Nonlinear regression curves were drawn according to the Hill equation. Total number of *n*=26 (DMSO), *n*=26 (BAPTA-AM), *n*=25 (Z-VAD-FMK), *n*=20 (Calpain inhibitor III), *n*=17 (Actinomycin) axons from 3 independent litters were counted. ***C***, Representative images of axonal spheroids after 18 hours of NGF deprivation. Fluo4-AM (green) indicates intra-axonal calcium, and Annexin V (magenta) indicates exposure of phosphatidylserine on the outer leaflet on the spheroid membrane. Scale bar = 5µm. ***D***, Quantification of the percentage of fluorescent Annexin V positive spheroids after 17 to 19.5 hours of NGF deprivation. Total number of *n*=15 axons from 3 independent litters were counted. Data are reported as mean±SEM.

Axonal spheroids develop membrane ruptures after NGF deprivation

Whereas Annexin V staining is consistent with PS flipping to the outer leaflet of the plasma membrane, it is also formally possible that the membrane integrity of growing spheroids is disrupted, allowing access of the 45 kDa Annexin V protein to the inner leaflet of the plasma membrane. To test this, we bathed control or NGF deprived axons in neutral fluorescent dextrans of different sizes (3, 10, 70 kDa). If there were any ruptures on the membrane after NGF deprivation, the dextran would immediately diffuse to the axoplasm (Fig.3*A*). The exclusion of dextran was maintained until 17 hours and 40 minutes after NGF deprivation, however by 17 hours and 50 minutes the axoplasm began to fill with 3 kDa fluorescent dextran (Fig.3*B*, Movie 3,5). The fraction of labeled spheroids decrease with increasing size of fluorescent dextran, and no significant spheroidal uptake was observed with 70 kDa dextran (Fig.3*D*), indicating that ruptures occur on a nano-scale and are permeable to molecules less than 10 kDa. Moreover, we observed non-punctate dextran positivity of spheroids simultaneously as Fluo4-AM dye was lost (Fig.3*C*), consistent with membrane rupture. We do observe some spheroids that have punctate dextran labeling, consistent with macropinocytosis, however the events that we consider rupture are quite distinct and involve rapid and complete filling of the spheroid (Movie 4). If the labeling of Annexin V on spheroids was due to entry of the dye through membrane rupture, the number of spheroids filled with dextran of similar or smaller sizes should be no less than the number of Annexin V positive spheroids. However, only 6.5±3.1% of 10 kDa dextran positive spheroids were observed after 18 hours of NGF deprivation, significantly less than 45 kDa Annexin V labeled spheroids (Fig.2*D*,3*C*), suggesting that the flipping of PS occurs prior to the entry of dextran or membrane rupture.

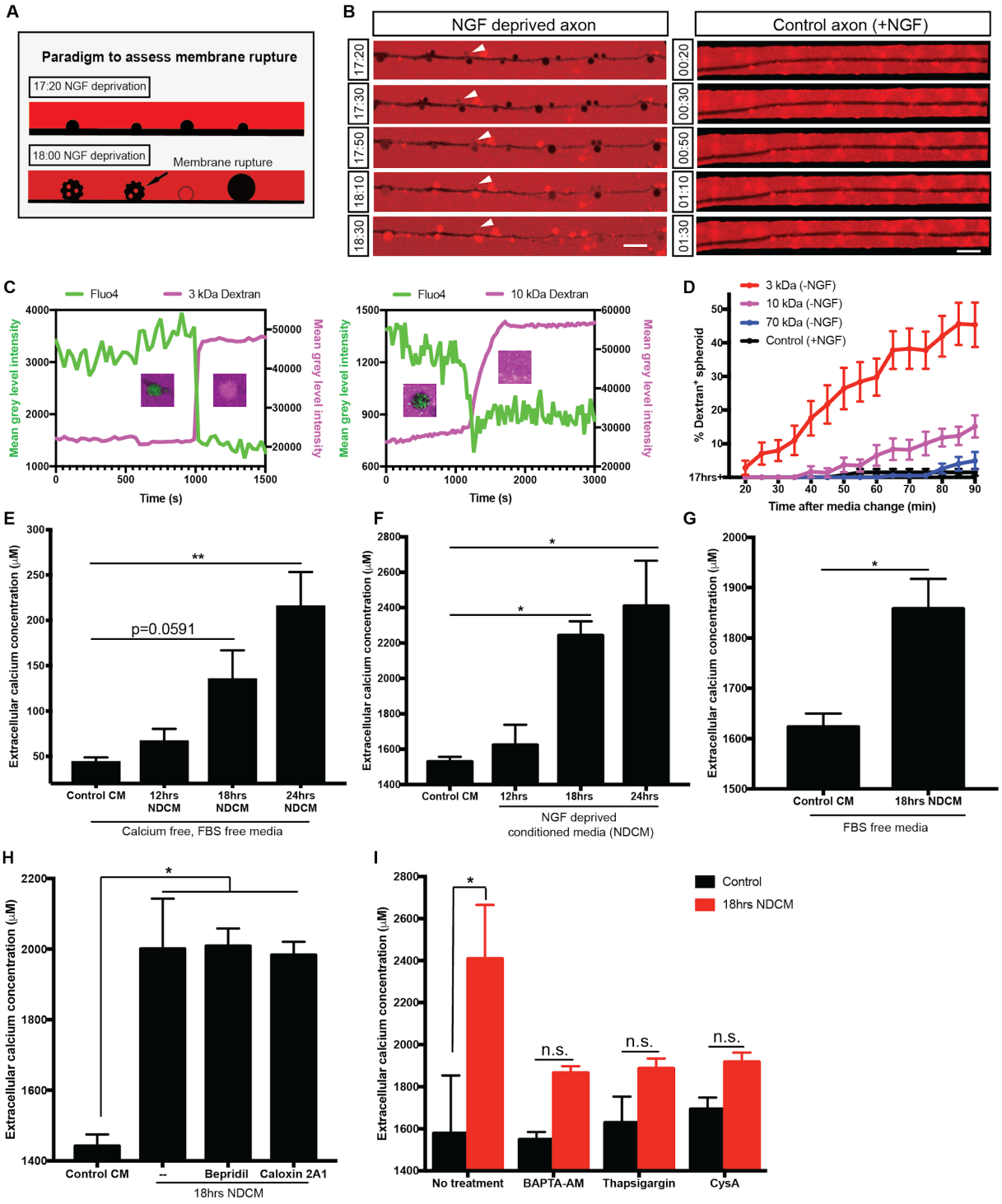

Figure 3: Axonal spheroids develop membrane rupture after NGF deprivation

A, Schematic representation of the experimental paradigm to assess membrane rupture model using fluorescent dextran. At 17 hours and 20 minutes of NGF deprivation, fluorescent dextran

(red) is not taken up by the axon (black, negative space). However, by 18 hours of NGF deprivation, as the plasma membrane loses integrity and ruptures, fluorescent dextran (red) can diffuse into spheroids, turning them red. Spheroids with intact membrane remain black. ***B***, Representative images of dextran 3 kDa (red) entry to axonal spheroids (black) from 17 hours and 20 minutes to 18 hours and 30 minutes of NGF deprivation (left column), and dextran exclusion in untreated axons (right column). White arrowheads indicate that dextran 3 kDa enter axonal spheroids after 18 hours of NGF deprivation. ***C***, Examples of individual spheroidal tracing on NGF deprived axons labeled with Fluo4-AM and bathed in 3 kDa (left) and 10 kDa (right) dextrans, respectively. Right y-axis is the mean grey level intensity of dextran fluorescence (megenta) after background subtraction, while left y-axis is the mean grey level intensity of Fluo4-AM (green) after background subtraction. Spheroids showing the red/green transition are captured. ***D***, Quantification of the percentages of fluorescent 3 kDa (red), 10 kDa (magenta), and 70 kDa (blue) dextran positive spheroids 20 to 90 minutes after 17 hours NGF deprivation. Black line (control) indicates the percentages of fluorescent 3 kDa dextran positive spheroids in the presence of NGF. Total number of n=15 (3 kDa), n=15 (10 kDa), n=12 (70 kDa), and n=9 (control) axons from 3 independent litters were counted. ***E,*** Measurement of extracellular calcium expelled from axons into calcium free, FBS free media. All axons were grown in regular DMEM then switched to calcium free, FBS free media prior to NGF deprivation. In the “Control CM” group, media was collected from axons grown in the presence of NGF. In “NDCM” groups, medium were collected at 12, 18, and 24 hours after NGF deprivation. Values were analyzed from n=7 (Control CM), n=5 (12hrs NDCM), n=6 (18hrs NDCM), and n=7 (24hrs NDCM) independent replicates. Compared to Control CM, p=0.0591 for 18hrs NDCM, p=0.0003 for 24hrs NDCM, one-way ANOVA with Dunnett’s multiple comparisons test. ***F***, Measurement of extracellular calcium concentration of untreated and NGF deprived conditioned media. Values were analyzed from n=7 (Control CM), n=4 (12hrs NDCM), n=6 (18hrs NDCM), and n=8 (24hrs NDCM) independent replicates. Compared to Control CM, p=0.0227 for 18hrs NDCM, p=0.0026 for 24hrs NDCM, one-

way ANOVA with Dunnett's multiple comparisons test. ***G***, Measurement of extracellular calcium extruded from axons into FBS free, IS21 supplemented DMEM with or without 18 hours of NGF deprivation. All axons were grown in FBS free, IS21 supplemented media prior to NGF deprivation. *n*=8 (Control CM) and *n*=3 (18hrs NDCM) independent replicates, *p*=0.0022, unpaired t-test. ***H***, Measurement of extracellular calcium concentrations in Control CM and 18hrs NDCM in the absence and presence of NCX blocker 10μM Bepridril or PMCA blocker 0.5mM Caloxin 2A1. *n*=4 for Control CM; *p*=0.0038, *n*=4 for 18hrs NDCM, --; *p*=0.0058, *n*=3 for 18hrs NDCM, Bepridril; *p*=0.0079, *n*=3 for 18hrs NDCM, Caloxin 2A1, one-way ANOVA with Tukey's multiple comparisons test. ***I***, Measurement of extracellular calcium concentration of untreated and NGF deprived conditioned media in the presence and absence of intracellular calcium chelator BAPTA-AM (10μM, 1hr incubation before NGF deprivation), SERCA inhibitor Thapsigargin (100nM, overnight treatment before NGF deprivation), and mitochondrial mPTP blocker Cyclosporin A (20μM, 1 hour treatment before NGF deprivation). *n*=3 for each group. *p*=0.0375 for No treatment; *p*=0.7952 for BAPTA-AM; *p*=0.8897 for Thapsigargin; *p*=0.9863 for CysA, two-way ANOVA with Sidak's multiple comparisons test. Data are reported as mean±SEM, n.s.=not significant, *p<0.05, **p<0.001. Scale bar = 10μm.

Rupture of axonal spheroids disrupts the electrochemical gradient and allows expulsion of axoplasmic material

Just as membrane rupture allows free diffusion of molecules under 10 kDa to enter spheroids, we predicted that these ruptures would allow small molecules to freely diffuse out of spheroids. Indeed, once spheroids reach approximately 400% of their original size, we observe a diminution of calcium signal, which we speculate is a function of diffusion of Fluo4-AM and calcium out of the spheroid. We sought to use calcium release to the extracellular space as a surrogate to test the hypothesis that small molecules may be released after spheroid rupture. We bathed axons in microfluidic devices in 100µL of calcium free media and measured extracellular calcium before and after spheroid formation using a Fluo4 spectrophotometric assay. Sympathetic neurons were cultured in media containing FBS and 1.8mM calcium, then switched to calcium free, FBS free media. We found that 24hrs NDCM contained approximately 4-fold higher calcium (215.50±37.68µM) compared to Control CM (43.88±4.97µM) (Fig.3*E*). Additionally, we were also able to observe an increase in extracellular calcium after spheroid rupture when experiments were performed using regular culture media containing FBS and 1.8mM calcium. We found that at 18hrs NDCM displayed a roughly 50% increase in calcium (2.24±0.08mM) over Control CM (1.53±0.03mM) (Fig.3*F*). To rule out the effect of FBS in regular culture media prior to calcium measurements, neurons were cultured in FBS free, IS21 supplemented DMEM media. Calcium level in 18hrs NDCM (1858.08±59.23mM) was significantly higher than calcium concentration in Control CM (1623.26±26.66mM) (Fig.3*G*), suggesting that this calcium release occurred regardless of the presence or absence of FBS in the media.

Beyond membrane rupture, it's formally possible that calcium release could be in part due to enhanced permeability of plasma membrane Ca^{2+} ATPase (PMCA) and/or reversal Na^{+}/Ca^{2+} exchanger (NCX) (Bano et al., 2007; Brini and Carafoli, 2011). To test this possibility, we treated

NGF deprived axons with PMCA inhibitor caloxin 2A1 or NCX inhibitor bepridil to test their ability to block elevation of extracellular calcium concentration. Axons deprived of NGF for 18 hours and treated with caloxin 2A1 or bepridil retained their ability to release calcium to the extracellular space (Fig.3*H*). Thus, spheroidal calcium is released to extracellular space independent of PMCA or NCX.

The observation that calcium in the media is elevated after membrane rupture is curious because the calcium concentration outside of the cell (1.8mM) is known to be much higher than in the axoplasm (100nM) (Clapham, 2007; LaFerla, 2002). How the axoplasm would have sufficient quantities of free calcium to appreciably elevate calcium levels in the media is unclear. To gain insight into this, we sought to determine the source of expelled intra-axonal calcium. We began by chelating all intracellular calcium with 10μM BAPTA-AM added 1 hour before NGF deprivation, which prevented calcium release to the extracellular space 18 hours after trophic deprivation (Fig.3*I*). Intracellular calcium is buffered and stored by a contiguous network of ER and mitochondria, and calcium flux is thought to contribute to axon degeneration (Mattson, 2007; Villegas et al., 2014). Depletion of ER or mitochondria calcium, by treating neurons with 100nM thapsigargin or 20μM cyclosporine A for 12 hours prior to NGF deprivation also blocked calcium increase in the extracellular space (Fig.3*I*). These results suggest that the elevated extracellular calcium come from intracellular calcium stores.

We expect that in physiological scenarios, membrane rupture would also allow disruption of the calcium electrochemical gradient between the inside and outside of the cell. In this way, elevated calcium level in the extracellular space may represent a surrogate for the release of other small molecules as well as a sustained elevation of intracellular calcium, which may lead to activation of calpain. Importantly, we are unable to observe sustained elevation of axoplasmic calcium after

rupture (Fig.1*D*) because the calcium indicator, Fluo4-AM, used in the above experiments would also diffuse out of the axon.

Expelled axoplasmic prodegenerative molecules hasten entry of axons into catastrophic phase

We speculated that contents released from ruptured spheroids may induce entry into the catastrophic phase of degeneration. To examine this, we collected media surrounding distal axons after 24 hours of NGF deprivation (24hrs NDCM) and incubated intact NGF deprived axons for 5 hours in 24hrs NDCM (Fig.4*A*). Importantly, in this paradigm the total time that recipient axons are incubated without NGF are 11 hours and 17 hours for "-NGF 6hrs" and "-NGF 12hrs" groups, respectively, prior to stereotypical morphological changes associated with degeneration. Neurons treated with control CM (from untreated axons at time 0 of NGF deprivation) displayed minimal degeneration, which is consistent with the kinetics of the trophic deprivation time course presented in Fig.1*C*. However, we found that intact axons treated with NDCM displayed 74.5±25.1% and 76.0±6.8% degeneration at 11 hours and 17 hours time points, respectively (Fig.4*B,C*). Additionally, in the presence of NGF, NDCM failed to promote degeneration in 5 hours of incubation (Fig.4*B,C*), indicating that loss of NGF pro-survival signal is necessary to drive catastrophic axonal degeneration.

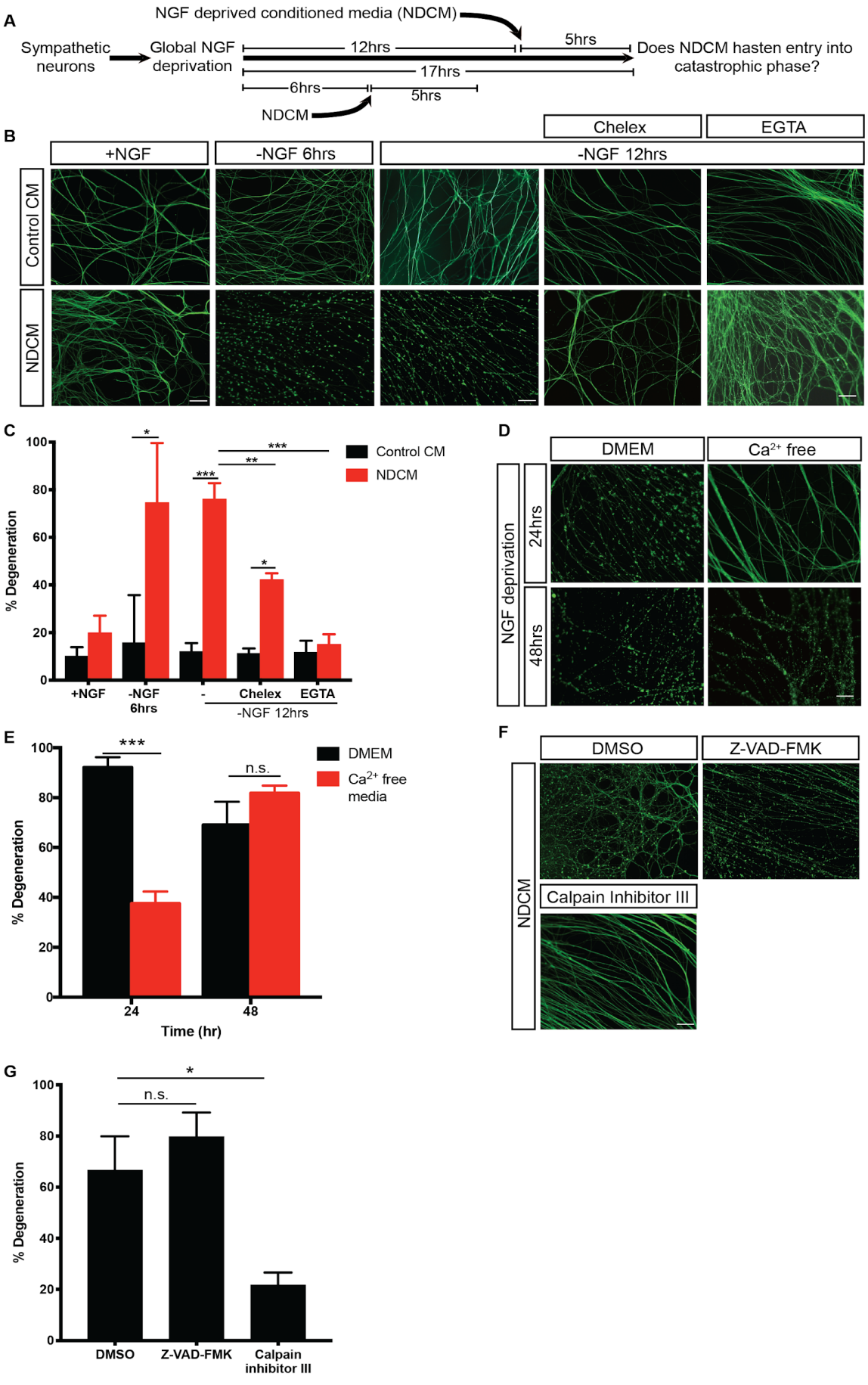
A
NGF deprived conditioned media (NDCM)
Sympathetic neurons
Global NGF deprivation
12hrs
5hrs
17hrs
6hrs
5hrs
NDCM
Does NDCM hasten entry into catastrophic phase?
B
Chelex
EGTA
+NGF
-NGF 6hrs
-NGF 12hrs
Control CM
NDCM
C
% Degeneration
Control CM
NDCM
+NGF
-NGF 6hrs
Chelex
EGTA
-NGF 12hrs
D
DMEM
Ca2+ free
NGF deprivation
24hrs
48hrs
E
% Degeneration
DMEM
Ca2+ free media
n.s.
24
48
Time (hr)
F
DMSO
Z-VAD-FMK
NDCM
Calpain Inhibitor III
G
% Degeneration
n.s.
DMSO
Z-VAD-FMK
Calpain inhibitor III

Figure 4: Calcium and calpain activation are required for NDCM-induced catastrophic axon degeneration

A, Conditioned media degeneration paradigm. WT sympathetic neurons were globally deprived of NGF for 6 hours or 12 hours followed by addition of conditioned media to the axons for 5 hours. NGF deprivation conditioned media (NDCM) was collected from degenerated axons after 24 hours of NGF deprivation. ***B, C***, Representative images (***B***) and quantification (***C***) of β3-tubulin immuno-stained distal sympathetic axons after treatment with Control CM and NDCM for 5 hours in the presence and absence of NGF, Chelex beads and EGTA (6mM). *n*=4 or more for each group. For each repeat, at least 100 axons were scored for degeneration. Compared to Control CM, *p*=0.0212 for -NGF 6hrs, NDCM; *p*<0.0001 for -NGF 12hrs, NDCM; *p*=0.0021 for -NGF 12hrs, Chelex, NDCM. Compared to -NGF 12hrs, NDCM, *p*=0.0002 for -NGF 12hrs, Chelex, NDCM; *p*<0.0001 for -NGF 12hrs, EGTA, NDCM, two-way ANOVA with Sidak's multiple comparisons test. ***D, E***, Representative images (***D***) and quantification (***E***) of β3-tubulin immunostained distal sympathetic axons after 24 and 48 hours of NGF deprivation in media with calcium (DMEM) and calcium free media. Axons were cultured in regular media (DMEM) and then switched to calcium free media at the time of NGF deprivation. *n*=3 for each group. For each repeat, at least 100 axons were scored for degeneration. *p*<0.0001 for 24 hours, *p*=0.4766 for 48 hours, two-way ANOVA with Sidak's multiple comparisons test. ***F, G***, Representative images (***F***) and quantification (***G***) of β3-tubulin immunostained distal sympathetic axons after treatment with NDCM for 5 hours in the presence of DMSO, 50μM Z-VAD-FMK, and 20μM Calpain inhibitor III, respectively. All cultures were globally deprived of NGF for 12 hours prior to NDCM incubation. Compared to DMSO (*n*=7), *p*=0.5328, *n*=9 for Z-VAD-FMK; *p*=0.0080, *n*=8 for Calpain inhibitor III, one-way ANOVA with Dunnett's multiple comparisons test. Data are reported as mean±SEM, n.s.=not significant, *p<0.05, **p<0.001, ***p<0.0001. Scale bar = 50 μm.

Extracellular calcium and calpain activation are required for entry into the catastrophic phase of degeneration

Small pro-degenerative molecules may be released to extracellular space and re-enter axoplasma via membrane rupture to promote degeneration. If sustained elevation of intracellular calcium is required for axons to trigger catastrophic degeneration, we would expect that blocking the pro-degenerative positive feedback step by depleting extracellular calcium would delay catastrophic degeneration. To this end we performed trophic deprivation using calcium free DMEM. NGF deprived wild-type axons maintained in DMEM with 1.85mM calcium, showed classic degenerative hallmarks like beading, blebbing and fragmentation by 24 hours (Fig.4*D*). Remarkably, when neurons were grown in calcium free media, their rate of degeneration slowed. After 24 hours of NGF deprivation only 38% of axons were degenerated in calcium free media, however maximal degeneration was observed 48 hours after NGF deprivation (Fig.4*D,E*). Moreover, both chelex resin which sequesters all divalent cations and EGTA which depletes calcium from NDCM suppressed the ability of NDCM to promote degeneration in recipient axons (Fig.4*B,C*). Thus, extracellular calcium is required to promote catastrophic degeneration in trophically deprived sympathetic axons. This is consistent with observations in trophically deprived sensory neurons and enucleated sympathetic neurons (George et al., 1995; Johnstone et al., 2019).

To explore the downstream effector of calcium influx during developmental axon degeneration, we applied NDCM to recipient axons in the presence of calpain inhibitor III or Z-VAD-FMK. Interestingly, after 5 hours of incubation, only 21.6±5.0% of axons were degenerated in cultures treated with calpain inhibitor III, significantly less than the DMSO group (66.6±13.3%), while axons bathed in Z-VAD-FMK displayed 79.7±9.6% of degeneration (Fig.4*F,G*). These results indicate

that calpain, instead of caspase, acts downstream of spheroid rupture and sustained calcium influx to promote catastrophic degeneration.

p75NTR but not DR6 regulates the timing of spheroid formation and axoplasmic content expulsion to the extracellular space

Based on the above results, we have identified three events prior to catastrophic axon degeneration: 1. An intra-axonal calcium increase; 2. Calcium independent spheroid formation and membrane rupture; and 3. Triggering of catastrophic degeneration by NDCM. What are the pathways upstream and downstream of these events? To address this we examined the role of two TNFR family members, DR6 and p75NTR, which we and others have implicated in axon degeneration following trophic withdrawal (Gamage et al., 2017; Olsen et al., 2014; Park et al., 2010; Twohig et al., 2011).

We first examined whether p75NTR or DR6 act upstream of spheroid formation and membrane rupture. To this end, we performed intra-axonal calcium imaging in NGF deprived *DR6*$^{-/-}$ and *p75NTR*$^{-/-}$ sympathetic axons. Both wild-type and *DR6*$^{-/-}$ axons displayed up to a 5 fold increase of spheroidal calcium levels, however, *p75NTR*$^{-/-}$ sympathetic axons did not display a significant increase in spheroidal calcium even after 20 hours and 30 minutes of NGF deprivation (Fig.5*A,B*). We next examined the role of p75NTR and DR6 in the accumulation of spheroids and the change in their size as a function of time after NGF deprivation. 18 hours after NGF deprivation, wild-type and *DR6*$^{-/-}$neurons display 12.0±1.0 and 6.1±0.7 spheroids per 100µm of axons, respectively (Fig.5*A,D*). However, *p75NTR*$^{-/-}$neurons displayed an approximately 2 hour delay in spheroid formation (Fig.5*D*), which is consistent with delayed onset of catastrophic degeneration (Gamage et al., 2017). We also observed that loss of *DR6* displayed a roughly 800% increase in spheroid size after trophic deprivation similar to wild-type controls, whereas *p75NTR*$^{-/-}$ neurons displayed a delayed accumulation of spheroids with a total size increase of less than 300% (Fig.5*C*). If spheroid formation is a prerequisite for membrane rupture, NGF deprived neurons isolated from *p75NTR*$^{-/-}$ mice would show diminished extracellular calcium expulsion whereas *DR6*$^{-/-}$ would

display normal calcium release, a surrogate for membrane rupture. Indeed, *p75NTR*$^{-/-}$ axons showed no difference in extracellular calcium levels before or after 18 hours of NGF deprivation, while *DR6*$^{-/-}$ neurons displayed a modest but significant increase (Fig.5*E*). We next examined whether NGF deprived conditioned media from *p75NTR*$^{-/-}$ or *DR6*$^{-/-}$ neurons was capable of inducing degeneration of WT axons (Fig.5*G*). Consistent with calcium release phenotypes, we found that NDCM derived from *p75NTR*$^{-/-}$ axons was incapable of inducing degeneration in WT axons (Fig.5*H,I*). In contrast, NDCM from *DR6*$^{-/-}$neurons contains prodegenerative activity (Fig.5*H,I*). Taken together, these data suggest that p75NTR but not DR6 is upstream of spheroid formation and membrane rupture.

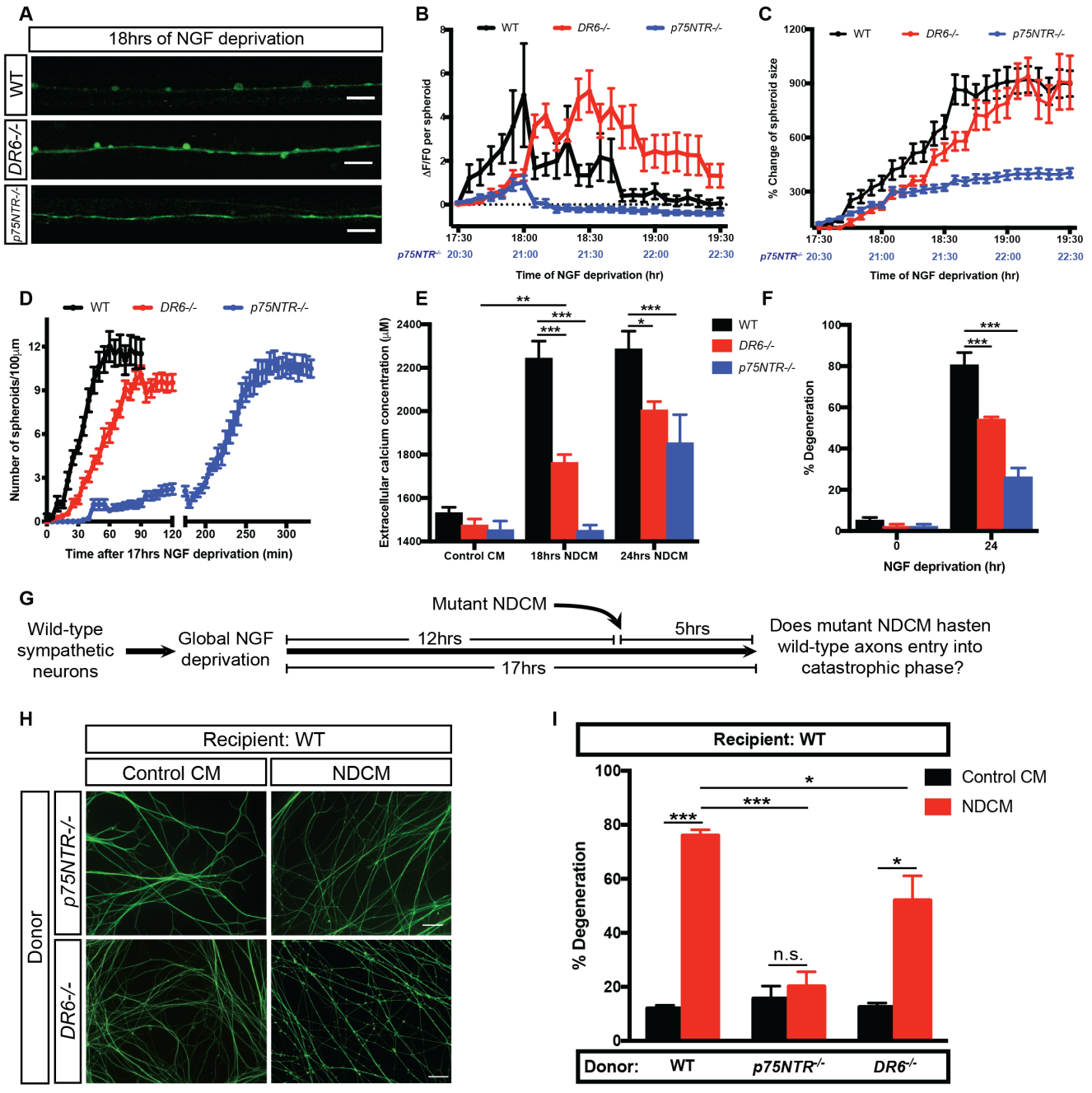

Figure 5: Depletion of p75NTR delays formation of spheroids and prodegenerative molecules exclusion after NGF deprivation

A, Fluo4-AM calcium imaging of wild-type, *DR6*$^{-/-}$ and *p75NTR*$^{-/-}$ sympathetic axons 18 hours of NGF deprivation. Scale bar = 10μm. ***B, C***, Spheroidal calcium fluorescence (***B***) and size change

(***C***) of wild-type, *DR6*$^{-/-}$ and *p75NTR*$^{-/-}$ sympathetic axons after indicated time of NGF deprivation. Black horizontal dotted line in (***B***) indicates the baseline without any calcium change. Lower x-axis labeled with blue correlates with time of NGF deprivation in *p75NTR*$^{-/-}$ sympathetic axons. Individual axonal spheroids were quantified: *n*=32 (wild-type), *n*=30 (*DR6*$^{-/-}$), and *n*=22 (*p75NTR*$^{-/-}$) spheroids from cultured neurons harvested from 3 independent litters. ***D***, Quantification of axonal spheroid number per 100μm of wild-type, *DR6*$^{-/-}$ and *p75NTR*$^{-/-}$ sympathetic axon at the indicated times after 17 hours of NGF deprivation. Individual axonal spheroids were counted: *n*=20 (wild-type), *n*=29 ((*DR6*$^{-/-}$), and *n*=22 (*p75NTR*$^{-/-}$) axons from cultured neurons harvested from 3 independent litters. ***E***, Measurement of extracellular calcium concentration of +NGF (Control CM), 18 hours and 24 hours NGF deprived conditioned media (NDCM) collected from wild-type, *DR6*$^{-/-}$and *p75NTR*$^{-/-}$ sympathetic axons. *n*=4 or more for each group. Compared to WT, 18hrs NDCM, $p<0.0001$ for *DR6*$^{-/-}$, 18hrs NDCM; $p<0.0001$ for *p75NTR*$^{-/-}$, 18hrs NDCM. Compared to WT, 24hrs NDCM, $p=0.0026$ for *DR6*$^{-/-}$, 24hrs NDCM; $p<0.0001$ for *p75NTR*$^{-/-}$, 24hrs NDCM. Compared to *DR6*$^{-/-}$, Control CM, $p=0.0045$ for *DR6*$^{-/-}$, 18hrs NDCM, two-way ANOVA with Dunnett's multiple comparisons test. ***F***, Quantification of degeneration of wild-type, *DR6*$^{-/-}$ and *p75NTR*$^{-/-}$ sympathetic axons with or without 24 hours of NGF deprivation. *n*=3 or more for each group. For each repeat, at least 100 axons were scored for degeneration. Compared to WT, 24hrs, $p<0.0001$ for *DR6*$^{-/-}$, 24hrs; $p<0.0001$ for *p75NTR*$^{-/-}$, 24hrs, two-way ANOVA with Dunnett's multiple comparisons test. ***G***. Catastrophic axon degeneration paradigm to test the pro-degenerative effect of mutant NDCM. Wild-type sympathetic neurons were globally deprived of NGF for 12 hours followed by addition of conditioned media derived from mutant axons for 5 hours. Mutant NDCM was collected from degenerating *p75NTR*$^{-/-}$ or *DR6*$^{-/-}$ axons 24 hours after NGF deprivation. ***H, I***, Representative images (***H***) and quantification (***I***) of wild-type distal sympathetic axons immunostained for β3-tubulin after treatment with Control CM and NDCM collected from *p75NTR*$^{-/-}$ and *DR6*$^{-/-}$ axons for 5 hours. Scale bar = 50 μm. Left two columns represent percentages of degeneration of wild-type sympathetic axons treated with wild-type

NDCM and Control CM, respectively. Compared to WT, NDCM (n=10), p<0.0001, n=7 for *p75NTR*$^{-/-}$, NDCM; p=0.0010, n=7 for *DR6*$^{-/-}$, NDCM, two-way ANOVA with Dunnett's multiple comparisons test. Compared to Control CM, p<0.0001 for WT, NDCM; p=0.8980 for *p75NTR*$^{-/-}$, NDCM; p=0.0014 *DR6*$^{-/-}$, NDCM, two-way ANOVA with Sidak's multiple comparisons test. Data are reported as mean±SEM, n.s.=not significant, *p<0.05, **p<0.001, ***p<0.0001.

p75NTR-Rho signaling is necessary and sufficient for spheroid formation and entry into catastrophic phase

How does p75NTR regulate spheroid formation prior to the catastrophic phase of degeneration? Previous work has shown that neurotrophins regulate growth cone dynamics by suppressing RhoA activation that occurs through p75NTR signaling (Gehler et al., 2004). p75NTR promotes RhoA activation to mediate sympathetic axonal degeneration in response to degenerative triggers like myelin (Park et al., 2010; Yamashita and Tohyama, 2003). The major downstream target of Rho activation is actin remodeling. We observed actin and β3-tubulin enrichment in axonal spheroids (Fig.6*A*), similar to previous observations (Beirowski et al., 2010). Active Rho in axonal spheroids was detected by incubation with GST-rhotekin Rho binding domain (RBD) fusion protein after 18 hours of NGF deprivation but not in cultures treated with Rho inhibitor C3 transferase (CT04) (Fig.6*B*). Moreover, inhibiting Rho family members using CT04 (1µg/mL, 2 hours prior to 17 hours NGF deprivation) prevented spheroid formation in wild-type axons (Fig.6*C,D*). We next tested whether actin remodeling is required for spheroid formation. Indeed, the actin polymerization inhibitor cytochalasin D (10µg/mL) inhibited spheroid formation (Fig.6*C,D*). Consistent with this, axons treated with CT04 or cytochalasin D delayed degeneration for up to 24 hours after NGF deprivation (Fig.6*E,F*). Taken together, these data suggest that activation of Rho and actin remodeling is necessary for spheroid formation and entry into the catastrophic phase of degeneration. Another downstream effector of Rho is the Rho-associated protein kinase 1 (ROCK1). During apoptosis, ROCK1 has been shown to be cleaved by caspase-3, resulting in constitutive kinase activity to promote phosphorylation of myosin light chain (MLC) and membrane blebbing (Coleman et al., 2001; Sebbagh et al., 2001). This may explain our finding of suppressed spheroid formation after NGF deprivation in the presence of caspase inhibitor (Fig.2*A,B*).

If Rho is downstream of p75NTR, ectopic activation of Rho would promote spheroid formation and axon degeneration in the absence of *p75NTR*. To test this, we incubated NGF deprived *p75NTR*$^{-/-}$ axons with Rho activator, CN03 (1µg/mL, 2 hours prior to 17 hours NGF deprivation). CN03 rescued the diminished spheroid formation and extracellular calcium release through membrane rupture in *p75NTR*$^{-/-}$ axons 18 hours after NGF deprivation (Fig.6*G-I*). We also found that CN03 could rescue the timing of degeneration in the absence of *p75NTR* (NGF deprived for 12 hours with CN03 for the final 5 hours) (Fig.6*J,K*). Taken together these data suggest that p75NTR-Rho signaling is necessary and sufficient to promote spheroid formation and entry into the catastrophic phase of degeneration.

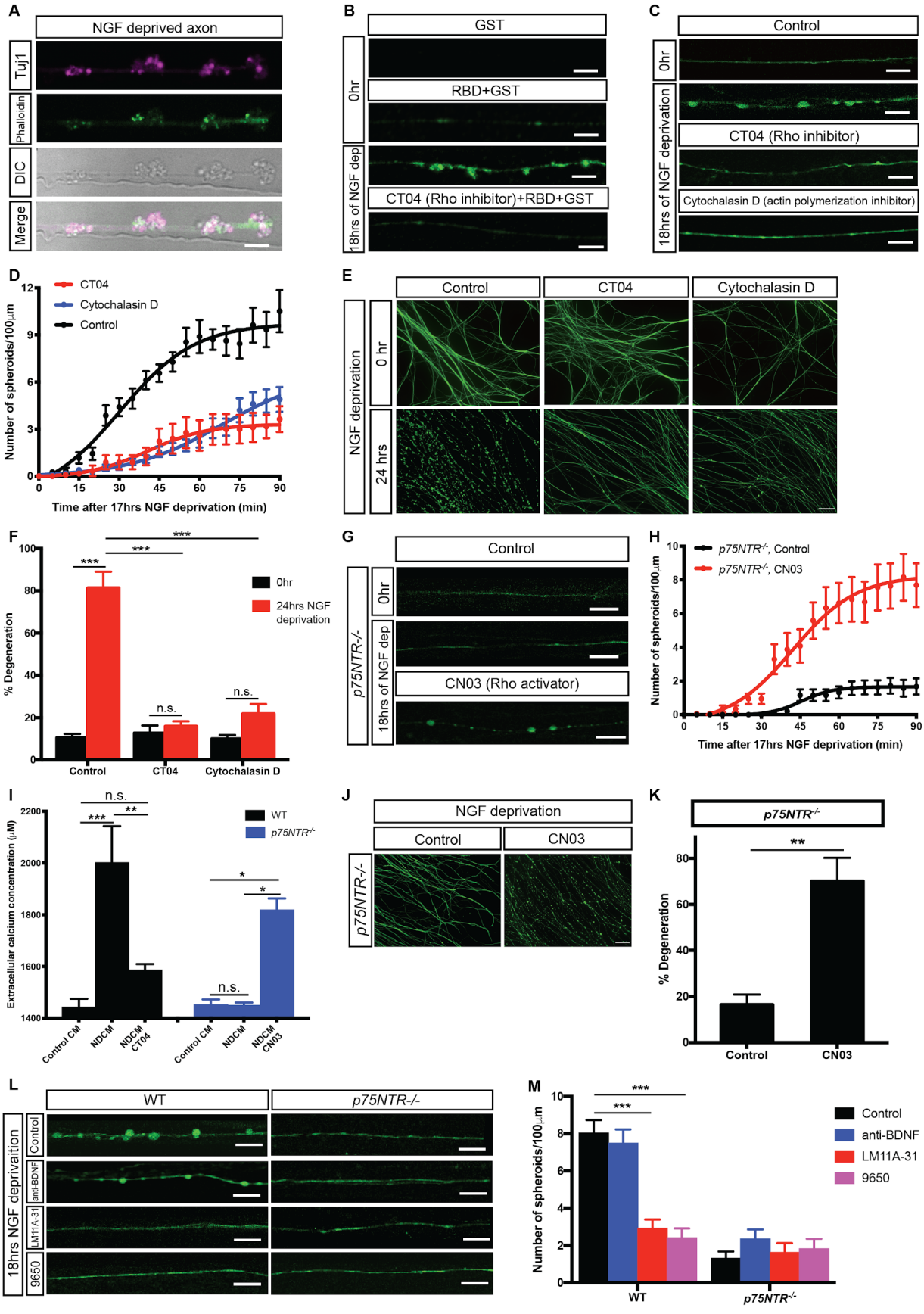
A
NGF deprived axon
Tuj1
Phalloidin
DIC
Merge
B
GST
0hr
RBD+GST
18hrs of NGF dep
CT04 (Rho inhibitor)+RBD+GST
C
Control
0hr
18hrs of NGF deprivation
CT04 (Rho inhibitor)
Cytochalasin D (actin polymerization inhibitor)
D
CT04
Cytochalasin D
Control
Number of spheroids/100μm
Time after 17hrs NGF deprivation (min)
E
Control
CT04
Cytochalasin D
NGF deprivation
0 hr
24 hrs
F
0hr
24hrs NGF deprivation
% Degeneration
Control
CT04
Cytochalasin D
n.s.
G
Control
p75NTR-/-
0hr
18hrs of NGF dep
CN03 (Rho activator)
H
p75NTR-/-, Control
p75NTR-/-, CN03
Number of spheroids/100μm
Time after 17hrs NGF deprivation (min)
I
WT
p75NTR-/-
Extracellular calcium concentration (μM)
Control CM
NDCM
NDCM CT04
NDCM CN03
n.s.
J
NGF deprivation
Control
CN03
p75NTR-/-
K
p75NTR-/-
% Degeneration
Control
CN03
L
WT
p75NTR-/-
18hrs NGF deprivaition
Control
anti-BDNF
LM11A-31
9650
M
Number of spheroids/100μm
Control
anti-BDNF
LM11A-31
9650
WT
p75NTR-/-

Figure 6: p75NTR-Rho signaling is required for axonal spheroid formation

A, Representative axons/spheroids visualized for β3-tubulin (Tuj1), Phalloidin and DIC after 18 hours of NGF deprivation. Scale bar = 5 μm. ***B***, Representative images of wild-type sympathetic axons immunostained for GST tag with or without NGF deprivation. All images except the first one show axons incubated with Rhotekin-RBD GST-fusion protein that binds active Rho proteins after fixation. Axon in the bottom image was NGF deprived and treated with 1μg/mL Rho inhibitor CT04 for 3 hours. Scale bar = 5 μm. ***C***, Fluo4-AM calcium imaging of wild-type sympathetic axons with or without drug treatment. For the "CT04" group, wild-type axons were incubated in SCG media containing 1μg/mL Rho inhibitor CT04, for 2 hours prior to 17 hours of NGF deprivation. For the "Cytochalasin D" group, wild-type axons were incubated in SCG media containing 10μg/mL actin polymerization inhibitor for 2 hours prior to 17 hours of NGF deprivation. Scale bar = 10μm. ***D***, Quantification of axonal spheroid number per 100μm of wild-type sympathetic axons at indicated time points after 17 hours of NGF deprivation in the absence and presence of CT04 or Cytochalasin D. Total number of n=9 (Control), n=8 (CT04), n=22 (Cytochalasin D) axons from cultured neurons harvested from 3 independent litters were quantified. Nonlinear regression curves were drawn according to Hill equation. ***E, F***, Representative images (***E***) and quantification (***F***) of wild-type distal sympathetic axons immuno-stained for β3-tubulin in the absence and presence of CT04 or Cytochalasin D. Scale bar = 50μm. Compared to 0hr, p<0.0001, n=3 for Control, 24hrs; p=0.9256, n=7 for CT04, 24hrs; p=0.1058, n=6 for Cytochalasin D, 24hrs, two-way ANOVA with Sidak's multiple comparisons test. Compared to Control, 24hrs, p<0.0001 for CT04, 24hrs; p<0.0001 for Cytochalasin D, 24hrs, two-way ANOVA with Dunnett's multiple comparisons test. ***G***, Fluo4-AM calcium imaging of *p75NTR*$^{-/-}$ sympathetic axons grown in the presence or absence of NGF with or without CN03 treatment. For "CN03" group, *p75NTR*$^{-/-}$ axons were incubated in SCG media containing 1μg/mL Rho activator CN03 for 2 hours before 17 hours of NGF deprivation. Scale bar = 10μm. ***H***, Quantification of number of spheroids per 100μm of *p75NTR*$^{-/-}$ sympathetic axons at indicated time points after 17 hours of NGF deprivation in the

absence and presence of CN03. Individual axons were counted: *n*=16 (*p75NTR*$^{-/-}$, Control) and *n*=12 (*p75NTR*$^{-/-}$, CN03) axons from 3 independent replicates. Nonlinear regression curves were drawn according to Hill equation. ***I***, Measurement of extracellular calcium concentration of untreated and NGF deprived conditioned media in the presence and absence of CT04 or CN03 collected from wild-type (black) and *p75NTR*$^{-/-}$ (blue) sympathetic axons. Compared to WT, Control CM (*n*=4),*p*<0.0001, *n*=4 for WT, NDCM; *p*=0.4701, *n*=6 for WT, NDCM CT04. Compared to WT NDCM, *p*=0.0004 for WT, NDCM CT04. Compared to *p75NTR*$^{-/-}$, Control CM (*n*=4), *p*>0.9999, *n*=5 for *p75NTR*$^{-/-}$, NDCM; *p*=0.0088, *n*=3 for *p75NTR*$^{-/-}$, NDCM CN03. Compared to *p75NTR*$^{-/-}$, NDCM, *p*=0.0055 for *p75NTR*$^{-/-}$, NDCM CN03, one-way ANOVA with Tukey's multiple comparisons test. ***J, K***, Representative images (***J***) and quantification (***K***) of *p75NTR*$^{-/-}$ distal sympathetic axons immuno-stained for β3-tubulin after treatment with or without CN03 for 5 hours. All cell cultures were pre-treated with 12 hours of NGF deprivation. Scale bar = 50μm. *p*=0.0006, *n*=3 for CN03 and *n*=7 for control, unpaired t test. ***L, M***, Fluo4-AM calcium imaging (***L***) and spheroid number per 100μm of wild-type and *p75NTR*$^{-/-}$sympathetic axons (***M***) after 18 hours of NGF deprivation in the absence and presence of 20μg/mL anti-BDNF, 2ng/mL p75NTR ligand/functional blocker LM11A-31, or 9650 immune serum (1:100). Scale bar = 10μm. Individual axons were counted: *n*=15 (WT, Control), *n*=16 (WT, anti-BDNF), *n*=37 (WT, LM11A-31), *n*=22 (WT, 9650), *n*=16 (*p75NTR*$^{-/-}$, Control), *n*=19 (*p75NTR*$^{-/-}$, anti-BDNF), *n*=18 (*p75NTR*$^{-/-}$, LM11A-31), and *n*=16 (*p75NTR*$^{-/-}$, 9650) axons from 3 independent replicates. Significance is determined by two-way ANOVA with Dunnett's multiple comparisons test. Data are reported as mean±SEM, n.s.=not significant, *p<0.05, **p<0.001, ***p<0.0001.

p75NTR dependent spheroid formation is ligand dependent

We next sought to determine whether p75NTR requires ligand to induce spheroid formation. Application of LM11A-31, a small nonpeptide p75NTR modulator (Massa et al., 2006; Simmons et al., 2014), suppressed spheroid formation on wild-type sympathetic axons after NGF deprivation (Fig.6*L,M*). Since there have been conflicting reports about whether LM11A-31 specifically blocks ligand binding (Massa et al., 2006; Xie et al., 2019), we also used the ligand-blocking antibody 9650 specific for p75NTR extracellular domain (Kraemer et al., 2014). Compared to control serum, 9650 significantly inhibited spheroid formation on wild-type sympathetic axons after NGF deprivation, and did not show additive effect on *p75NTR*$^{-/-}$ axons (Fig.6*L,M*). However, blocking brain-derived neurotrophic factor (BDNF), which has been shown to activate p75NTR apoptotic signaling (Kohn et al., 1999), failed to inhibit development of spheroids on NGF deprived axons (Fig.6*L,M*). These results suggest that p75NTR mediated spheroid formation can be activated by binding pro-degenerative ligands other than BDNF.

DR6, but not p75NTR, gates entry into the catastrophic phase of degeneration in response to NDCM

We next asked whether DR6 or p75NTR are downstream of the prodegenerative activity of NDCM using the paradigm described in Fig.4*A*. We applied NDCM collected from wild-type axons to recipient neurons derived from *DR6*$^{-/-}$ and *p75NTR*$^{-/-}$ mice. After a 5 hour treatment of NDCM, *p75NTR*$^{-/-}$ axons showed 71.6±5.8% degeneration, while *DR6*$^{-/-}$axons displayed minimal degeneration (Fig.7*A,B*). These data suggest that DR6 but not p75NTR is downstream of the prodegenerative effects of NDCM.

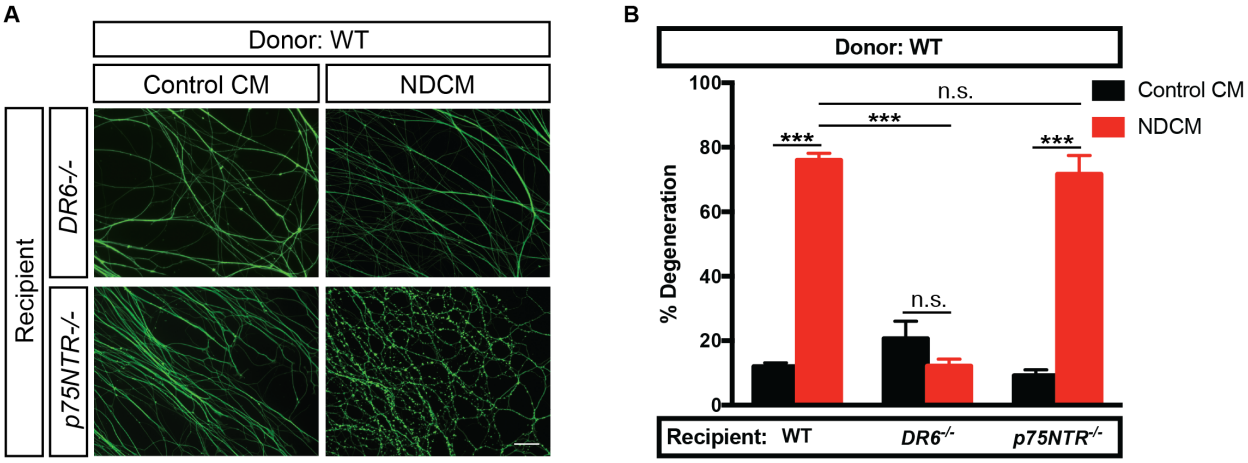

Figure 7: DR6 is required for catastrophic degeneration induced by NDCM

A, B, Representative images (***A***) and quantification (***B***) of distal sympathetic axons from *DR6*$^{-/-}$ and *p75NTR*$^{-/-}$ animals immuno-stained for β3-tubulin after treatment with NDCM and Control CM collected from wild-type neurons for 5 hours, respectively. All cultures were NGF deprived for 12 hours prior to the addition of CM. Left two columns represent percentages of degeneration of wild-type sympathetic axons treated with wild-type NDCM and Control CM, respectively. Compared to NDCM, $p<0.0001$, $n=10$ for WT, Control CM; $p=0.5437$, $n=3$ for *DR6*$^{-/-}$, Control CM; $p<0.0001$, $n=7$ for *p75NTR*$^{-/-}$, Control CM, two-way ANOVA with Sidak's multiple comparisons test. Compared to WT, NDCM ($n=10$), $p<0.0001$, $n=9$ for *DR6*$^{-/-}$, NDCM; $p=0.5422$, $n=11$ for *p75NTR*$^{-}$

$^{-/-}$, NDCM, two-way ANOVA with Dunnett's multiple comparisons test. Data are reported as mean±SEM, n.s.=not significant, ***p<0.0001. Scale bar = 50 μm.

Discussion

By investigating calcium dynamics during the transition from latent to catastrophic phases of degeneration after trophic withdrawal, we identified several novel events: **1.** Intra-axonal calcium rise and spheroid formation between latent and catastrophic phases of degeneration. This spheroid formation is triggered by p75NTR-Rho signaling, caspase activation and actin remodeling. The timing of p75NTR-Rho-actin signaling and upregulation of pro-degenerative transcriptional programs may define the duration of the latency phase. **2.** The membranes of growing spheroids rupture, leading to expulsion of axoplasmic material to the extracellular environment. This may represent a novel mechanism by which pro-degenerative molecules are released to influence neighboring cells. **3.** The material expelled from ruptured spheroids triggers catastrophic degeneration. DR6 is required for responding to this prodegenerative signal thereby gating entry into the catastrophic phase of degeneration (Fig.8).

Formation of axonal spheroids has been reported in many neurological disorders, including Alzheimer's disease, ALS, and neurocysticercosis (Beirowski et al., 2010; Griffin and Watson, 1988; Mejia Maza et al., 2018). After injury or oxidative stress, spheroids arise along the length of axons with accumulation of cytoskeleton degradation products and calcium overload (Beirowski et al., 2010); (Barsukova et al., 2012). While spheroids have been extensively described in the literature, whether they have a function in promoting degeneration has remained unknown. We propose that the function of these spheroids is to trigger catastrophic degeneration by releasing pro-degenerative molecules into the extracellular environment. Here, we report localized annexin V positivity (i.e. PS flipping) (Fig.2*C*), which suggests that they are marked for phagocytic engulfment reminiscent of apoptotic bodies (Ravichandran, 2010; Segawa et al., 2014). Indeed, we observed several instances of spheroids detaching from the axon, which is a unit that

presumably would be phagocytosed (Movie 4). Importantly, the exposure of PS on the outer leaflet of the spheroid membrane but not the axon shaft indicates that spheroids might be 'hot-spots' on degenerating axons to recruit nearby glia or macrophages, clearing damaged components. In correlation with the growth of spheroids, we also observe 3 kDa and 10 kDa fluorescent dextran entering the cytosol, consistent with disrupted or ruptured plasma membrane (Fig.3*B-D*). It is unclear where membrane integrity is disrupted; it may be at the belly of the spheroid and/or at axon/spheroid junctions. Whether or not spheroid rupture also occurs in aforementioned neurodegenerative disorders remains an open question.

What signaling pathways are upstream of spheroidal rupture? We found that disrupting caspase activation, p75NTR, Rho or actin polymerization delays spheroid formation after NGF deprivation (Fig.2*A,B*; Fig.6*C,D*). The intracellular domain (ICD) of p75NTR has been shown to modulate RhoA activation by interacting with Rho GDP-dissociation inhibitor (RhoGDI) to inhibit axonal outgrowth and promote axon pruning (Park et al., 2010; Yamashita et al., 1999, 2002). In the presence of NGF, the interaction of p75NTR with RhoGDI-RhoA complex is disrupted, leading to RhoA inactivation and neurite outgrowth (Mathew et al., 2009). Consistent with these findings, we show that activation of RhoA in the absence of *p75NTR* promotes entry into catastrophic phase by triggering spheroid formation (Fig.6*G-K*). Proneurotrophin activation of p75NTR in the absence of Trk signaling leads to caspase mediated neuronal death(Gentry et al., 2004; Troy et al., 2002). Sublethal executioner caspase activity plays an important role in nervous system development (Unsain and Barker, 2015). Interestingly, inhibition of caspases suppressed spheroid formation, but failed to protect axons from NDCM induced catastrophic degeneration (Fig.4*F,G*). Thus, in the absence of NGF, spheroid formation is induced by p75NTR, caspase, RhoA and actin remodeling, which are all requisite for transitioning from latent to catastrophic degeneration.

Our findings are consistent with the notion that p75NTR controls the window of latency prior to catastrophic degeneration. What is the molecular basis for the putative timer controlling the window of latency after trophic withdrawal? Classically, biological timers have been associated with transcriptional programs that form feedback loops (Mitrophanov and Groisman, 2008; Santos and Ferrell, 2008). Inhibition of transcription by applying actinomycin D to the soma during NGF deprivation blocked spheroid formation and degeneration (Fig.2*A,B*), indicating the involvement of a degenerative transcriptional program. This pathway has been shown to up-regulate TNFα-converting enzyme (TACE), which is necessary for p75NTR cleavage (Kenchappa et al., 2010). Liberation of the p75NTR ICD retrograde degenerative signal is accompanied by secondary activation of JNK and up-regulation of proapoptotic factors like p53-upregulated modulator of apoptosis (Puma) (Kenchappa et al., 2010; Pathak et al., 2018; Simon et al., 2016). The time it takes to engage this transcriptional program and cleave p75NTR by TACE and γ-secretase may represent a molecular timer governing the duration of the latency window (Pathak and Carter, 2017). This molecular timer may account for the delay of spheroid formation in NGF deprived *p75NTR*$^{-/-}$ axons (Fig.5*D*).

What signaling pathways are downstream of spheroidal rupture? Similar to p75NTR, DR6 is required for axon degeneration after trophic withdrawal (Gamage et al., 2017; Olsen et al., 2014). Does DR6 regulate the same signaling events as p75NTR after trophic factor deprivation? We conclude that this is unlikely given that these TNFR family members govern distinct phases of degeneration. Unlike *p75NTR*$^{-/-}$, *DR6*$^{-/-}$ axons are capable of expelling prodegenerative axoplasmic materials to the surrounding environment via membrane rupture after NGF deprivation (Fig.5*H,I*). *DR6*$^{-/-}$ axons are protected from entry into catastrophic phase in response to a 5 hour incubation of NDCM (Fig.7*A,B*). These findings suggest that DR6 is downstream of spheroidal rupture and the destructive factor(s) found in NDCM, however whether there is a direct or indirect interaction between these factors and DR6 remains to be determined. DR6 was

previously shown to interact with β-amyloid precursor protein (APP) to regulate developmental axonal pruning and synapse restriction (Kallop et al., 2014; Nikolaev et al., 2009). Given the fact that depletion of APP could partially protect sensory axons from degeneration after NGF withdrawal (Olsen et al., 2014), it's possible that DR6 promotes developmental catastrophic degeneration via an APP dependent pathway. Previous findings show that DR6 potently activates NF-κB and JNK to induce apoptosis (Benschop et al., 2009; Hu et al., 2014). Consistent with this, loss of *DR6* suppressed phosphorylation of JNK after injury (Gamage et al., 2017). Thus, we speculate that direct or indirect activation of DR6 by the prodegenerative factor emanating from ruptured spheroids may promote the activation of JNK and calpain, which are known to trigger catastrophic degeneration (Fig.8). It is also possible that activation of DR6 independently activates catastrophic degeneration by engagement of receptor mediated caspase pathways.

While the calcium dependent protease, calpain, is known to be required for catastrophic degeneration (Fig.4*F,G*), it is unclear why the initial intracellular wave of calcium prior to catastrophic degeneration is insufficient to trigger this event. One clue may come from Tessier Lavigne and colleagues who suggest that depletion of the calpain inhibitor, calpastatin, is required for catastrophic degeneration (Yang et al., 2013). The membrane ruptures that we observe at the onset of catastrophic degeneration is likely to cause equilibration of external and internal calcium concentrations. Post-rupture, intraxonal calcium levels are likely to be persistently high. However, depletion of calpastatin is likely a prerequisite for calcium dependent catastrophic degeneration. Recent studies show that chelation of extracellular calcium by EGTA in late but not early phases of degeneration rescues axons from trophic deprivation induced degeneration (Johnstone et al., 2019). Additionally, the transient receptor potential vanilloid family member 1 (TRPV1) cation channel is required for calcium influx to promote developmental sensory axon degeneration, while plasma membrane nanoruptures allow entry of extracellular calcium to drive axon degeneration in multiple sclerosis (Johnstone et al., 2019; Witte et al., 2019). Thus, extracellular calcium may

enter the axoplasma via calcium channels like TRPV1 or spheroidal ruptures. Both routes of sustained intracellular calcium elevation converge on calpain to trigger catastrophic degeneration.

In summary, our data reveal novel signaling emanating from two different death receptors to govern latent and catastrophic phases of degeneration. After NGF deprivation, prodegenerative transcription, caspase activation and p75NTR-Rho dependent actin remodeling promote formation of axonal spheroids. Axoplasmic materials containing prodegenerative molecules like calcium are then released to the extracellular space via membrane rupture, which may act as a positive feedback loop to hasten the entry of axons into catastrophic phase degeneration. Entry into the catastrophic phase of degeneration appears to be gated by DR6 (Fig.8). Whether or not this represents a mechanism whereby axons might coordinate their degeneration requires further study. Nevertheless, the notion of destructive spheroids and subsequent inter-axonal communication during degeneration facilitates our understanding of neural refinement during development and presents intriguing possibilities with respect to therapeutic intervention to alleviate bystander degeneration in disease.

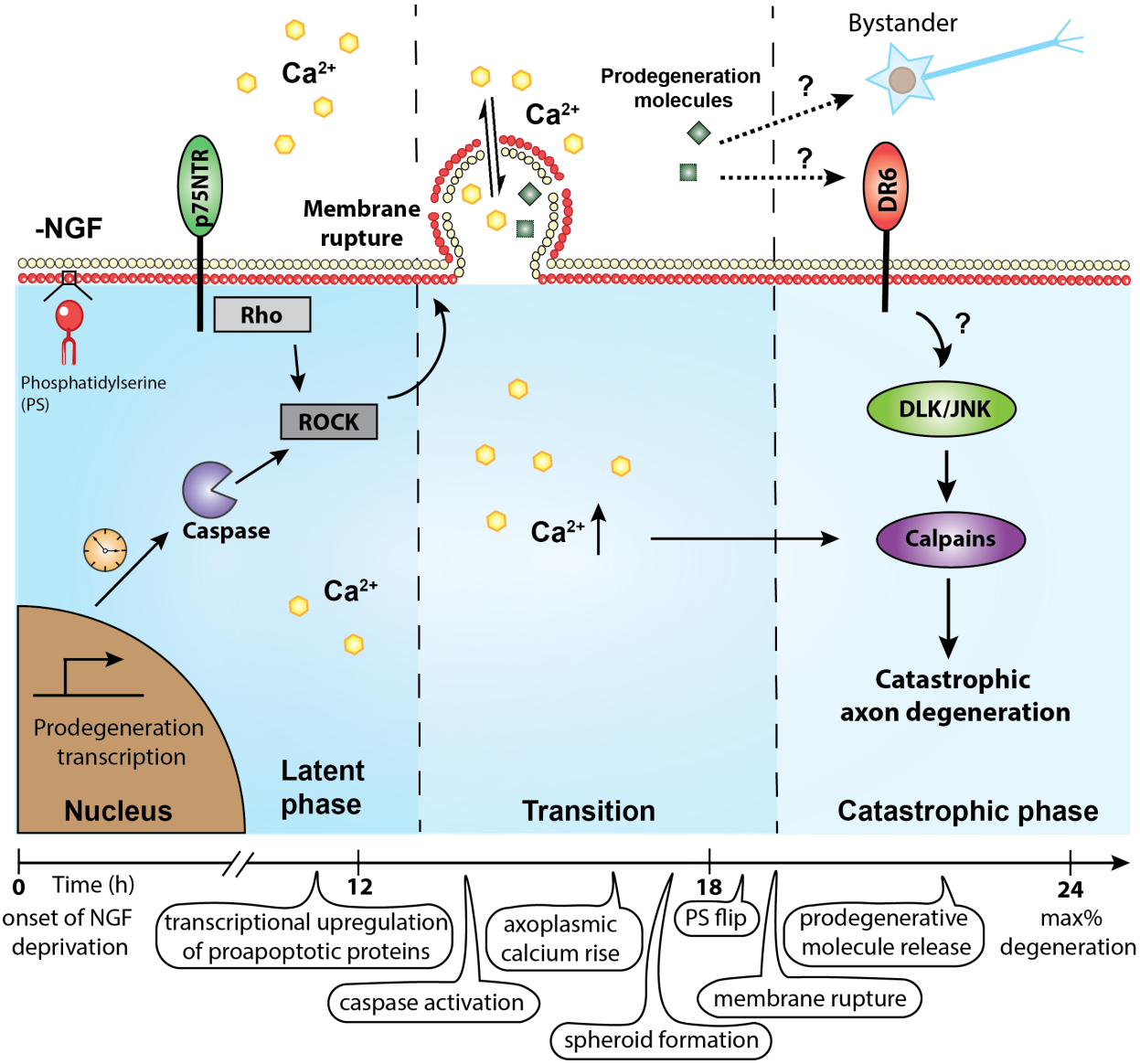

Figure 8: Time course of events associated with NGF-deprivation induced axon degeneration of sympathetic neurons.

After NGF deprivation, prodegenerative transcription is upregulated. Axoplasmic calcium is increased and enriched in spheroids prior to catastrophic phase. Spheroid formation is regulated by p75NTR, Rho activity, and caspase activation. The calcium electrochemical gradient across the membrane is disrupted by spheroidal rupture, which may also lead to the release of intra-axonal prodegenerative molecules to extracellular space, acting as extrinsic factors to promote degeneration in a paracrine or autocrine manner. We speculate that p75NTR plays an important

role in calcium dynamics during the latent phase, while DR6 can be activated by prodegenerative NDCM to mediate downstream catastrophic degeneration pathways (e.g. DLK/JNK, calpastatin, calpain).

Chapter 3[3]

Regulation of degenerative spheroids after injury

Authors

Yu Yong[1], Kanchana Gamage[2], Courtny Cushman[3], Anthony Spano[1], Christopher Deppmann[1,3*]

Author affiliations

[1]Department of Biology, University of Virginia, Charlottesville, VA, 22903, USA

[2]Amgen, Massachusetts & Department of Stem Cell and Regenerative Biology, Harvard University, Cambridge, MA, 02138, USA

[3]Department of Neuroscience, University of Virginia, Charlottesville, VA, 22903, USA

Correspondence

*To whom correspondence should be sent:

Christopher D. Deppmann

Departments of Biology, Cell Biology, Neuroscience and Biomedical Engineering

University of Virginia

Charlottesville, VA 22904-4328

email: deppmann@virginia.edu

[3] Y. Yong *et al.,* Regulation of degenerative spheroids after injury. *Scientific Reports* (2020, *in press*).

Abstract

Neuronal injury leads to rapid, programmed disintegration of axons distal to the site of lesion. Much like other forms of axon degeneration (*e.g.* developmental pruning, toxic insult from neurodegenerative disorder), Wallerian degeneration associated with injury is preceded by spheroid formation along axons. The mechanisms by which injury leads to formation of spheroids and whether these spheroids have a functional role in degeneration remain elusive. Here, using neonatal mouse primary sympathetic neurons, we investigate the roles of players previously implicated in the progression of Wallerian degeneration in injury-induced spheroid formation. We find that intra-axonal calcium flux is accompanied by actin-Rho dependent growth of calcium rich axonal spheroids that eventually rupture, releasing material to the extracellular space prior to catastrophic axon degeneration. Importantly, after injury, *Sarm1*$^{-/-}$ and *DR6*$^{-/-}$, but not *Wld*^{S} (excess NAD^+) neurons, are capable of forming spheroids that eventually rupture, releasing their contents to the extracellular space to promote degeneration. Supplementation of exogenous NAD^+ or expressing WLD^S suppresses Rho-dependent spheroid formation and degeneration in response to injury. Moreover, injured or trophically deprived *Sarm1*$^{-/-}$ and *DR6*$^{-/-}$, but not *Wld*^{S} neurons, are resistant to degeneration induced by conditioned media collected from wild-type axons after spheroid rupture. Taken together, these findings place Rho-actin and NAD^+upstream of spheroid formation and may suggest that other mediators of degeneration, such as DR6 and SARM1, mediate post-spheroid rupture events that lead to catastrophic axon disassembly.

Introduction

Axons are the primary information conduits of the nervous system. Failure to maintain the integrity of axons is a feature of many neurological disorders. In response to injury, a process of axonal fragmentation, or Wallerian degeneration (WD) occurs, often resulting in permanent loss of neural function (Waller, 1851). Immediately after injury, the severed axon goes through a latent phase where its overall morphology remains unchanged for 1-2 hours *in vitro* and up to 48 hours *in vivo* (Beirowski et al., 2005; Wang et al., 2012). Intracellular calcium increases transiently during the latent phase, followed by a second global calcium wave just prior to axon fragmentation (Vargas et al., 2015). Elevation of intracellular calcium through L-type calcium channels and sodium-calcium exchanger (NCX), together with impaired mitochondrial motility and calcium buffering capacity, results in activation of the calpain protease and irreversible disassembly of the axon (Adalbert et al., 2012; Avery et al., 2012; George et al., 1995; Ma et al., 2013; Yang et al., 2013; Yong et al., 2019). In addition to calcium flux, severed axons display cessation of axonal transport, formation of axonal swellings called spheroids, fragmentation of neurofilaments and removal of debris by recruited phagocytes. This rapid and near synchronous axonal disintegration period is called the catastrophic/execution phase of degeneration and can also be observed in developmental and other pathological regressive contexts (Coleman, 2005; Llobet Rosell and Neukomm, 2019; Saxena and Caroni, 2007).

The field's first insight into the non-passive nature of WD signaling came from the *Wld*^{s} mouse which harbors a neomorphic gain of function mutation and displays axon degeneration that is 10 times slower after injury compared to wild-type neurons (Brown et al., 1992; Lunn et al., 1989). The *Wld*^{s} gene encodes a chimeric fusion protein, consisting of the full-length nicotinamide mononucleotide adenyltransferase 1 (NMNAT1), which synthesizes NAD^{+} from its substrate nicotinamide mononucleotide (NMN), and a fragment of the ubiquitination factor UBE4B (Conforti

et al., 2000). The perdurance of high NAD^+ levels in axons is sufficient to delay Wallerian degeneration (Sasaki et al., 2006). As such, depletion of NAD^+ is known to be an important trigger for WD and is achieved in several ways after injury: **1.** Turnover of NMNAT2 regulated by the ubiquitin proteasome system (UPS), palmitoylation of cysteines in NMNAT2 for membrane targeting and mitogen-activated protein kinase (MAPK) signaling (Gilley and Coleman, 2010; Milde et al., 2013; Summers et al., 2018; Walker et al., 2017) and **2.** Activation of sterile alpha and armadillo motif (SARM1), which has intrinsic NAD^+ cleavage activity (Essuman et al., 2017; Gerdts et al., 2015; Osterloh et al., 2012). Beyond proteins that influence NAD^+ levels, several other factors have been implicated in promoting Wallerian degeneration including death receptor 6 (DR6), calpain, Phr1 E3 ubiquitin ligase, dual leucine zipper kinase (DLK), c-jun n-terminal kinase (JNK), and axundead (Axed) (Babetto et al., 2013; Gamage et al., 2017; George et al., 1995; Larhammar et al., 2017; Murata et al., 2018; Neukomm et al., 2017; Yang et al., 2015; Zhai et al., 2003). Whether these factors all converge on similar signaling hubs such as NAD^+ remains to be determined.

Because the cytoskeleton is crucial for maintaining axon integrity, signaling pathways that promote disassembly of microtubules and actin filaments likely contribute to axon degeneration. The Rho/Rac/Cdc42 family of small G-proteins are well known for their effects on reorganization of actin, which affect cell survival, migration and vesicle trafficking (Ridley, 2001). In neurons, RhoA and its downstream effector Rho-associated protein kinase (ROCK) has been shown to regulate axon retraction, degeneration, regeneration and neural death in both developmental and pathological conditions (Koch et al., 2014; Luo and O'Leary, 2005; Stankiewicz and Linseman, 2014). Importantly, RhoA/ROCK has been shown to be activated in injured axons and its pharmacological inhibition delays degeneration (Dubreuil et al., 2003; Yamagishi et al., 2005). Moreover, we recently found that Rho activation is required in axonal spheroid formation and

degeneration triggered by trophic deprivation (Yong et al., 2019). Whether Rho also regulates WD through mechanisms similar to developmental degeneration requires further investigation.

Formation and growth of axonal spheroids has been identified in various models of degeneration, including optic nerve injury, Alzheimer's disease, Parkinson's disease and amyotrophic lateral sclerosis (Coleman, 2005; Mi et al., 2005; Sasaki et al., 2005). Recently, we found that these spheroids are not merely a morphological hallmark of degeneration induced by trophic withdrawal but are also functionally consequential, mediating the transition from latent to catastrophic phase (Yong et al., 2019). Additionally, axonal spheroids arised after injury has been shown to be blocked by *Wld*^{s} (Beirowski et al., 2010). Despite a handful of descriptive reports about the content of these spheroids (Coleman, 2005), whether spheroid formation is influenced by the aforementioned regulators of WD (e.g. NMNATs, SARM1, DR6) remains unresolved.

Here, we demonstrate that prior to catastrophic degeneration, intra-axonal calcium increases and decreases corresponding to growth and rupture of axonal spheroids. We further demonstrate that Rho activation and changes to the actin cytoskeleton are required for spheroid formation after injury. We also find that consistent with previous observations, neurons derived from *Wld*^{s} mice display impaired spheroid formation and rupture after injury (Beirowski et al., 2010). We show that upstream of Rho activation, both exogenous supplementation of NAD^{+} and the presence of a more stable axonally targeted NMNAT, such as WLD^{s}, suppress spheroid formation. In contrast, loss of *DR6* or *SARM1* has minimal effect on spheroid formation and rupture after injury. Moreover, we find that SARM1 and DR6, but not $WLD^{s}$are required for responding to spheroid-derived pro-degenerative cues to promote catastrophic degeneration. These findings indicate a separable role of classic Wallerian degeneration effectors with respect to spheroid formation after axotomy.

Results

Intra-axonal calcium increases in enucleated axons and accumulates in spheroids prior to catastrophic degeneration

We first sought to determine whether calcium accumulates in spheroids after injury as we have observed previously for degeneration associated with trophic deprivation. To this end, we cultured mouse sympathetic neurons in microfluidic devices, which separate soma and axons (Fig.1a). Cell bodies of sympathetic neurons were enucleated by aspiration of the cell body chamber in PBS, which leaves axons residing in the distal axon chamber and microgrooves intact. After injury, these axons remain intact for roughly an hour as measured by microtubule integrity (β3-tubulin staining). At the conclusion of the latent phase, the majority of axons rapidly degenerate, going from 7.5±2.08% to 82.75±3.9% of degeneration within 90 minutes (Fig.1b,c). This is referred to as the catastrophic or execution phase of degeneration (Conforti et al., 2014). We applied the Fluo4-AM calcium dye to axons 30 minutes prior to imaging and recorded the calcium dynamics for 90 minutes after injury (Fig.1d). For injured axons, intra-axonal calcium had a roughly 2-fold increase from baseline prior to onset of the catastrophic phase (Fig.1e). Much of this calcium was concentrated in nascent spheroids (Fig.1d), consistent with previous *in vivo* and *in vitro* injury studies (Barsukova et al., 2012; Beirowski et al., 2010) and similar to our recent findings in the context of trophic withdrawal (Yong et al., 2019). After observing the initial formation of calcium rich spheroids, these structures increase in size from 3.2±0.4μm^2 to 13±1.2μm^2 (roughly 400%) between 20 and 80 minutes after injury. Spheroidal calcium levels increased by roughly 5-fold at 1 hour after injury (Fig.1g). Interestingly, spheroidal calcium levels decrease as spheroids increase in size. Besides the increase in size and calcium level in individual spheroids, the number of spheroids increased from 0.54±0.14 to 6.8±0.53 per 100μm of axon between 5 and 60 minutes after injury (Fig.1f). We also examined spheroidal calcium as a function of spheroidal area and

found the same trend (Fig.1h). Taken together, these results indicate that the formation of calcium rich axonal spheroids is a morphological hallmark that occurs prior to entry into the catastrophic phase of degeneration after injury.

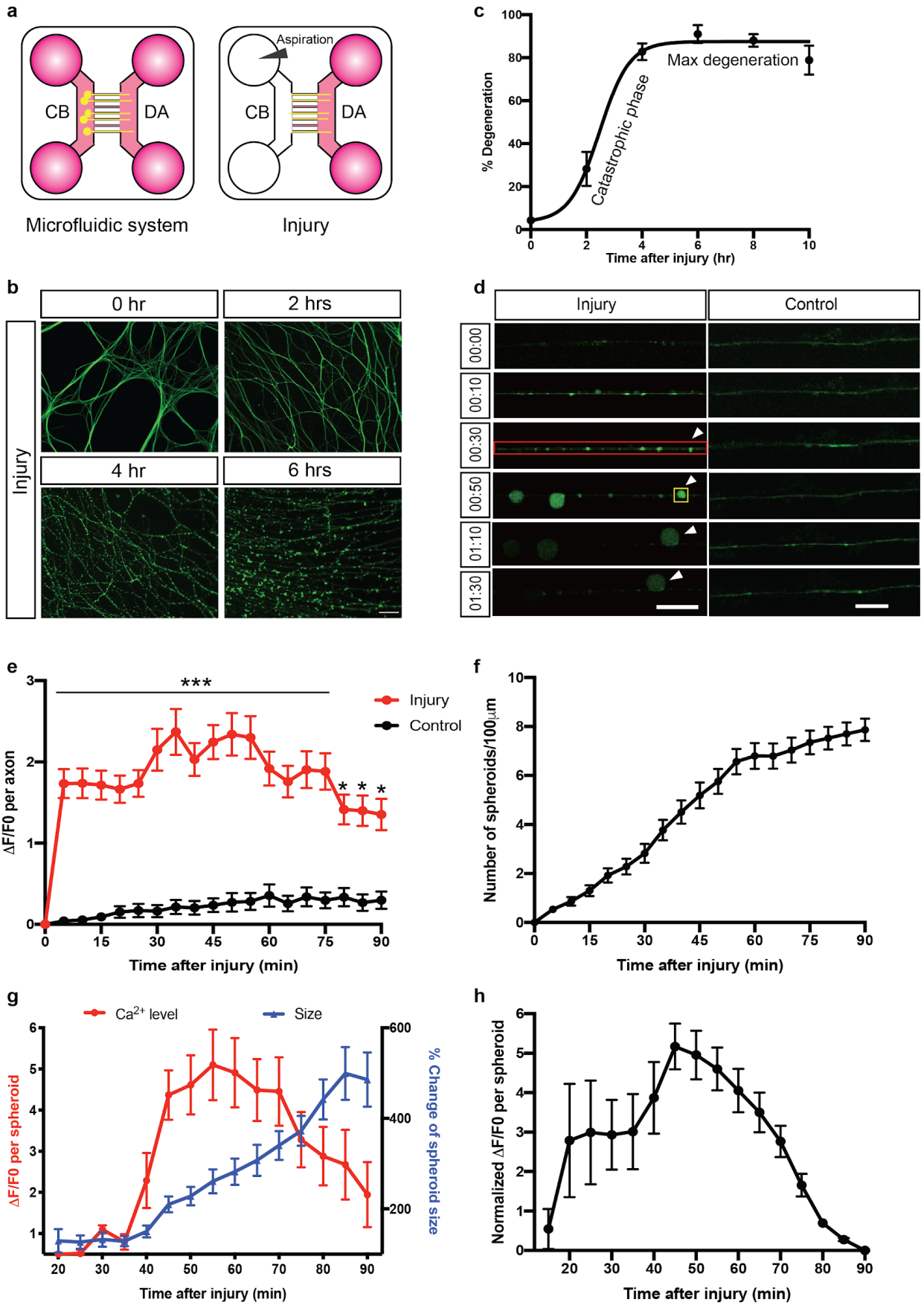
a
CB
DA
Microfluidic system
Aspiration
CB
DA
Injury
b
0 hr
2 hrs
4 hr
6 hrs
Injury
c
% Degeneration
Catastrophic phase
Max degeneration
Time after injury (hr)
d
Injury
Control
00:00
00:10
00:30
00:50
01:10
01:30
e
***
Injury
Control
ΔF/F0 per axon
Time after injury (min)
f
Number of spheroids/100μm
Time after injury (min)
g
Ca2+ level
Size
ΔF/F0 per spheroid
% Change of spheroid size
Time after injury (min)
h
Normalized ΔF/F0 per spheroid
Time after injury (min)

Figure 1: Axoplasmic calcium dynamics and formation of spheroids prior to catastrophic degeneration in response to injury

(a) Schematic representation of injury paradigm in microfluidic devices. Cell bodies (CB) and distal axons (DA) are seperated. All the cultures were maintained in the presence of 45ng/mL NGF. For the "injury" condition, neurons were enucleated by aspiration in PBS. (b) Representative images of β3-tubulin immuno-stained distal sympathetic axons before treatment (0hr), 2, 4 and 6 hours after injury. Scale bar = 50μm. (c) Degeneration time course after injury. Catastrophic phase and maximum of degeneration are noted. Nonlinear regression curve was drawn according to the Hill equation. *n*=3 for each time point. (d) Fluo4-AM calcium imaging of sympathetic axons at the indicated times after injury. For the "injury" condition, neurons were enucleated by aspiration in PBS and then incubated with Fluo4-AM for calcium imaging. For the "Control" condition, no injury was performed. Red box indicates the individual axon as a region of interest. Yellow box indicates axonal spheroid as a region of interest. White arrowheads indicate the formation and growth of spheroid. Scale bar = 10μm. (e) Calcium fluorescence change of control or injured axons over time. Total number of *n*=76 (injury) and *n*=30 (control) of axons from 3 independent litters were quantified. (f) Quantification of axonal spheroid number per 100μm of axon at the indicated times after injury. Total number of *n*=47 axons from 3 independent litters were counted. (g) Calcium fluorescence and size change of axonal spheroid at the indicated times after injury. Total number of *n*=14 axonal spheroids from 3 independent litters were quantified. (h) Quantification of normalized calcium fluorescence of axonal spheroids from 20 to 90 minutes after injury. Individual axonal spheroids were quantified: *n*=14 spheroids from 3 independent replicates. Data are reported as mean±SEM, *p<0.05, ***p<0.0001, two-way ANOVA with Sidak's multiparisons test.

Formation of axonal spheroids requires Rho activation and actin remodeling

What signaling pathways trigger axonal spheroid formation after injury? Given the dramatic outgrowth of membrane, we speculated that spheroid formation may involve cytoskeletal remodeling, similar to what we observed after trophic deprivation (Yong et al., 2019). To examine actin and β3-tubulin abundance in spheroids we stained enucleated axons with phalloidin and Tuj1 1 hour after injury. We found that actin accumulated in 47.5±3.9% of the spheroids examined, while β3-tubulin accumulated in 32.1±4.4% of spheroids (Fig.2a). We next sought to determine whether the formation of spheroids involves actin remodeling. To examine this, cultures were pre-treated (3hrs prior to injury) with the actin polymerization inhibitor cytochalasin D (10μg/μL), which delayed spheroid formation (Fig.2b,c). Rho activation is known to influence actin assembly (Hall, 1998), and may serve as a molecular switch to govern spheroid formation. Indeed, inhibiting Rho family members using the C3 transferase, CT04 (1μg/mL, 2hrs prior to injury), also suppressed spheroid formation (Fig.2b,c). Interestingly, pretreatment with cytochalasin D or CT04 delayed degeneration for up to 4 hours after injury (Fig.2d,e).

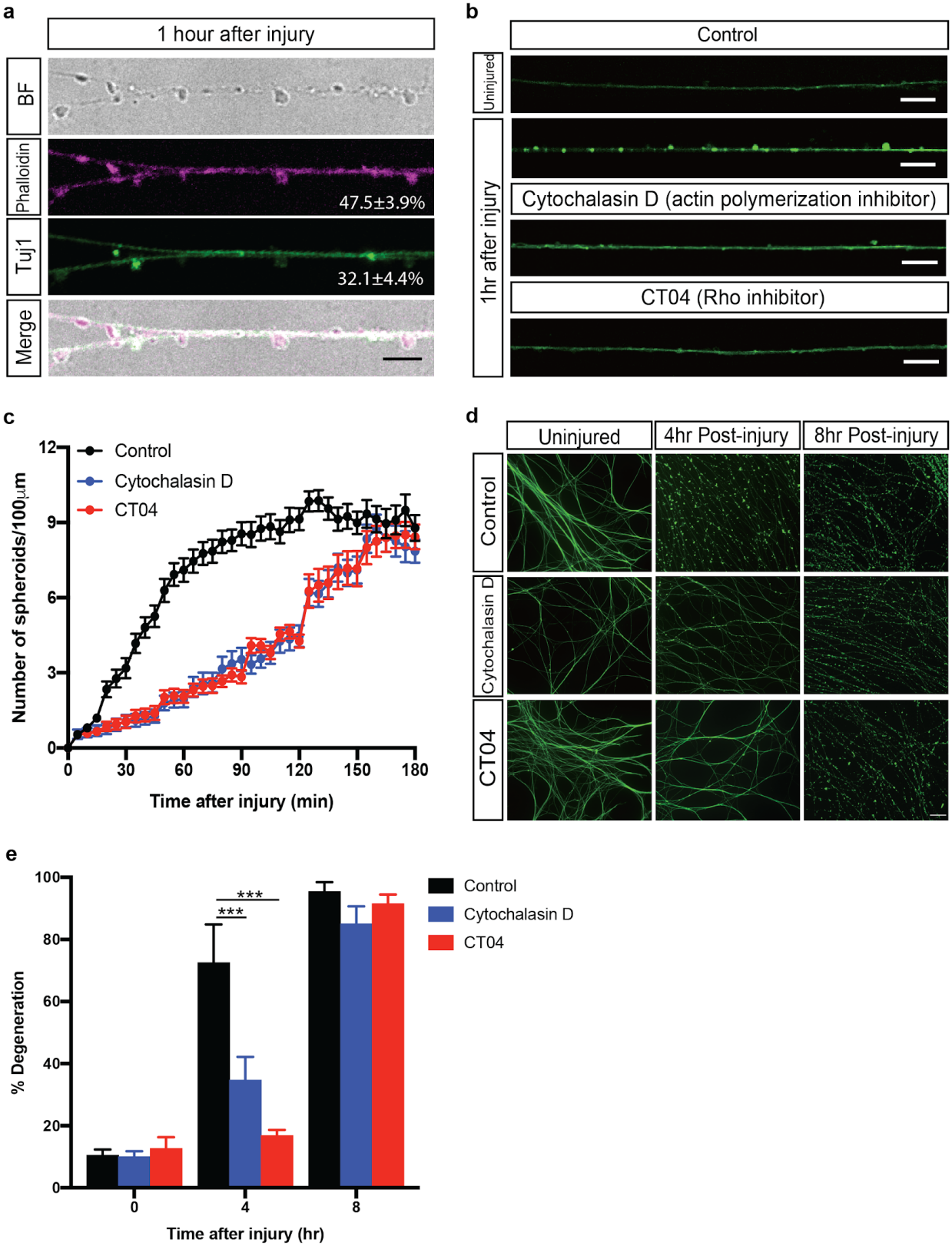
a
1 hour after injury
BF
Phalloidin
47.5±3.9%
Tuj1
32.1±4.4%
Merge
b
Control
Uninjured
1hr after injury
Cytochalasin D (actin polymerization inhibitor)
CT04 (Rho inhibitor)
c
Control
Cytochalasin D
CT04
Number of spheroids/100μm
Time after injury (min)
d
Uninjured
4hr Post-injury
8hr Post-injury
Control
Cytochalasin D
CT04
e
Control
Cytochalasin D
CT04
% Degeneration
***
***
Time after injury (hr)

Figure 2: Rho activation and actin remodeling are required for axonal spheroid formation in response to injury

(a) Representative axons/spheroids visualized for bright field, Phalloidin and β3-tubulin (Tuj1) 1 hour after injury. Scale bar = 5 μm. Percentages of Phalloidin positive and Tuj1 positive spheroids were quantified next to the images, respectively. Total number of *n*=10 axons were quantified. (b) Fluo4-AM calcium imaging of wild-type sympathetic axons with or without drug treatment. For the "CT04" group, wild-type axons were incubated in SCG media containing 1μg/mL Rho inhibitor CT04, for 2 hours prior to injury. For the "Cytochalasin D" group, wild-type axons were incubated in SCG media containing 10μg/mL actin polymerization inhibitor for 2 hours prior to injury. Scale bar = 10μm. (c) Quantification of axonal spheroid number per 100μm of wild-type sympathetic axons at the indicated times after injuryin the absence and presence of CT04 or Cytochalasin D. Total number of *n*=50 (Control), *n*=28 (Cytochalasin D), *n*=32 (CT04) axons from cultured neurons harvested from 3 independent litters were quantified. (d) Representative images and (e) quantification of degeneration of wild-type distal sympathetic axons immuno-stained for β3-tubulin in the absence and presence of CT04 or Cytochalasin D. Scale bar = 50μm. Compared to Control, 4hr post-injury (*n*=4), $p<0.0001$, *n*=6 for Cytochalasin D, 4hr post-injury; $p<0.0001$, *n*=5 for CT04, 4hr post-injury, two-way ANOVA with Dunnett's multiple comparisons test. Data are reported as mean±SEM, *p<0.05, ***p<0.0001.

Axonal spheroids develop membrane rupture after injury

We and others have shown that the electrical chemical gradient can be disrupted through membrane rupture on axonal spheroids in models of developmental degeneration and multiple sclerosis (Witte et al., 2019; Yong et al., 2019). To determine whether the axonal spheroids that we observed on injured sympathetic axons develop ruptures, we bathed axons in neutral fluorescent dextran beginning 20 minutes after injury, which is sufficient time for the initial site of lesion to re-seal (Eddleman et al., 1998). If there were any ruptures on the membrane after injury, the 3 kDa red dextran would immediately diffuse to the axoplasm (Fig.3a). As expected, the exclusion of dextran was maintained for 40-50 minutes after injury, however after 50 minutes, the axoplasm begins to fill with fluorescent dextran (Fig.3b). An additional movie file shows the dextran filling axonal spheroids in more detail [see Supplementary video 1]. We also examined the size of ruptures using different sized dextrans. We observed that 70, 10, and 3 kDa dextran filled 11.5±2.6%, 33±6.6% and 63.6±7.1% of axonal spheroids by 90 minutes after injury, respectively (Fig.3c). This indicates permeability of small to medium sized molecules and suggests the same physiology of spheroidal rupture in WD as other degeneration paradigms. To determine whether dextran diffusion correlates with the size of spheroids, we counted the numbers and sizes of 3 kDa dextran positive and negative spheroids 30, 60, and 90 minutes after injury, respectively (Fig.3d). Most of the axonal spheroids are 5-10μm^2 in size. However, regardless of their sizes, more spheroids develop membrane rupture at later times after injury suggesting that the probability of rupture is more impacted by time than size of spheroid.

Based on the diminution of spheroidal calcium signal 1 hour after injury and the permeability of the spheroidal membrane, we speculate that intra-axonal calcium may diffuse to the extracellular space after spheroidal rupture. To test this hypothesis, we bathed axons in microfluidic devices in 100µL of regular culture media or calcium free, serum free media and measured extracellular

calcium before and 1 hour after injury using a Fluo4 spectrophotometric assay (Yong et al., 2019). For the cultures maintained in regular SCG media, calcium levels in conditioned media taken from injured axons (ICM) (2409.51±212.17μM) was significantly higher than calcium concentration in Control CM (1578.16±275.57μM) (Fig.3e). Additionally, we were able to observe an increase in extracellular calcium after spheroidal rupture when experiments were performed using calcium free, FBS free media (Fig.3e). Whether or not this calcium extrusion is physiologically relevant remains to be determined. However, in this *in vitro* system it represents a complementary paradigm to the aforementioned dextran assay for assessing membrane integrity.

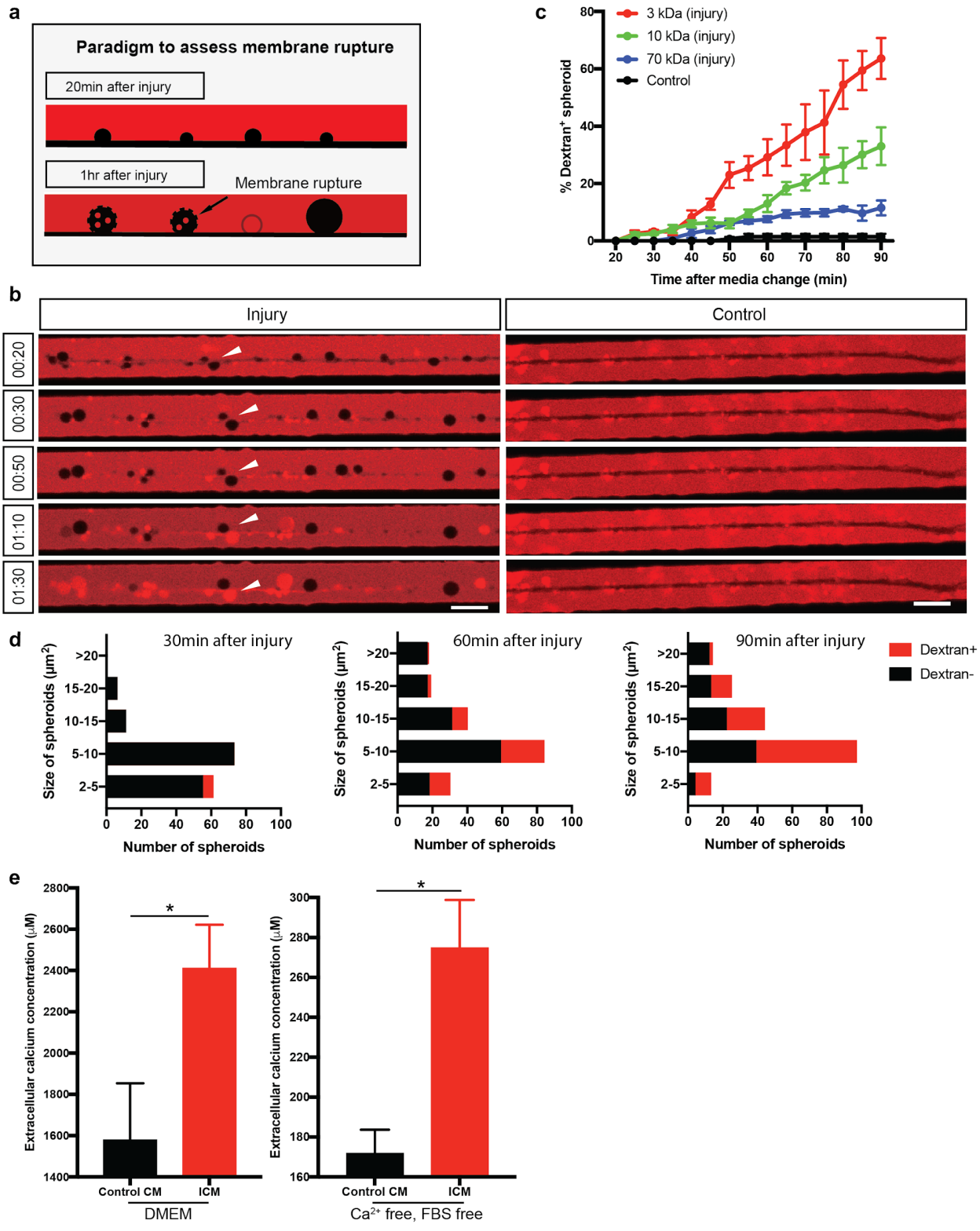

Figure 3: Axonal spheroids develop membrane rupture after injury

(a) Schematic representation of the experimental paradigm to assess membrane rupture model using fluorescent dextran. 20 minutes after injury, fluorescent dextran (red) is not taken up by the axon (black, negative space). However, by 1 hour after injury, as the plasma membrane loses integrity and ruptures, fluorescent dextran (red) can diffuse into spheroids, turning them red. Spheroids with intact membrane remain black. (b) Representative images of dextran 3 kDa (red) entry to axonal spheroids (black) from 20 to 90 minutes after injury (left column), and dextran exclusion in untreated axons (right column). White arrowheads indicate that dextran 3 kDa enter axonal spheroids 1 hour after injury. Scale bar = 10 μm. (c) Quantification of the percentages of fluorescent 3 kDa (red), 10 kDa (green), and 70 kDa (blue) dextran positive spheroids 20 to 90 minutes after injury. Black line (control) indicates the percentages of fluorescent 3 kDa dextran positive spheroids without injury. Total number of n=12 (3 kDa), n=12 (10 kDa), n=9 (70 kDa), and n=27 (control) axons from 3 independent litters were counted. (d) Histogram of 3 kDa dextran negative (black) and positive (red) spheroids 30, 60, and 90 minutes after injury. (e) Measurements of extracellular calcium expelled from axons into regular SCG culture media (DMEM, left) and calcium free, FBS free media (right). In the “Control CM” group, media was collected from uninjured axons. In the “ICM” group, media was collected 1 hour after injury. For DMEM groups, compared to Control CM (n=4), p=0.0414, n=4 for ICM; For calcium free, FBS free groups, compared to Control CM (n=3), p=0.0185, n=3 for ICM, unpaired t test. Data are reported as mean±SEM, *p<0.05, ***p<0.0001.

Spheroid formation in WD deficient mutants

We next examined the spheroid formation in genotypes reported to have impaired Wallerian degeneration: *Wld*^{s}, *DR6*$^{-/-}$ and *Sarm1*$^{-/-}$. Calcium imaging revealed that *Wld*^{s} did not display a late stage calcium wave, and had a greatly diminished capacity to form spheroids in response to injury (Fig.4a-c). This is consistent with previous observations demonstrating that mitochondria in *Wld*^{s} neurons have increased calcium buffering capacity and a delay in spheroid formation (Adalbert et al., 2012; Avery et al., 2012; Beirowski et al., 2010; Vargas et al., 2015). Interestingly, neurons from *DR6*$^{-/-}$ and *Sarm1*$^{-/-}$ mice also had attenuated spheroidal calcium compared to wild-type but significantly higher than *Wld*^{s} neurons (Fig.4c). We also examined the Fluo4-AM signals in the inter-spheroidal regions of wild-type and WD mutant axons after injury. No obvious calcium wave was detected in the axons outside of spheroids after injury, suggesting that spheroids are the predominant contributor to axoplasmic calcium change (Fig. 4d). We next examined the role of WLD^{s}, DR6 and SARM1 in the change in spheroid size and the accumulation of spheroids as a function of time after injury. 1 hour after injury, we observed that loss of *DR6* or *SARM1* displayed a roughly 100% increase in spheroid size (Fig.4e). Moreover, wild-type, *DR6*$^{-/-}$, and *Sarm1*$^{-/-}$ neurons displayed 7.5±0.8, 9.1±0.5, and 9.7±0.7 spheroids per 100μm of axons, respectively, whereas *Wld*^{s} neurons only displayed 1.4±0.5 spheroids per 100μm of axons 1 hour after injury (Fig.4b). We next examined spheroid rupture and calcium extrusion in sympathetic axons from *Wld*^{s}, *DR6*$^{-/-}$ and *Sarm1*$^{-/-}$ mice. WT, *DR6*$^{-/-}$ and *Sarm1*$^{-/-}$ all displayed similar levels of 3 kDa dextran spheroid filling after injury, however *Wld*^{s} axons displayed negligible filling indicating a lack of spheroid rupture (Fig.4f,g). Consistent with this, *Wld*^{s} axons showed no difference in extracellular calcium levels before or 1 hour after injury, while *DR6*$^{-/-}$ and *Sarm1*$^{-/-}$ displayed elevation in extracellular calcium levels (Fig.4h). Taken together, these findings suggest that WLD^{s}/NMNAT is upstream of spheroid formation while the other players tested have minimal roles in this process.

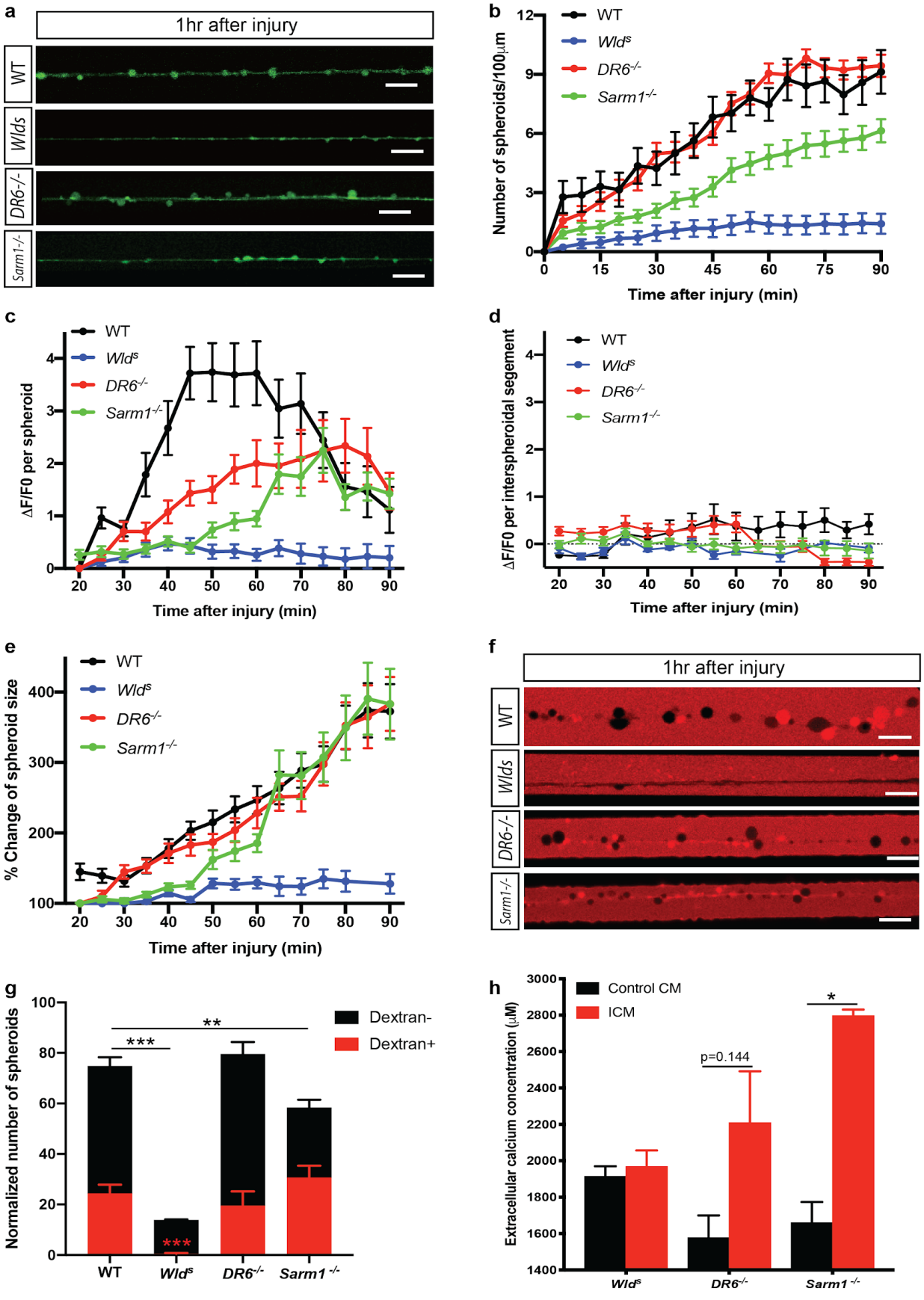
a
1hr after injury
WT
Wlds
DR6-/-
Sarm1-/-
b
WT
Wld^S
DR6^-/-
Sarm1^-/-
Number of spheroids/100μm
Time after injury (min)
c
ΔF/F0 per spheroid
Time after injury (min)
d
ΔF/F0 per interspheroidal segement
Time after injury (min)
e
% Change of spheroid size
Time after injury (min)
f
1hr after injury
g
Normalized number of spheroids
Dextran-
Dextran+
***
**
***
h
Control CM
ICM
Extracellular calcium concentration (μM)
p=0.144
*

Figure 4: *DR6*$^{-/-}$ and *Sarm1*$^{-/-}$ develop axonal spheroids and spheroidal rupture after injury, while *Wld*^{s} does not

(a) Fluo4-AM calcium imaging of wild-type, *Wld*^{s}, *DR6*$^{-/-}$, and *Sarm1*$^{-/-}$ sympathetic axons 1hr after injury. Scale bar = 10μm. (b) Quantification of numbers of axonal spheroids, (C) spheroidal calcium level, (d) interspheroidal calcium level, and (e) size change of axonal spheroids on the wild-type, *Wld*^{s}, *DR6*$^{-/-}$, and *Sarm1*$^{-/-}$ axons 1 hour after injury, respectively. Total number of n=29 (WT), n=17 (*Wld*^{s}), n=57 for (*DR6*$^{-/-}$), and n=54 (*Sarm1*$^{-/-}$) axons from 3 independent litters were counted. (f) Representative images of dextran 3 kDa (red) entry to axonal spheroids (black) on wild-type, *Wld*^{s}, *DR6*$^{-/-}$, and *Sarm1*$^{-/-}$ axons 1 hour after injury. Scale bar = 10μm. (g) Normalized numbers of 3 kDa dextran negative (black) and positive (red) axonal spheroids on wild-type, *Wld*^{s}, *DR6*$^{-/-}$, and *Sarm1*$^{-/-}$ axons 1 hour after injury. Compared to WT, Dextran^{+}, p<0.0001, n=21 for *Wld*^{s}, Dextran^{+}. Compared to WT, Dextran^{-}, p<0.0001, n=22 for *Wld*^{s}, Dextran^{-}; p=0.0003, n=17 for *Sarm1*$^{-/-}$, Dextran^{-}, two-way ANOVA with Dunnett's multiple comparisons test. (h) Measurement of extracellular calcium concentration in media surrounding injured and uninjured *Wld*^{s}, *DR6*$^{-/-}$and *Sarm1*$^{-/-}$ axons. All injured conditioned media was collected from distal axon chamber 1hr after injury. Compared to Control CM, p=0.9982, n=3 for *Wld*^{s}, ICM; p=0.1440, n=6 for *DR6*$^{-/-}$, ICM; p=0.0141, n=3 for *Sarm1*$^{-/-}$, ICM, two-way ANOVA with Sidak's multiple comparisons test. Data are reported as mean±SEM, *p<0.05, **p<0.001, ***p<0.0001.

NAD^+ acts upstream of Rho activation to suppress spheroid formation

The Wld^S protein stably targets NMNAT1 to axons to maintain high NAD^+ levels for prolonged periods following injury, which is known to protect axons from degeneration (Di Stefano et al., 2015). To test whether NAD^+ contributes to the formation of axonal spheroids, we treated sympathetic axons with 1mM exogenous NAD^+ overnight prior to injury. Supplementation of NAD^+ to wild-type sympathetic axons suppressed spheroid formation after injury (Fig.5a,b), and phenocopied observations in *Wld*^{S} axons (Fig.4a,b). We next examined whether NAD^+ is upstream of Rho activation with respect to regulating spheroid formation. To this end, axons were incubated with the Rho activator, CN03 in the presence of exogenouse NAD^+. Activation of Rho is able to promote spheroid formation even in the presence of exogenous NAD^+(Fig.5a,b). NAD^+ levels are known to decline in injured axons and nerves, due to both turnover of NMNAT2 and SARM1-dependent NAD^+ degradation (Gilley and Coleman, 2010; Sasaki et al., 2016; Wang et al., 2005). However, loss of *SARM1* failed to inhibit spheroid formation, whereas *Sarm1*$^{-/-}$ neurons pre-treated with NAD^+ or Rho inhibitor CT04 displayed only 1.16±0.52 and 0.85±0.31 spheroids per 100μm of axons 1 hour after injury, respectively (Fig.5c,d). Moreover, activation of Rho by CN03 in *Wld*^{S}neurons increased the number of spheroids to 3.59±0.87 per 100μm of axons 1 hour after injury (Fig.5e,f). We further examined the protection effects of NAD^+ in the presence and absence of Rho activation. 4 hours after injury, wild-type sympathetic axons treated with exogenous NAD^+ remained intact, but degeneration was partially rescued (41.7±0.3%) by CN03 incubation (Fig.5g,h). 8 hours after injury, *Wld*^{S} axons treated with CN03 displayed 60.5±3.4% degeneration, significantly higher than control *Wld*^{S} cultures with 13.8±7.1% degeneration (Fig.5g,h).

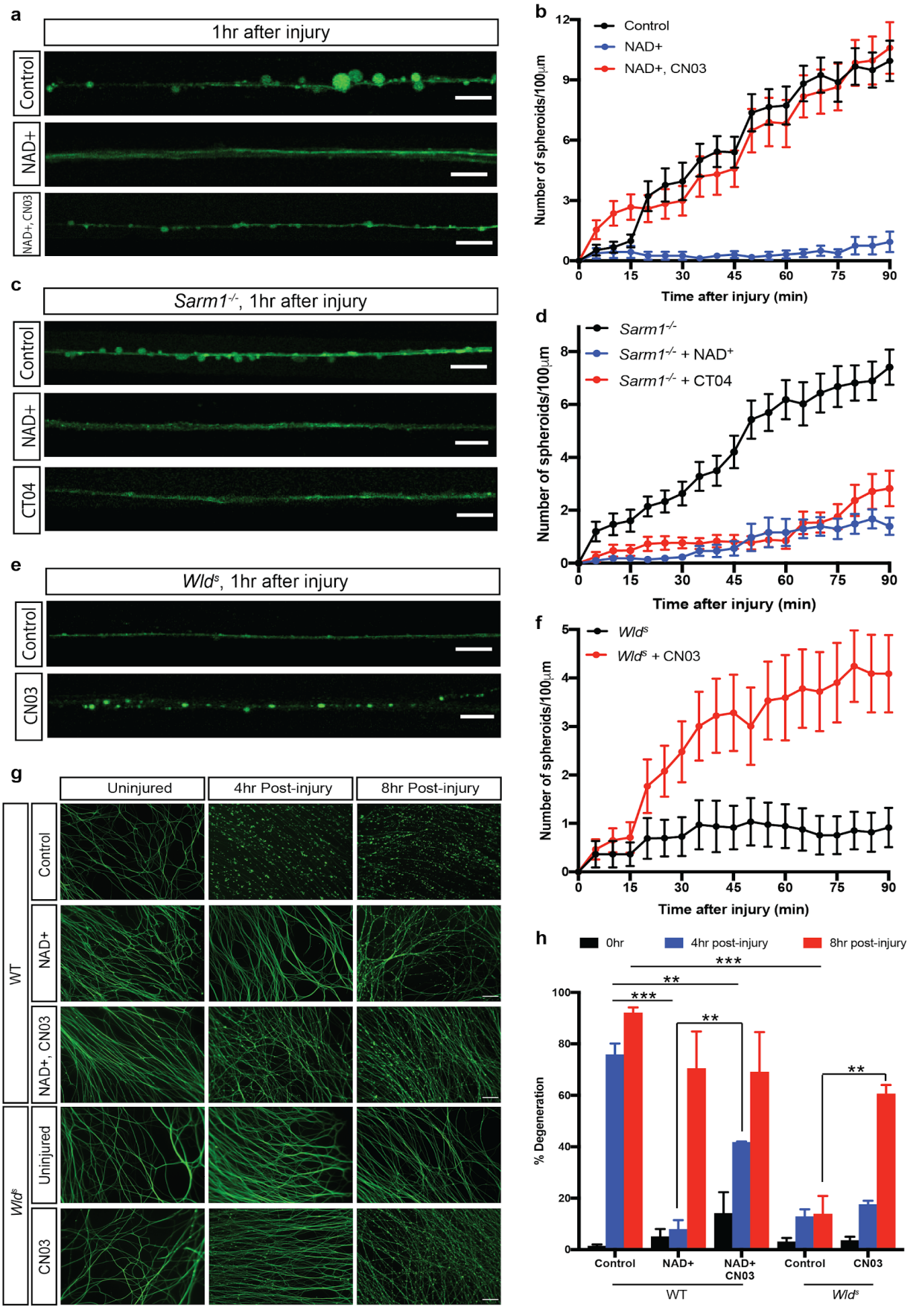
a
1hr after injury
Control
NAD+
NAD+, CN03
b
Control
NAD+
NAD+, CN03
Number of spheroids/100μm
Time after injury (min)
c
Sarm1-/-, 1hr after injury
Control
NAD+
CT04
d
Sarm1-/-
Sarm1-/- + NAD+
Sarm1-/- + CT04
Number of spheroids/100μm
Time after injury (min)
e
Wlds, 1hr after injury
Control
CN03
f
Wlds
Wlds + CN03
Number of spheroids/100μm
Time after injury (min)
g
Uninjured
4hr Post-injury
8hr Post-injury
WT
Control
NAD+
NAD+, CN03
Wlds
Uninjured
CN03
h
0hr
4hr post-injury
8hr post-injury
% Degeneration
Control
NAD+
NAD+ CN03
Control
CN03
WT
Wlds

Figure 5: NAD^+ acts on upstream of Rho activation to suppresses spheroid formation after injury

(a) Fluo4-AM calcium imaging of wild-type sympathetic axons 1hr after injury with or without drug treatment. Scale bar = 10μm. (b) Quantification of axonal spheroid number per 100μm of wild-type sympathetic axons at the indicated times after injury in the absence and presence of NAD^+ or CN03. Total number of *n*=23 (Control), *n*=13 (NAD^+), *n*=21 (NAD^+, CN03) axons from cultured neurons harvested from 3 independent litters were quantified. (c) Fluo4-AM calcium imaging of *Sarm1*$^{-/-}$ sympathetic axons 1hr after injury with or without drug treatment. Scale bar = 10μm. (d) Quantification of axonal spheroid number per 100μm of *Sarm1*$^{-/-}$ sympathetic axons at the indicated times after injury in the absence and presence of NAD^+ or CT04. Total number of *n*=30 (Control), *n*=16 (NAD^+), *n*=25 (CT04) *Sarm1*$^{-/-}$axons from cultured neurons harvested from 3 independent litters were quantified. (e) Fluo4-AM calcium imaging of *Wld*^{S} sympathetic axons 1hr after injury in the presence and absence of CN03. Scale bar = 10μm. (f) Quantification of axonal spheroid number per 100μm of *Wld*^{S} sympathetic axons at the indicated times after injury in the absence and presence of CN03. Total number of *n*=25 (Control), *n*=24 (CN03) *Wld*^{S} axons from cultured neurons harvested from 3 independent litters were quantified. (g) Representative images and (h) quantification of degeneration of wild-type and *Wld*^{S} distal sympathetic axons immuno-stained for β3-tubulin with different treatments. Scale bar = 50μm. For the "NAD^+" group, axons were incubated in SCG media containing 1mM NAD^+ supplement overnight prior to injury. For the "CN03" and CT04" groups, axons were incubated in SCG media containing 1μg/mL Rho activator CN03 and Rho inhibitor CT04 for 2 hours prior to injury, respectively. Data are reported as mean±SEM, *p<0.05, **p<0.001, ***p<0.0001, two-way ANOVA with Tukey's multiple comparisons test.

DR6 and SARM1 act downstream of spheroid formation

How could injured *Sarm1*$^{-/-}$ and *DR6*$^{-/-}$ axons remain resistant to degeneration even though they are competent to form and rupture spheroids? We recently showed that loss of *DR6* in trophically deprived axons could prevent catastrophic degeneration downstream of spheroid rupture (Yong et al., 2019). Therefore, we hypothesize that SARM1 and DR6 acts downstream of spheroid rupture to promote catastrophic degeneration instead of gating exit from the latent phase of degeneration. To examine this, we collected media surrounding injured distal axons from *Wld*^{s}*, DR6*$^{-/-}$ and *Sarm1*$^{-/-}$cultures and applied this injured conditioned media (ICM) to uninjured trophic deprived wild-type axons (Fig.6a). These morphologically intact recipient wild-type axons underwent complete degeneration within 5 hours of incubation with ICM derived from *Sarm1*$^{-/-}$ and *DR6*$^{-/-}$ axons (Fig.6b,c). However, ICM collected from injured *Wld*^{s} axons didn't hasten catastrophic axon degeneration in trophic deprived wild-type neurons (Fig.6b,c), consistent with the diminished spheroid formation and rupture in these mutants (Fig.4).

To determine whether SARM1, DR6 or WLD^{s} are downstream of spheroid rupture to regulate degeneration, we applied ICM collected from wild-type axons to intact recipient trophic deprived neurons derived from *Wld*^{s}*, DR6*$^{-/-}$ and *Sarm1*$^{-/-}$ mice (Fig.6d). Remarkably, in this paradigm *Wld*^{s} axons showed 78.4±5.8% degeneration, while *DR6*$^{-/-}$ and *Sarm1*$^{-/-}$ showed 16.3±5.9% and 12.7±1.4% degeneration when exposed to ICM from wild-type axons, respectively (Fig.6e,f). We next performed a similar experiment on injured recipient axons. We applied wild-type ICM to mutant axons 4 hours after injury and then incubate for another 4 hours (Fig.6g). Consistent with the delayed WD in these mutants (Gamage et al., 2017), injured *Sarm1*$^{-/-}$, *DR6*$^{-/-}$ and *Wld*^{s} axons displayed less than 20% degeneration 8 hours after injury with the final 4 hours in the presence of Control CM incubation (Fig.6h,i). Remarkably, injured *Wld*^{s} axons displayed 42.5±9.7% degeneration after WT ICM incubation (Fig.6h,i). Injured *DR6*$^{-/-}$ and *Sarm1*$^{-/-}$ axons only showed

16.5±3.5% and 2.0±0.6% when exposed to WT ICM, respectively (Fig.6h,i). These results raise the possibility that *Sarm1*$^{-/-}$ and *DR6*$^{-/-}$ protects axons from WD by perturbing pathways required for the catastrophic degenerative response to spheroid contents, while *Wld*^{S} delays WD by suppressing the development of axonal spheroids thereby delaying exit from latency.

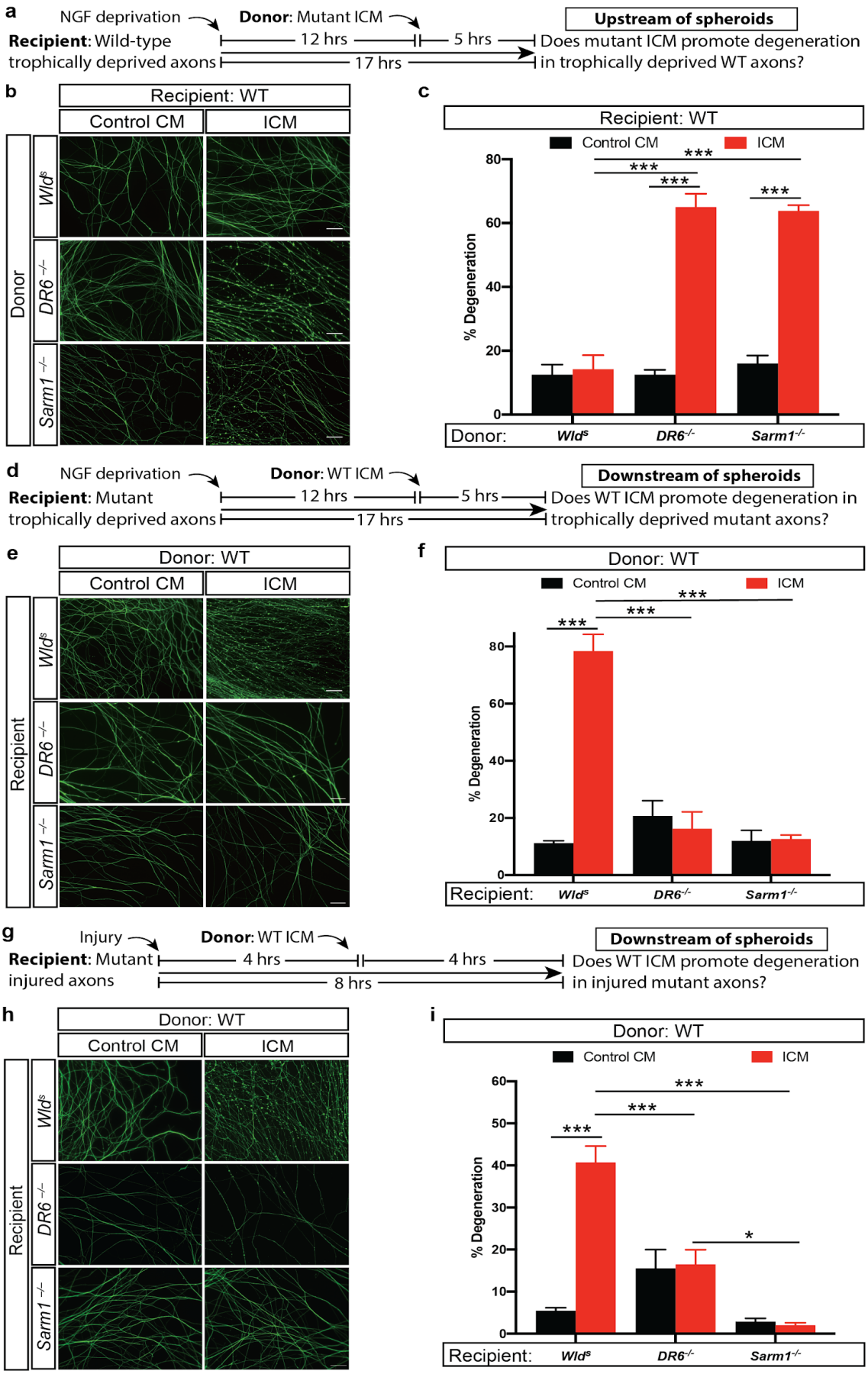
a
NGF deprivation
Donor: Mutant ICM
Recipient: Wild-type trophically deprived axons
12 hrs
5 hrs
17 hrs
Upstream of spheroids
Does mutant ICM promote degeneration in trophically deprived WT axons?
b
Recipient: WT
Control CM
ICM
Donor
Wlds
DR6 -/-
Sarm1 -/-
c
Recipient: WT
Control CM
ICM
% Degeneration
Donor:
Wlds
DR6-/-
Sarm1-/-
d
NGF deprivation
Donor: WT ICM
Recipient: Mutant trophically deprived axons
12 hrs
5 hrs
17 hrs
Downstream of spheroids
Does WT ICM promote degeneration in trophically deprived mutant axons?
e
Donor: WT
Control CM
ICM
Recipient
f
Donor: WT
Control CM
ICM
% Degeneration
Recipient:
g
Injury
Donor: WT ICM
Recipient: Mutant injured axons
4 hrs
4 hrs
8 hrs
Downstream of spheroids
Does WT ICM promote degeneration in injured mutant axons?
h
Donor: WT
Control CM
ICM
Recipient
i
Donor: WT
Control CM
ICM
% Degeneration
Recipient:

Figure 6: *DR6*$^{-/-}$ and *Sarm1*$^{-/-}$ suppress ICM induced axon degeneration, while *Wld*^{s} does not

(a) Wild-type and (d) mutant sympathetic neurons were globally deprived of NGF for 12 hours followed by addition of conditioned media collected from distal axons for 5 hours, respectively. (b) Representative images and (c) quantification of β3-tubulin immunostained trophic deprived distal sympathetic axons from wild-type animals after treatment with ICM and Control CM collected from *DR6*$^{-/-}$, *Sarm1*$^{-/-}$ and *Wld*^{s} neurons. Compared to *Wld*^{s}, Control CM (n=4), p=0.9811, n=5 for *Wld*^{s}, ICM. Compared to *DR6*$^{-/-}$, Control CM (n=3), p<0.0001, n=5 for *DR6*$^{-/-}$, ICM. Compared to *Sarm1*$^{-/-}$, Control CM (n=3), p<0.0001, n=5 for *Sarm1*$^{-/-}$, ICM. (e) Representative images and (f) quantification of β3-tubulin immunostained trophic deprived distal sympathetic axons from *DR6*$^{-/-}$, *Sarm1*$^{-/-}$ and *Wld*^{s} animals after treatment with ICM and Control CM collected from wild-type neurons. Compared to Control CM, *Wld*^{s} (n=5), p<0.0001, n=5 for ICM, *Wld*^{s}. Compared to Control CM, *DR6*$^{-/-}$ (n=3), p=0.8921, n=4 for ICM, *DR6*$^{-/-}$. Compared to Control CM, *Sarm1*$^{-/-}$ (n=7), p=0.9988, n=6 for ICM, *Sarm1*$^{-/-}$. (g) Mutant neurons were injured for 4 hours in the presence of NGF followed by addition of conditioned media collected from wild-type axons for 4 hours. (h) Representative images and (i) quantification of β3-tubulin immunostained injured distal sympathetic axons from *DR6*$^{-/-}$, *Sarm1*$^{-/-}$ and *Wld*^{s} animals after treatment with ICM and Control CM collected from wild-type neurons. Compared to Control CM, *Wld*^{s} (n=7), p<0.0001, n=11 for ICM, *Wld*^{s}. Compared to Control CM, *DR6*$^{-/-}$ (n=2), p=0.9983, n=4 for ICM, *DR6*$^{-/-}$. Compared to Control CM, *Sarm1*$^{-/-}$ (n=7), p=0.9951, n=8 for ICM, *Sarm1*$^{-/-}$. In the “Control CM” group, media was collected from uninjured axons. In the “ICM” group, media was collected 4 hours after injury. Data are reported as mean±SEM, *p<0.05, ***p<0.0001. Significant difference is determined by two-way ANOVA with Sidak’s multiple comparison test. Scale bar = 50μm.

Discussion

Here we describe the regulated formation of calcium rich axonal spheroids as injured axons transition from latent to catastrophic phase of degeneration. Importantly, among three WD deficient mutants, only *Wld*^{s} suppresses spheroid formation, suggesting that depletion of axonal NMNAT/NAD^+ acts upstream of spheroid formation during the latent phase, whereas SARM1 and DR6 activation might promote degeneration during catastrophic phase (Fig.7). This is somewhat surprising given that the mechanism of SARM1 action is thought to be through NAD^+ degradation (Essuman et al., 2017; Gerdts et al., 2015). This sets up a scenario whereby NAD^+ may be acting at different points in the degeneration timeline after injury. It is known that the initial decay of NAD^+ after injury is independent of SARM1 and we suggest that this reduction is sufficient for the disinhibition of Rho induced spheroid formation. After spheroid rupture, we suggest that DR6 and SARM1 are activated by an as yet unknown mechanism to further drive down the level of NAD^+ and promote catastrophic axon degeneration (Fig.7).

Axonal spheroids have been characterized as a common morphological hallmark during axon degeneration (Coleman, 2005). These spheroids arise continuously in axons and show different degrees of swelling in response to a range of molecular triggers, including the focal blockage of axonal transport, ROS mediated actin aggregation, and NMNAT deficiency (Barsukova et al., 2012; Mi et al., 2005; Sasaki et al., 2005). Here, we report the formation of calcium rich spheroids on severed sympathetic axons *in vitro*(Fig.1). Similar to our observations in developmental degeneration models (Yong et al., 2019), we find that spheroid formation requires Rho dependent actin remodeling. Inhibition of this pathway not only blocks spheroid formation but also delays injury induced degeneration (Fig.2). However, pharmacological manipulations of actin dynamics or Rho may affect degeneration events other than spheroid regulation, such as remodeling of the

actin-spectrin-based membrane associated periodic skeleton, axon transport or ERK signaling (Lorenzo et al., 2019; Wang et al., 2019a; Zhong et al., 2014; Zhou et al., 2019). Therefore, it's likely that spheroid formation is the phenotypic result of actin remodeling and Rho activation during axon degeneration, and perhaps an indirect driver of catastrophic fragmentation.

By comparing axoplasmic calcium dynamics of WD deficient mutants with wild-type sympathetic axons, we demonstrated that neurons from *Wld*^{s} animals display minimal axonal calcium flux from 20 to 90 minutes after injury, significantly fewer and smaller axonal spheroids formed, and no calcium extrusion to the extracellular space (Fig.4). These findings suggest that injury induced NMNAT2 depletion is likely an upstream trigger for calcium rich spheroid formation and rupture. SARM1 has been proposed to be in the same pathway as Wld^{s}/NMNAT1 in promoting axon degeneration due to its intrinsic NAD^+ cleavage activity (Coleman and Höke, 2020; Essuman et al., 2017; Gerdts et al., 2015, 2016). Surprisingly, unlike *Wld*^{s}, *Sarm1*$^{-/-}$ axons are capable of forming axonal spheroids after injury suggesting that at least in the context of spheroid formation and rupture, these pathways operate independently. Importantly, this finding is not in conflict with reports that NMNAT/NAD^+ depletion is involved in catastrophic degeneration (Sasaki et al., 2016). Studies in mouse dorsal root ganglion (DRG) neuron cultures have shown that there is slow NAD^+ decline loss for roughly 2 hours after transection likely owing to NMNAT2 degradation, followed by a fast SARM1-dependent NAD^+ decay (Sasaki et al., 2016, 2020; Wang et al., 2005). To explain the different phenotypes of *Sarm1*$^{-/-}$ and *Wld*^{s} with respect to spheroid formation after injury, we propose a working model by which SARM1 is inactive during the latent phase and then becomes active after spheroidal rupture to accelerate NAD^+depletion during the catastrophic phase of axon degeneration.

The mechanism by which NAD^+ inhibits Rho activity and spheroid formation remains unknown and will be the subject of future inquiry. We envision a few possibilities: **1.** The replenished axonal

NAD^+ pool might inhibit the calcium release from intracellular stores, which contributes to the formation of calcium enriched spheroids. NAD^+ depletion after injury leads to the increase of relative concentrations of calcium-mobilizing agents including cADPR and ADPR over axonal NAD^+, stimulating intra-axonal calcium rise by activation of ryanodine receptors on ER and calcium channels on plasma membrane, respectively (Guse, 2015). In addition, blocking ER calcium channels has been shown to protect injury-induced axonal degeneration in DRG cultures and secondary degeneration of severed CNS axons (Orem et al., 2017; Villegas et al., 2014). However, whether blocking intracellular calcium stores would suppress spheroid formation on injured sympathetic axons must be investigated in the future. **2.** Depletion of NAD^+ pools after injury alters axonal redox state and ATP synthesis (Nikiforov et al., 2015) which may contribute to spheroid formation and rupture by regulating Rho GTPase activity (Fig.7). Studies have shown that the cellular oxidation state mediates activation of Rho GTPase via a redox-sensitive cysteine at the end of p-loop motif (Heo and Campbell, 2005; Mitchell et al., 2013). Moreover, application of Rho activator CN03 is able to promote spheroid formation on injured axons in the presence of NAD^+ supplementation (Fig.5a,b). The disruption of redox state or NAD^+/NADH balance caused by NMNAT2 degradation may therefore activate Rho to mediate actin remodeling and spheroid formation.

The mechanism by which SARM1 is activated after spheroid rupture remains unclear, but the recent finding that NMN analogue can activate SARM1 to induce non-apoptotic cell death appears to provide one possible answer to this question (Zhao et al., 2019). In a neuroinflammatory model, activation of mixed lineage kinase domain-like pseudokinase (MLKL) can induce loss of axonal survival factors NMNAT2 and SCG10/STMN2 to trigger SARM1 NADase activity, which indicates that necroptotic pathways could disinhibit SARM1 to activate pathological axon degeneration (Ko et al., 2020; Llobet Rosell and Neukomm, 2019). Activation of SARM1 has been shown to promote phosphorylation of JNK to trigger neuronal immune response after axon injury (Wang et al., 2018).

Moreover, phosphorylation of SARM1 by JNK regulates NAD^+ cleavage to inhibit mitochondrial respiration in response to oxidative stress (Murata et al., 2018). Therefore, SARM1 may also be activated by JNK to promote further NAD^+ depletion (Fig.7). Both overexpression of NMNATs and knocking out SARM1 have been shown to decrease injury-induced degradation of the calpain inhibitor, calpastatin, which protects neurons from degeneration (Galindo et al., 2017; Yang et al., 2013). It is possible that NAD^+ depletion and further energy deficits lead to calpastatin degradation, which would disinhibit calpain to promote catastrophic degeneration. Similar to the phenotype of *Sarm1*$^{-/-}$, injured *DR6*$^{-/-}$ axons showed formation of spheroids and spheroidal calcium accumulation (Fig.4). Indeed, we've shown in the past that DR6 is also required for JNK activity after injury (Gamage et al., 2017). Because of our previous work examining the role of DR6 in trophic withdrawal induced degeneration, it is tempting to speculate that DR6 gates entry into the catastrophic phase WD by activating SARM1 (Yong et al., 2019). Injured *Sarm1*$^{-/-}$ and *DR6*$^{-/-}$ axons are competent for spheroid formation and rupture yet still degenerate much later than injured wild-type axons (Fig.4). Remarkably, *Sarm1*$^{-/-}$ or *DR6*$^{-/-}$ neurons, but not *Wld*^{S} neurons are resistant to degeneration induced by ICM collected after spheroidal rupture (Fig.6). Based on these results, we propose that SARM1 and DR6 are likely to promote WD by regulating signaling pathways downstream of spheroid formation and rupture. However, whether and how DR6 and SARM1 would work together to do this is unclear (Fig.7).

Spheroid formation is a common hallmark for many neurodegenerative disorders including Alzheimer's disease (AD), glaucoma, amyotrophic lateral sclerosis (ALS) (Adalbert et al., 2007; Conforti et al., 2014; Howell et al., 2007; Kanaan et al., 2013; Sasaki et al., 2005). Our previous work suggests that these spheroids play a functional role as axons transition from latent to catastrophic phases of degeneration (Yong et al., 2019). Recently, overactivation of calcium influx in neurons has been shown to trigger degeneration in *Sarm1*$^{-/-}$ zebrafish *in vivo*, suggesting that calcium could be one of the effectors downstream of Sarm1 to drive degeneration (Tian et al.,

2020b). However, we only observed minor attenuation of spheroidal calcium flux in injured *Sarm1*$^{-/-}$ and *DR6*$^{-/-}$ axons (Fig.4), indicating that SARM1 and DR6 likely promotes WD independent of calcium signaling. While the pathways downstream of spheroid formation require further investigation, it is intriguing to speculate that the rupture of these spheroids and release of their contents may recruit macrophages and/or modulate Schwann cell injury response. Interestingly, *Sarm1*$^{-/-}$ and *Wld*^{s} failed to affect macrophage recruitment after injury, while macrophages in injured *Wld*^{s} nerve stump showed 'nerve scanning' behavior, elongating and extending their process along the distal nerve before fragmentation (Rosenberg et al., 2012; Tian et al., 2020a). Lack of spheroids along *Wld*^{s} axons might contribute to macrophage scanning behavior as they are looking for the potential targets to engulf. Whether the formation and rupture of axonal spheroids mark the location for phagocytic cells to react or trigger other immune responses during WD remains unclear. As such, understanding the regulation and consequence of these spheroids may help to rationalize therapeutic targets for a range of degenerative disorders.

In summary, this study demonstrates that: 1) severed sympathetic axons develop calcium rich spheroids and membrane ruptures prior to catastrophic degeneration. 2) Mechanistically, we show that sufficient NAD^+ pool is able to suppress the formation of axonal spheroids and delay WD after injury through a Rho-dependent pathway. 3) DR6 and SARM1 do not regulate spheroid formation, but are required for catastrophic degeneration downstream of spheroidal rupture. Based on our results and recent findings, we propose that 4) NMNAT degradation-dependent NAD^+ depletion contributes to spheroid formation, while SARM1 activation-dependent NAD^+ hydrolysis executes axon degeneration after spheroidal rupture in response to injury. Our findings contribute to further understanding of protective NAD^+mechanisms in regulating the development

of axonal spheroids that aid in the application of WD-blocking therapies for neurodegenerative disorders.

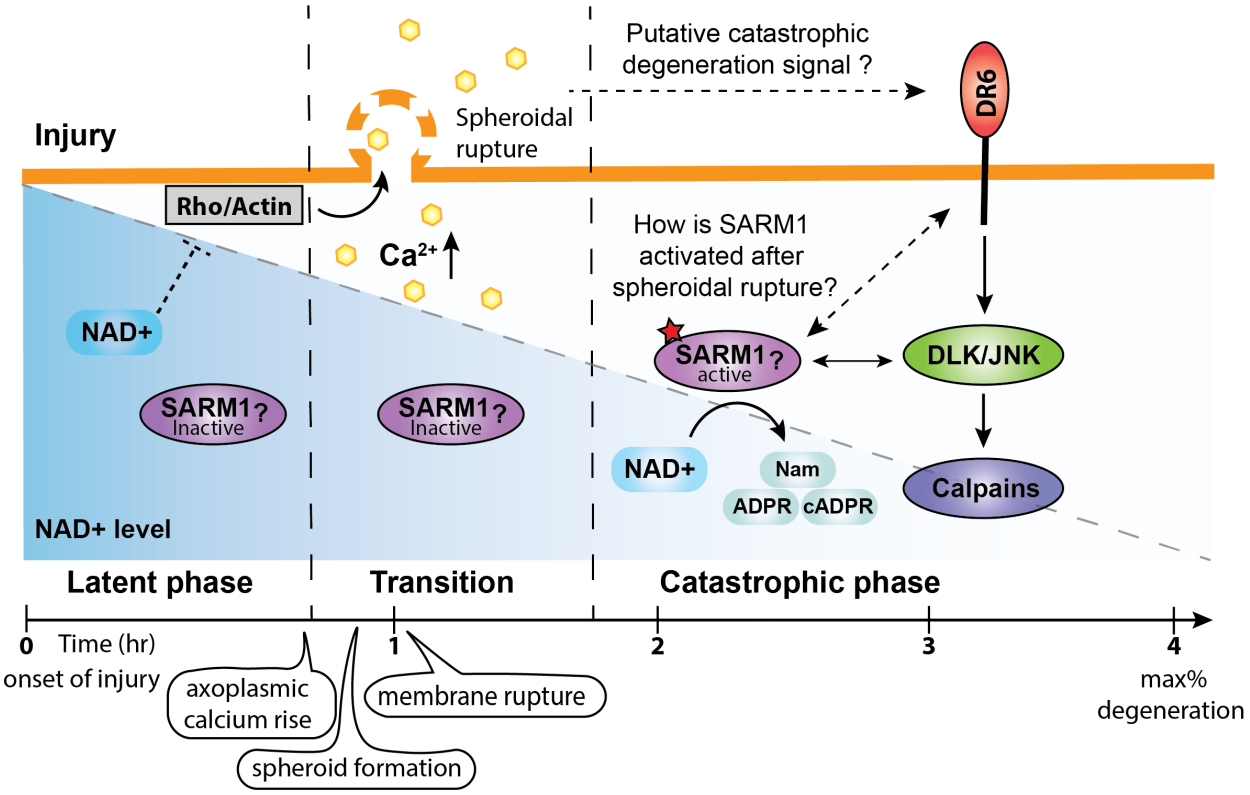

Figure 7: Proposed model for events associated with injury induced axon degeneration of sympathetic neurons

After injury, axoplasmic calcium is increased and enriched in spheroids prior to catastrophic phase. Spheroid formation is regulated by Rho activity and actin remodeling, which is suppressed by NAD^+. The calcium electrochemical gradient across membrane is disrupted by spheroidal rupture. We speculate that axonal NAD^+ level decreases via SARM1 independent catalysis while SARM1 stays inactive prior to spheroidal rupture. DR6 and SARM1 can be activated to promote further NAD^+ depletion and catastrophic degeneration. However, how DR6 and SARM1 get activated downstream of spheroid rupture remains unclear. The schematic representation of the model was drawn in Adobe Illustrator.

Chapter 4[4]

Discussion

Axonal spheroids and neurodegeneration

Abstract

The emergence of axonal spheroids is a universal pathological hallmark of neurodegeneration. Most of them are stationary, while few of them can move and fuse as they grow (see Appendix 1). They are often filled with calcium, NF, membrane bound vesicles, and organelles. Depending on the pathological insult, they sometimes co-localize with disease-related proteins like APP and motor proteins. Initial formation of axonal spheroids depends on the disruption of axonal and membrane tension governed by cytoskeleton and membrane skeleton. Various degenerative triggers, such as injury, oxidative stress, inflammatory factors, and neurotoxic molecules promote the development of axonal spheroids through either convergent pathways regulating cytoskeleton and membrane skeleton (*e.g.* Rho activation) or positive feedback mechanisms associated with impairment of axonal transport. Axonal spheroids have PS exposure, becoming the hotspots for macrophage engulfment. Axonal spheroids are degenerative because they could rupture, providing the gateway for pro-degenerative factor transmission across the membrane.

[4] Y. Yong & C. Depmann. Axonal spheroids and neurodegeneration, *in prep*.

A primary and early effect of dynamic deformation of axons during neurodegeneration is the formation of axonal swellings that appear in a periodic arrangement along axons. These axonal “varicosities”, “spheroids”, or “swellings” have been likened to beads on a string or branches bearing fruit, and are nearly universal (Ramón y Cajal, 1928; Sasaki et al., 1989). They not only have been found in developmental degeneration and the aging brain but also appear in injury, neuropathy, neuroaxonal dystrophy and many neurodegenerative diseases (Kikuchi et al., 1990; Kilinc et al., 2008; Lauria et al., 2003; Luo and O’Leary, 2005; Stokin et al., 2005). Cajal hypothesized that these voluminous balls were often the seat of destructive processes, autolytic in nature (Azmitia, 2002; Ramón y Cajal, 1928). Although spheroids are a common hallmark in degeneration, their characterization, regulation and function have been scarcely examined in the 100 years since Cajal’s initial description.

Recently, we’ve revealed that axonal spheroids are important for damaged axons transitioning from latent phase to catastrophic phase of degeneration in response to trophic deprivation or injury (Yong et al., 2019, 2020). Live and electron imaging, together with biochemical analysis and biophysical modeling have shed light on the mechanism and functional roles of spheroid formation in neurodegeneration. In this review, we summarize the features of axonal spheroids in different degeneration etiologies, propose a potential working model for the regulation of spheroid formation, and emphasize the degenerative roles of axonal spheroids in disease progression and phagocyte recruitment.

Contents within axonal spheroids

Accumulation of cytoskeletal elements in spheroids

Because axoskeletal changes correlate with morphological changes in degenerating axons, it is perhaps intuitive that cytoskeleton elements accumulate in many axonal spheroids. As a significant feature of the pathology of motor neuron disease, axonal spheroids with accumulation of neurofilaments have been observed in ALS cases (Delisle and Carpenter, 1984). Immunohistochemical studies of the post-mortem brains and spinal cords of patients indicate that these spheroids are strongly positive for neurofilament (NF), kinesin and phosphorylated neurofilament and weakly positive for ubiquitin and synaptophysin (Takahashi et al., 1997; Toyoshima et al., 1989, 1998). Similarly, mouse models of neuroaxonal dystrophy and nerves obtained from patients with gracile axonal dystrophy (GAD) showed neurofilament rich axonal spheroids (Prineas et al., 1976; Shinzawa et al., 2008). High levels of tubulin and actin was also detected in spheroids of live cortical neurons treated with hydrogen peroxide as well as mechanically injured chick forebrain neurons (Barsukova et al., 2012; Kilinc et al., 2008). We also found accumulation of tubulin and actin in spheroids of the injured and NGF deprived sympathetic axons (Yong et al., 2019, 2020).

Accumulation of organelles in spheroids

Although distant from the nucleus, axons have constant synthesis, processing, and turnover of proteins and lipids to support neural function. This is achieved through an ER network and a steady stream of mitochondria and vesicles throughout the extent of axonal and dendritic processes (Hollenbeck and Saxton, 2005; Wu et al., 2017). This organelle distribution is maintained by active retrograde and anterograde transport. In response to degenerative triggers, accumulated organelles are often found in axonal spheroids, indicating the disruption of axonal

transport at the site of spheroid formation. Indeed, electron dense bodies, multivesicular bodies, mitochondria, and double membrane bound vesicles are observed in spheroids across a range of degenerative triggers (Kilinc et al., 2008; Griffiths et al., 1998; Beirowski et al., 2010). Importantly, some of the organelles present in spheroids are swollen or deformed, consistent with their behavior in degenerative etiologies (Ferreirinha et al., 2004). In addition, ER and mitochondria are the primary sources of intracellular calcium, which could contribute to the increase of spheroidal calcium level and disrupted calcium homeostasis during axon degeneration.

Accumulation of pathological proteins in spheroids

Impaired axonal transport also affects protein distribution in the axon. As such, many pathological proteins are often found in axonal spheroids in various neurological disorders. In parasitic brain diseases like neurocysticercosis, axonal spheroids were observed across species and demonstrated increased immunoreactivity to APP and ubiquitin (Mejia Maza et al., 2018). Moreover, accumulated APP and ubiquitin in axonal spheroids were shown in various models of AD, hereditary spastic paraplegia (HSP), tramatic brain injury (TBI) (Dawson et al., 2010; Ferreirinha et al., 2004; Griffiths et al., 1998; Johnson et al., 2013; Ohgami et al., 1992; Wirths et al., 2006). In some cases of neuroaxonal dystrophy and PD, α-synuclein immunoreactivity was also present in axonal spheroids (Martin et al., 2006; Newell et al., 1999). Additionally, the microtubule associated protein (MAP), tau and its phosphorylated form have been linked to AD and other neurodegenerative diseases. Similar to APP, phospho-tau has been shown to accumulate in spheroids in a mouse model of AD (Stokin et al., 2005). However, not all axonal spheroids are filled with pathological protein aggregates, some spheroids on injured nerves remain “empty” as lucent cavities under electron microscopy (Beirowski et al., 2010). Interestingly, enrichment of calcium in spheroids has been shown on trophic deprived, injured, stretched, or

toxin-treated axons by us and other groups (Barsukova et al., 2012; Gu et al., 2017; Yong et al., 2019).

Different contents within axonal spheroids have been observed in neurodegeneration. However, how these contents vary as a function of degenerative triggers is unknown. Whether the disrupted cytoskeleton, organelles, and pathological proteins are randomly distributed in spheroids, or they are dependent on the specific signaling pathway remains unclear. Moreover, whether these contents are functionally significant with respect to the formation of spheroids or progression of neurodegeneration needs further investigation.

Regulation of axonal spheroids

The role of the cytoskeleton in spheroid formation

Despite an abundance of evidence correlating axonal spheroids with degeneration, the mechanisms that regulate the formation and growth of these spheroids remain largely unknown. Because these structures represent a significant disruption in the architecture of the axon, it stands to reason that cytoskeletal rearrangements underlie their formation. Indeed, shifting from a uniform cylindrical shape into a “beads on a string” configuration involves localized constriction and bulging due to changes in membrane skeleton and the subaxolemmal network comprised of spectrin/fodrin, actin, ankyrin, integrins, and other transmembrane proteins (Budde and Frank, 2010; Ochs et al., 1997). Moreover, spheroids emerged at regions of cytoskeleton disruption following injury or toxic insult, which could be suppressed by pre-incubation of cytoskeleton stabilizers (Kilinc et al., 2008; Tang-Schomer et al., 2012; Barsukova et al., 2012). Consistently, We also found that actin-stabilizing drug cytochalasin D was able to delay spheroid formation on NGF deprived or injured axons (Yong et al., 2019, 2020). In addition, the membrane periodic skeleton (MPS) composed of actin rings and spectrin tetramers has been shown to regulate axon diameter, swellings and degeneration (Costa et al., 2018; Wang et al., 2019a). Thus, regulation of the cytoskeleton is likely to contribute to the formation of axonal spheroids during degeneration.

Regulation of the cytoskeleton prior to spheroid formation

Actin remodeling is one of the early responses to NGF deprivation and injury, prior to axonal fragmentation (Unsain et al., 2018). Rho GTPases are essential regulators of the cytoskeleton remodelling, which contributes to several aspects of neuronal development and degeneration (Govek et al., 2005). Accumulating evidence suggests an increase in RhoA/ROCK signaling in WD, neuroinflammation and neurodegenerative diseases such as AD, ALS and SCI (Stankiewicz

and Linseman, 2014). RhoA/ROCK may be relevant to axonal deformation since it is known to change the properties of the F-actin cytoskeleton from promoting protrusive activity to generating contractile forces in response to retraction cues (Gallo, 2006). Importantly, we detected RhoA activation in axonal spheroids. Inhibition of RhoA by CT04 suppressed spheroid formation, while activation of RhoA by CN03 promotes spheroid formation in axons that are normally refractive to degenerative cues, suggesting that Rho activation is both necessary and sufficient to drive the formation of axonal spheroids (Yong et al., 2019, 2020).

Disruption of axonal transport

The axonal transport system is a unique and important feature of neurons, allowing efficient, long-distance signal transduction, trafficking of axonal building blocks, and delivery of organelles throughout the axon (Roy et al., 2005). In the anterograde direction, the slow transport system conveys the bulk of the axoplasmic constituents, including cytoskeletal elements. In contrast, the fast transport system functions bidirectionally and carries small vesicles and other organelles (Griffin and Watson, 1988). Many neurological disease-linked genes have been identified as motor proteins, adaptor proteins, and microtubule network proteins, indicating that disrupted axonal transport may be causative and not simply a non-specific by-product of neurodegeneration (Guedes-Dias and Holzbaur, 2019; Sleigh et al., 2019). In fact, there has been a long debate about whether axonal spheroids in neurological disorders is a consequence of impaired axonal transport, or whether it causes the transport defect, or both (Mi et al., 2005). Both light and electron microscopy imaging have revealed focal accumulation of APP, tau, motor proteins and some membrane-bound organelles like mitochondria in the axonal spheroids in various pathological conditions (Ferreirinha et al., 2004; Götz et al., 2006; Kilinc et al., 2008; Tang-Schomer et al., 2012). However, impaired axonal transport in axonal spheroids does not demonstrate causality. Direct evidence comes from a study in a mouse model of AD where impairing axonal transport by reducing the dosage of kinesin-I enhanced the formation of axonal

spheroids and increased amyloid deposition (Stokin et al., 2005). This argues that axonal transport defects could cause spheroid formation, at least in the case of AD. However, in models of trophic deprivation, stretch injury and axotomy, the formation of axonal spheroids is unlikely a result of traffic jams based on the following observations: **1.** Continuous microtubule tracks were seen in a large fraction of spheroids (Tang-Schomer et al., 2012). **2.** No accumulation of vesicles or mitochondria were seen in axonal spheroids at early stages (Beirowski et al., 2010). **3.** Axonal spheroids were not fixed and they could migrate and fuse along the axon as they form (Yong et al., 2019). **4.** The spheroid shapes (lemon like at early stages and clamshell or ball like at late stages) are typical of a surface maintained under tension as opposed to a shape defined by a collection of organelles (Datar et al., 2019). Overall, the formation of axonal spheroids is often associated with the disruption of axonal transport, while its mechanism is not solely dependent on transport blockage.

Transition in size and shape of spheroids

As we described early, axonal spheroids are not fixed in size and shape. The pathways involved in the volume regulation are likely to regulate spheroid growth and related pathology. Osmolarity change at the sites of axonal spheroids is considered to be a major player because that elastic stresses in the cytoskeleton would provide the driving force for water and ions to leak through channels on the membrane to effect volume regulation (Fernández and Pullarkat, 2010; Pullarkat et al., 2006). Additionally, mechanical stress could induce spheroid formation by activating transient receptor potential cation channel subfamily V member 4 (TRPV4). The resulting persistent calcium influx brought in water to cause volume expansion and also reduced the microtubule stabilizing binding protein STOP by calmodulin to promote further spheroid formation (Gu et al., 2017). Consistent with the idea of osmolarity shock driven by calcium flux, focal aggregation of the NCX and VGCC subunits was found at the sites of spheroids in stressed axons (Barsukova et al., 2012). Although accumulated calcium in axonal spheroids has been shown in

many degeneration models across species, we found that depleting intracellular calcium by BAPTA-AM failed to suppress the generation axonal spheroids but decreased their average size (maintaining a lemon-like shape instead of clamshell or ball like shape) (Yong et al., 2019). This does not argue against the importance of calcium in spheroid formation, but supports the hypothesis that calcium flux and attendant osmolarity changes likely contribute to growth and maturation of pre-existing axonal spheroids.

Biophysical model for spheroid formation

The morphological changes and formation of spheroids we observed on degenerating axons is known as “pearling instability” in the physics community. Theoretical models and computational simulations of this axonal behavior have been established suggesting that spheroid formation is a tension-driven shape instability, dependent on axonal tension and membrane surface energy (Datar et al., 2019; Shao et al., 2020). Based on the pathogenesis analysis and biophysical measurements of axonal spheroids, we propose a model of spheroid formation (Fig.1). Specifically, in response to pathological insult, minor changes of membrane skeleton and cytoskeleton, such as the breakage of few but not all microtubules and actin remodeling by Rho activation, lead to localized release of axonal tension and reduction of membrane tension, driving the initial formation of axonal spheroids. The expanding membrane and cytoskeletal stress near spheroids then induces ion and water flow to drive growth of these spheroids. Calcium flux, axonal transport impairment, and energy deficits due to initial spheroid formation further promote

development of these spheroids along the axons at later stages. This positive feedback loop eventually drives irreversible spheroid formation that contributes to neurodegeneration.

Figure 1: Proposed model of axonal spheroid in neurodegeneration

In the latent phase of degeneration, no morphological change is observed in axons. NGF deprivation (indicated in violet) triggers *de novo* synthesis of pro-degenerative molecules, caspase activation, p75NTR and Rho activation, while injury (indicated in red) leads to

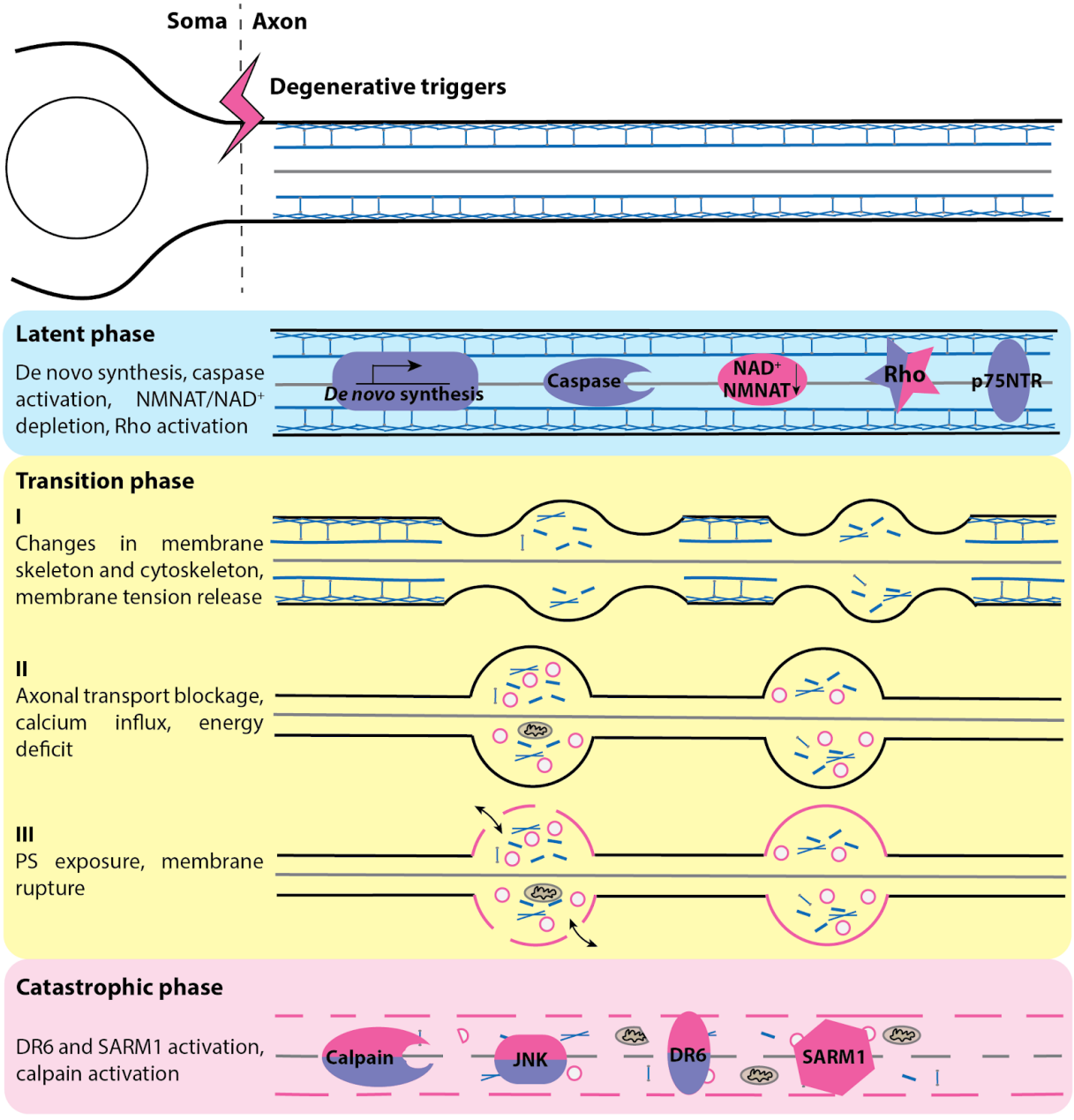

NMNAT/NAD^+ depletion and Rho activation. These upstream events promote the formation of axonal spheroids in the transition phase. Early changes in membrane skeleton and cytoskeleton promote the release of membrane tension and emergence of the lemon-like shape of spheroids. Subsequent disruption of axonal transport, calcium dysregulation, and energy deficit further promote the growth of axonal spheroids, becoming clamshell or ball-like shape. These spheroids have PS exposure on the outer surface of the membrane and develop membrane rupture that allows the transmission of prodegenerative molecules across the membrane. Ruptured axonal spheroids, together with the activation of calpain, JNK, DR6 and SARM1 promote cytoskeleton breakdown and catastrophic axon degeneration. Other molecules, such as UPS, Bax, Axed, MAPK signaling cascade, have not been assigned to particular phases of degeneration. And their roles in regulating spheroid formation remain unclear.

Rupture of axonal spheroids

As the early phenotypic representation of dying neurons, axonal spheroids also share similar features with neuron death. Plasma membrane rupture that is commonly seen in necrotic cell death is also observed in axonal spheroids, which appeared more frequently at later stages of axonal degeneration. Fluorescent neutral dextrans less than 10 kDa are able to enter the spheroids via membrane rupture, indicating that the pores on the spheroidal membrane are likely non-selective (Yong et al., 2019, 2020; Zhang et al., 2018).

Beyond membrane rupture, there is also evidence for regulated pore formation in axon degeneration. Recent studies have revealed the involvement of necroptosis activation in axon degeneration. Pharmacological inhibition of the necroptotic kinase RIPK1, knockdown of the key necroptotic regulator RIP3 or the downstream effector MLKL (mixed lineage kinase domain like pseudokinase) delayed axonal degeneration on sensory neurons after mechanical and toxic insults (Arrázola et al., 2019). As the final executioner of necroptosis, MLKL translocates to the plasma membrane creating pores capable of allowing molecules less than 10kDa to exchange between the axoplasm and extracellular space (Heckmann et al., 2019; Ros et al., 2017). Whether MLKL pores contribute to spheroidal membrane rupture remains an open question. Interestingly, although MLKL is transiently activated after axonal damage, MLKL does not induce membrane rupture and calcium influx in axons as its function in cell bodies. Instead, it has been proposed that MLKL may stimulate SARM1 dependent axon degeneration (Arrázola et al., 2019; Ko et al., 2020). Additionally, it has been shown that necroptosis is dispensable in motor neuron degeneration in ALS (Wang et al., 2020). While the contribution of necroptotic mediators in axon degeneration varies in different neuronal types, the membrane rupture on axonal spheroids might be regulated by MLKL independent mechanisms. Another pathway to induce membrane rupture

in dying cells is the activation of the pore-forming protein gasdermin D (GSDMD) in pyroptosis (McKenzie et al., 2020). Emerging evidence suggest the formation of GSDMD pores in microglia, macrophages, and oligodendrocytes in neurodegeneration (McKenzie et al., 2018). Interestingly, neurons with little or low GSDMD expression seem to be susceptible to caspase-1 mediated but GSDMD independent cell death (Tsuchiya et al., 2019). However, whether the spheroid rupture is driven by the formation of GSDMD pores or simply the result of disrupted membrane tension requires further investigation.

Function of axonal spheroids

Evolutionarily speaking, why do organisms develop spheroids in the nervous system? Are they merely decorative or are spheroids functionally significant for axon degeneration and regeneration allowing the system to defend against harmful environmental stress? Similar to WD in the distal nerves after transection, axonal spheroids might promote localized degeneration and clearance of debris of an axon without influencing the main neurite and cell body (Coleman, 2005; Luo and O'Leary, 2005).

Phosphatidylserine exposure and clearance

Similar to the phosphatidylserine (PS) exposure on the outer surface of cell membrane during apoptosis, PS exposure was also observed on the membrane of degenerating DRG axons after NGF deprivation or vincristine treatment (Shacham-Silverberg et al., 2018). Interestingly, studies have shown that PS is exposed on non-apoptotic degenerating neurites in a specific spatiotemporal pattern, which causes phagocytes to engulf the neurites (Sapar et al., 2018; Shlomovitz et al., 2019). Consistently, we showed the PS flip specifically on the spheroids of SCG axons after NGF deprivation (Yong et al., 2019), suggesting that PS exposure can be targeted to selective parts of the cell membrane. As a well defined phagocytotic signal, PS externalization is promoted by phospholipid scramblases mediated by calcium or capsease (Nagata et al., 2016; Segawa et al., 2014). Interestingly, blocking extracellular calcium influx did not prevent PS exposure, while inhibiting caspase activity suppressed PS exposure only in apoptotic dependent axon degeneration (Shacham-Silverberg et al., 2018). Moreover, transected axons of retinal ganglion cells isolated from *Wld*^{s} rats with suppressed axonal spheroid formation showed a delay of PS exposure and lower speed of PS exposure spread compared to injured wild-type axons (Almasieh et al., 2017). And PS exposure on injured dendrites depended on NAD^{+} depletion, not

caspase activity (Sapar et al., 2018). Local ATP production through autophagy could also promote PS exposure on injured DRG axons (Wakatsuki and Araki, 2017). These results suggest that while localized perturbation of PS asymmetry is common in degenerating axons, the trigger of PS exposure on axonal spheroids or different axon domains is context dependent. As a neuronal "eat-me" signal, localized externalization of PS mediates developmental synaptic pruning by microglia in mouse hippocampal neurons, while PS exposure on damaged axons acts as a "save-me" signal to promote axonal fusion after injury in *C. elegans* (Abay et al., 2017; Scott-Hewitt et al., 2020). Therefore, It is possible that axonal spheroids with PS exposure function as the trash cans laid out on the curb of damaged axons to promote phagocytosis and clearance.

In vivo studies of degenerating nerves and staining of postmortem brain slices revealed that axonal spheroids were detected throughout the white and gray matter in disease-specific regions in some cases, but are particularly abundant in non-myelinated regions and and where small-diameter, lightly myelinated axons reside (Griffiths et al., 1998; Ochs et al., 1997). Additionally, numerous axonal spheroids were observed in proximity to macrophages (Takahashi et al., 1997), indicating that axonal spheroids may affect macrophage infiltration. Supporting this notion, PS exposure on axonal spheroids could act as the "eat-me" signal to recruit macrophages in response to pathological insult (Shacham-Silverberg et al., 2018; Yong et al., 2019). However, macrophage recruitment was not impaired in *Wld*^{S} expressing zebrafish, which did not develop axonal spheroids after injury. A novel "nerve scanning" behavior of macrophages was observed in these animals (Rosenberg et al., 2012), indicating that macrophage engulfment, instead of recruitment may be associated with axonal spheroids. We also examined the behaviors of macrophages near injured axons and found the formation of phagocytic cups around the axonal spheroids (see appendix 2). These suggest that axonal spheroids with PS exposure might be the hotspots for macrophage engulfment to promote clearance and regeneration.

Rupture and progression of degeneration

Membranes compartmentalize the cell and organize cellular processes, whose perturbation has been shown in many neurodegenerative diseases (de Groot and Burgas, 2015). Membrane rupture in dying neurons allow the release of intracellular contents to trigger inflammatory response and damage to neighboring cells (Fricker et al., 2018). It also allows the influx of pathological molecules like calcium from extracellular space to drive axon degeneration (Witte et al., 2019). Interestingly, we found the development of membrane rupture on axonal spheroids, which led us to speculate that disrupted electrochemical gradient across membrane and diffusion of pro-degenerative factors via spheroidal rupture could promote catastrophic axon degeneration. Indeed, treatments of both NDCM and ICM collected after spheroidal rupture were able to hasten the entry of catastrophic phase of degeneration in recipient axons that were originally in latent phase *in vitro* (Yong et al., 2019). Thus, ruptured axonal spheroids could be the gateway for pro-degenerative factor transmission across the membrane to coordinate degeneration of nearby vulnerable axons or axon fragments.

However, the identity of these pro-degenerative factors have yet to be identified. We detected increased calcium levels in conditioned media after spheroidal rupture, which promoted catastrophic degeneration of injured or NGF deprived axons (Yong et al., 2019, 2020). Importantly, depleting intracellular calcium stores suppressed the increase of extracellular calcium after membrane rupture. Chelating calcium in conditioned media by EGTA or chelex was able to suppress the pro-degenerative effect (Yong et al., 2019). These results suggest that calcium could be one of the pro-degenerative factors transmitted via spheroidal rupture. However, the intracellular calcium level is usually kept relatively low with respect to extracellular space (Maravall et al., 2000). Spatiotemporal patterning of calcium contributes to neuronal function and signaling transduction (Bagur and Hajnóczky, 2017). How intracellular calcium gets released into the extracellular environment against overall electrochemical gradient is unknown. It's possible

that localized spheroidal calcium concentration is higher than the extracellular calcium level prior to membrane rupture. But whether the ruptured spheroids are sufficient to drive the calcium-dependent catastrophic degeneration remains an open question.

Moreover, the downstream receptors of prodegenerative ligands derived from ruptured axonal spheroids have not been characterized. We showed that DR6 was likely to act downstream of spheroidal rupture to coordinate catastrophic degeneration in response to NGF deprivation and injury (Yong et al., 2019, 2020). However, no calcium binding site or sensitive motif in DR6 has been identified. Interestingly, DR6 can be cleaved by α-secretase ADAM10 (a disintegrin and metalloproteinase 10) that plays important role in neuronal homeostasis and pathology (Endres and Deller, 2017). Increased calcium, together with surface-exposed PS, trigger ADAM10 sheddase function (Bleibaum et al., 2019). Whether accumulated spheroidal calcium and PS exposure promote the ADAM10-dependent DR6 cleavage and whether cleaved DR6 activate downstream death signaling to coordinate axon degeneration require further investigation.

Concluding remarks

Although the field is making headway in elucidating the regulation and function of axonal spheroids in neurodegeneration, a number of questions remain unanswered. First, how do axonal spheroids develop in the context of a myelin sheath? Most evidence related to the regulation of spheroid formation comes from *in vitro* studies of pure neuronal cultures. Histological analysis of brain slices and nerve sections reveal uneven distribution of axonal spheroids across regions (Beirowski et al., 2010; Kikuchi et al., 1990). It's possible that spheroids are only relevant in degenerating unmyelinated or pre-myelinated axon tracts. Alternatively, they may have a role in coordinating glial response in developmental and pathological degeneration.

Second, is the formation and rupture of axonal spheroids a conduit for disease progression? For example, disease related molecules such as tau, APP, and α-synuclein accumulate in some axonal spheroids, which could potentially be exposed to extracellular environment and contaminate "by-stander" neurons via spheroid rupture (Newell et al., 1999; Ohgami et al., 1992; Tang-Schomer et al., 2012). Since the spheroidal rupture is non-selective, neurotoxic factors in the extracellular space could also enter the axon segments to speed up the degeneration process. Further identification of spheroid-derived degenerative molecules is required.

Third, many features of the axonal spheroids, such as PS exposure, NF accumulation, RhoA activation, actin remodeling and cation channel aggregation, point to cytoskeleton reorganization and signaling domains distinct from non-spheroidal regions of the axons. What are the membrane and cytoskeleton coupled signaling complexes in the axonal spheroid? Does spheroidal signaling complexes contribute to the progression of degeneration?

As a convergent point common to all degenerative processes, axonal spheroid represents a worthwhile target for therapeutic consideration. Characterization of axonal spheroids with various contents and functions in axon degeneration has shed new light in the development and progression of neurodegeneration. Moreover, further understanding of these axonal spheroids will help provide great therapeutic perspectives for neurodegenerative disorders.

Chapter 5[5]

Materials and Methods

Mice

All experiments were carried out in compliance with the Association for Assessment of Laboratory Animal Care policies and approved by the University of Virginia Animal Care and Use Committee. All mice are on a C57BL/6J.129S mixed background except for *Wld*^{s} mice, which were FVB/NJ background. *Wld*^{s}, *p75NTR*$^{-/-}$ and *Sarm1*$^{-/-}$ animals were purchased from the Jackson labs. *DR6*$^{-/-}$ animals were a generous gift from Genentech. Males and females were mixed in all experiments.

Primary Sympathetic neuronal cultures

Sympathetic neuron cultures were established as described previously (Deppmann et al., 2008). Briefly, neurons were obtained by dissociation of P0-P2 mouse superior cervical ganglia. These neurons (from each litter of pups) were plated in compartmentalized microfluidic devices in DMEM supplemented with 10% FBS, penicillin/streptomycin (1U/mL), and 45 ng/mL of NGF purified from mouse salivary glands. Glia are removed from cultures using 5 μM cytosine arabinofuranoside (Ara-C) (Sigma) for 48-72 hours. For NGF deprivation, cultures were washed three times with media lacking NGF and then maintained in NGF- deficient media containing a neutralizing antibody (1μg/mL anti-NGF antibody, Millipore) through designated time points at 37^{0}C.

Axotomy experiments in vitro

Neurons from each litter of pups were allowed to project their axons to the axonal chamber (3-7 DIV) after plating. After the axons had grown into the axonal chamber, neurons were enucleated

[5] Published in part in Y. Yong *et al.,* A microfluidic culture platform to assess axon degeneration. In Babetto E (Ed.). *Axon degeneration: methods and protocol. Springer publishers* (2020).

by aspirating 3mL of 1x PBS through the cell body chamber leaving the axons intact in their respective chamber. Unless otherwise indicated, both compartments were replaced with DMEM supplemented with 10% FBS, penicillin/streptomycin (1U/mL) and 45 ng/mL of NGF and incubated at 37^0C and 10% CO_2 for indicated times. For technical consistency, we used encleation in microfluidic chambers for injury. In our experimental system, axons originating from wild-type dissociated SCG neurons degenerate within 2 hours after injury, while neurites originating from SCG explant degenerate within 8 hours after scalpel cut (Loreto et al., 2015). The difference in axon degeneration time window could be due to dissociation procedure and time in culture. We suspect that the most likely explanation for this difference is in the media volume of these cultures, where spheroid derived pro-degenerative molecules are more concentrated in the 200µL volume of an MFD as opposed to the 1-3mL volume bathing explants. Nevertheless, the morphological changes from latent to catastrophic phase, as well as the calcium wave in "physical cut method" remain the same as what we observed in our model (Loreto et al., 2015).

Fabrication and use of microfluidic devices

Microfluidic devices were generated as described previously (Park et al., 2006). These chambers were affixed to coverglass coated with poly-D-lysine (50µg/mL) and laminin (1µg/mL).

Macrophage axon co-culture

SCG neurons were cultured in microfluidic devices for 6-7 days. Bone marrow drive macrophages (BMDMs) were harvested from *hCD68-GFP* mice and maintained in IMDM media supplemented with heat inactivated FBS, L929 cell conditioned media, non-essential amino acids, and penicillin-streptomycin in 150mm plates for 5-6 days. BMDMs were then collected from plates and seeded in the distal axon channels of the SCG microfluidic cultures (6000 cells/plate for live imaging). Live imaging and other experiments were performed 1 day after the co-culture.

Immunocytochemistry

Immunocytochemistry was carried out as previously described (Singh et al., 2008). Briefly, at the indicated times, axons were fixed in 4% paraformaldehyde (w/v)/ phosphate buffered saline (PBS) at room temperature for 20 minutes, washed 3x5min with 1x PBS, and blocked/permeabilized (5% goat serum, 0.05% Triton-x-100 in PBS) for 1 hour at room temperature. Axons were then incubated overnight at 4^0C with primary antibody diluted in blocking buffer. Cells were then washed 3x5 min with 1x PBS and incubated with fluorescent secondary antibody for 1 hour at room temperature. Cells were again washed with 1x PBS three times and imaged using a fluorescent inverted microscope. The antibodies used in this study are mouse anti-Tuj1 (1:1000, Covance), and goat anti-mouse Alexa 488 (1:800, Life Technologies). For active Rho staining, axons were incubated with 50µg/mL of GST-Rhotekin-RBD fusion protein in blocking solution for 1 hour at room temperature, washed 3x5min with 1x PBS. Cells were then incubated with anti-GST (1:800, Sigma G1160) diluted in blocking buffer for 1 hour, washed 3x5min with 1x PBS and incubated with fluorescent secondary antibody for 1 hour at room temperature. All *in vitro* experiments were performed in triplicate with at least two microfluidic devices used for each condition.

Live imaging

Sympathetic neuron cultures were washed 3 times with DMEM/F-12, Phenol Red free, and incubated for 30 minutes at 37^0C and 10% CO_2 with live imaging dyes diluted in DMEM/F-12, Phenol Red free. Cells were then imaged under Leica SP5 X confocal microscope in W.M. Keck Center at the University of Virginia. Axons in grooves of microfluidic chamber were imaged after NGF deprivation or injury. For assessing flipping of phosphatidylserine on axonal spheroids, Annexin V red reagent (IncuCyte, 4641) was diluted in DMEM/F-12, Phenol Red free (1:200) after NGF deprivation. For membrane rupture, dextran dyes diluted in DMEM/F-12, Phenol Red free were added to the microfluidic chamber after 17 hours of NGF deprivation or 20 minutes after

injury. The dyes used in this study are Fluo-4 AM (1μM, F14201) and Dextran Texas Red, neutral, 3 kDa (50μM, D3329), 10 kDa (50μM, D1828) and 70 kDa (50μM, D1830). All dyes were purchased from Thermo Fisher Scientific. Drugs used for manipulating spheroid formation are Z-VAD-FMK (50μM, Enzo, ALX-260-020), Calpain inhibitor III (20μM, Millipore, 208722), Actinomycin D (1μg/mL, Sigma, A9415), CT04 (1μg/mL, Cytoskeleton Inc), Cytochalasin D (10μg/mL, Sigma, C2618), CN03 (1μg/mL, Cytoskeleton Inc), LM11A-31 (2ng/mL, Cayman Chemicals, 21982), anti-BDNF (20μg/mL, Millipore, AB1779SP). 9650 immune serum was a gift from Bruce Carter in Vanderbilt University. For macrophage-axon co-culture, plates were imaged under the Zeiss 980 confocal airyscan microscope in W.M. Keck Center at the University of Virginia.

Image Processing and analysis

Axon degeneration in culture was quantified from β3-tubulin stained fluorescence images by counting the number of individual axons at the leading edge that had at least three beads/blebs as described (Zhai et al., 2003). A blinded investigator counted ten representative pictures of the axons, in two microfluidic chambers per condition/time point. On each image 10 50μm boxes were randomly assigned to single axons. The investigator took care not to box bundles of axons, which may confound analysis. Then the number of boxes, which had 3 or more beads/blebs were counted and categorized as degenerating axons. Equal to or more than 80% degeneration was considered maximum degeneration and equal to or less than 10% degeneration of axons was considered as minimum degeneration. The percentage of the total number of degenerating axons was calculated using Microsoft Excel. At least 300 total axons were counted for each condition. The standard error of the mean was considered as error. In live imaging, Ca^{2+} intensity (ΔF/F0), the size (S/S0) and number of axonal spheroids were quantified in selected ROI (single axon or axonal spheroid) by Fiji software (Schindelin et al., 2012). Each experiment was repeated at least 3 times with separate litters of mouse pups of the same genotype. For quantification of

macrophage protrusions, cell edge and protrusions were isolated by the FiloQuant plug-in in Fiji software. Center of the macrophage was manually set in each movie.

Conditioned media experiments

Established compartmentalized recipient neuron cultures were deprived of NGF by washing with NGF free DMEM three times and incubating at 37^0C with a neutralizing anti-NGF antibody for 12 hours. To collect NGF deprivation conditioned media (NDCM), donor neuron cultures were washed with NGF free DMEM three times and treated with a neutralizing anti-NGF antibody at 37^0C for 24 hours. To collect injury conditioned media (ICM), donor neuron cultures were injured by PBS aspiration in the cell body chamber at 37^0C for 4 hours. For each device, a volume of ~100µL of NDCM was collected, including the media in the wells of the device on the axonal side and the media in the axonal channel. NDCM or control conditioned media was applied on recipient axons for 5 hours. ICM was applied on recipient axons for 4 hours.

Calcium measurement

Conditioned media was diluted to milliQ water (1:20) and mixed thoroughly. 100µL of reaction mixture was made with 1µL HEPES, 2µL 1mM Fluo-4 (20mM working concentration, Life Technologies), 10µL diluted conditioned media, and 87µL water. Black 96 well plate was used in Spectrophotometric assay. Eight $CaCl_2$ standards (2.54µM, 4.87µM, 9.75µM, 19.5µM, 39µM, 78µM, 156µM, and 313µM) were used to calculate standard curve for analyzing Ca^{2+} concentration in conditioned media.

Exogenous Calcium assay

Sympathetic neuron cultures were washed three times with DMEM supplemented with 10% FBS, penicillin/streptomycin (1U/mL), and then incubated in NGF deficient media containing a neutralizing antibody (1µg/mL anti NGF antibody, Millipore) for 12 hours. For exogenous calcium

concentration below 1.8mM (DMEM), cells were washed 3 times with DMEM Ca^{2+} free media. $CaCl_2$ was added to DMEM Ca^{2+} free media to indicated final concentrations, which was then applied to cultures 37^0C and 10% CO_2 for 5 hours.

Experimental design and statistical analysis

Statistical analysis was performed in Prism 8.0 software (GraphPad). All measurements are shown as mean ± SEM. For samples defined by one factor, data were compared by unpaired two-tailed *t* tests for two samples or one-way ANOVA with Tukey's *post hoc* multiple comparisons test for three or more samples. For samples defined by two factors, data were compared by two-way ANOVA with Sidak's *post hoc* multiple comparisons test. Sample size (n) was defined as the number of axons or axonal spheroids counted in the live imaging experiment, or the number of independent cultures that were quantified in each experiment. The null hypothesis was rejected at the 0.05 level. *P* values <0.05 are considered significant and represented by asterisks. The statistical test, sample size (n), and the *p* values are reported in the figure legends.

Appendix 1

Growth and movement of axonal spheroids

Live imaging of injured or stressed axons have revealed that axonal beading or varicosity starts at the early stages of degeneration, which grow bigger and become spheroids at later time yet prior to axon fragmentation (Barsukova et al., 2012; Beirowski et al., 2010; Yong et al., 2019). As we described in both trophic deprived and injured axons grown in microfluidic devices, calcium rich axonal spheroids could grow 4-fold bigger than their initial size within an hour in the transition from latent to catastrophic phase of degeneration. Moreover, we developed a negative staining strategy where the fluorescent neutral dextran dye was added in the culture media to allow us to visualize and trace individual axonal spheroids over time. Importantly, we found that most of the spheroids were stationary in response to NGF deprivation or injury. Only 2.9±1.4% and 10.4±6.0% of spheroids moved anterogradely and retrogradely after NGF deprivation, respectively. Interestingly, 17.8±3.6% and 7.1±3.3% of spheroids moved anterogradely and retrogradely after injury, respectively (Fig.1A,C). Our observation that moving spheroids favor anterograde direction on injured axons might indicate the direction of degeneration, consistent with previous reports about anterograde WD in transected distal nerves (Beirowski et al., 2005). Additionally, few fusion events in multiple axonal spheroids were observed in our recordings (Fig.1B), suggesting dynamic membrane remodeling in these spheroids. Nevertheless, we still don't know what mechanisms drive the movement of axonal spheroids during degeneration.

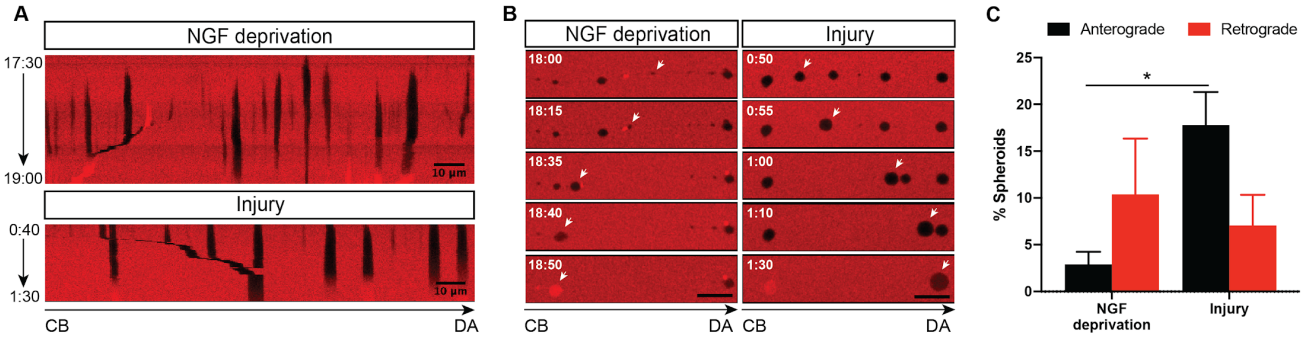

Appendix figure 1: Movement of axonal spheroids

(A) Representative images, (B) kymographs, and (C) quantification of the movement of axonal spheroids after NGF deprivation or injury. White arrows indicate the movement and fusion of spheroids. Scale bar = 10µm. Data are reported as mean±SEM, *p<0.05, two-way ANOVA with Tukey's multiple comparison test.

Appendix 2

Macrophage engulf axonal spheroids

To determine whether axonal spheroids are the sites of phagocytosis, we examined the behaviors of macrophages near axonal spheroids by co-culturing GFP labeled bone marrow derived macrophage (BMDMs) with injured axons. Interestingly, we found that nearby macrophage sent processes towards axonal spheroid and formed a phagocytic cup near it, while some macrophages seated on the regions with clusters of axonal spheroids and used them as anchors for engulfment (Fig.2A, B). Moreover, BMDM protects distal axons from catastrophic degeneration in response to injury, which is partially diminished in cultures after incubation of annexin V that masks PS exposure on axonal spheroids (Fig.2C, D). These data suggest that axonal spheroids might be the hotspots for macrophage targeting and engulfment to promote clearance and regeneration.

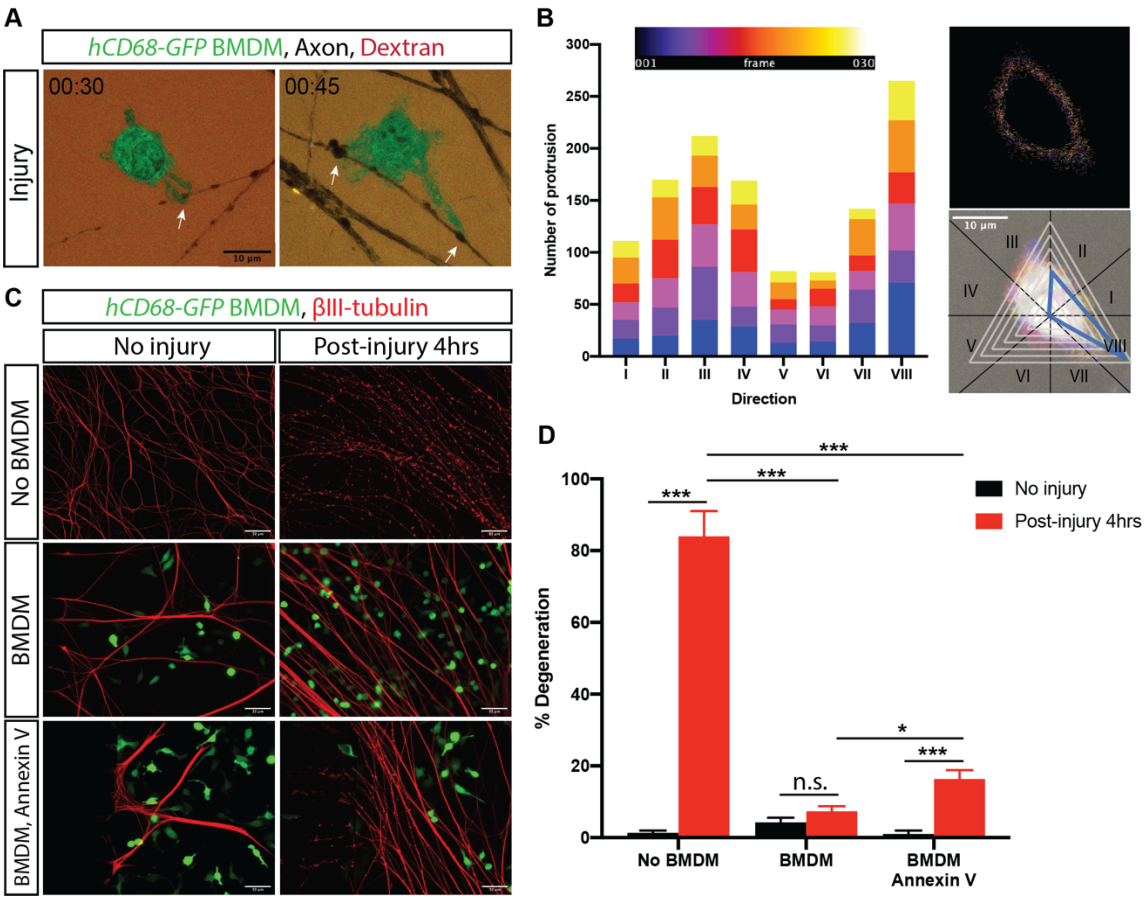

Appendix figure 2: Macrophage send protrusions toward axonal spheroids and suppress degeneration

(A) Representative images of GFP-BMDM and axonal spheroids after injury. White arrow in the left panel indicates the phagocytic cup of macrophage near the axonal spheroid, while the white arrows in the right panel mark the anchor points of macrophage along the axon. Scale bar = 10µm (B) Color coded temporal representation of extracted protrusions (upper right) of the macrophage, distribution of the maximum extension (lower right), and quantification of the protrusion numbers in different direction zones over time (left). (C) Representative images and (D) quantification of percentages of degeneration in pure neuronal cultures and co-cultures of axons and BMDMs in response to injury with or without Annexin V incubation. For axon-BMDM co-cultures, BMDMs were plated in the distal axon chamber 1 day prior to injury. Annexin V was applied to distal axon

chamber immediately after injury. Scale bar = 50μm. Data are reported as mean±SEM, n.s.=not significant, *p<0.05, ***p<0.0001. Significant difference is determined by two-way ANOVA with Tukey's and Sidak's multiple comparison tests.

Appendix 3

Distinctive roles of DR6 and p75NTR in degeneration

Death receptors are members of TNFRSF characterized by the presence of a conserved intracellular death domain and are able to trigger cell death. In the nervous system, death receptors regulate neurite growth and apoptosis in physiological condition, and contribute to pathology of neurodegenerative disease (Mc Guire et al., 2011). Here, we focus on two death receptors widely expressed by neurons and required for axon degeneration, DR6 and p75NTR, whose expressions are developmentally regulated, showing high expression in early development or pathological conditions (Haase et al., 2008; Meeker and Williams, 2014). As a orphan receptor, DR6 stimulation by APP binding or prion peptide resulted in caspase 3-dependent neuronal cell death and caspase 6-dependent axonal degeneration (Nikolaev et al., 2009; Wang et al., 2015; Zeng et al., 2012). p75NTR, on the other hand, binds to all neurotrophins and initiates survival or destructive signaling cascade depending on the trigger and condition (Ibáñez and Simi, 2012). In this thesis, we've characterized distinctive roles of DR6 and p75NTR in axonal degeneration *in vitro*. In response to trophic deprivation, *p75NTR*$^{-/-}$ axons showed extended latent phase of degeneration and diminished spheroid formation. *DR6*$^{-/-}$ axons were resistant to NDCM-induced degeneration (Gamage et al., 2017; Yong et al., 2019). We found that p75NTR regulates spheroid formation by activating RhoA, while DR6 acts downstream of spheroid formation and rupture to gate catastrophic axon degeneration (Yong et al., 2019). Interestingly, in response to injury, knocking out p75NTR axons did not protect axons from developing axonal spheroids or degeneration. Moreover, DR6 was required for coordinate ICM induced degeneration downstream of spheroid rupture. Collectively, these data suggest that p75NTR acts on upstream of axonal spheroid formation in developmental degeneration, while DR6 regulates pathways downstream of axonal spheroids in both developmental and Wallerian degeneration. However,

the molecular mechanisms of DR6 activation and downstream signaling related to degenerative players including calpain, JNK, and SARM1 require further investigation.

Neurons are not the only player in the nervous system. Axons are often wrapped by myelin sheath and surrounded by Schwann cells *in vivo*. During development, neurotrophins and cell adhesion molecules guide the axo-glial contact. The Schwann cells that are closely associated with the axon then myelinate, extending the myelin process around target axons and forming segments and nodal regions (Rao and Pearse, 2016; Sherman and Brophy, 2005). Studies have shown that endogenous BDNF activates p75NTR to enhance myelin formation and inhibit Schwann cell migration by Src kinase dependent activation of RhoA, whereas NT-3 inhibits myelin formation by TrkC receptors (Bentley and Lee, 2000; Cosgaya et al., 2002; Yamauchi et al., 2004). In addition, asymmetrical localization of polarity protein Par-3 in Schwann cells recruits p75NTR to the axo-glial junction, forming a complex necessary for myelination (Chan et al., 2006). In contrast to the pro-myelin effect of p75NTR during development, DR6 is a negative regulator of oligodendrocyte maturation. Blocking DR6 promotes precocious myelination in CNS (Mi et al., 2011; Popko, 2011). Interestingly, DR6 is not expressed in Schwann cells, but has similar effect in myelination in PNS. Neuronal DR6 was found to be cleaved by ADAM10, releasing soluble DR6 ectodomain to inhibit Schwann cell proliferation and myelination during early development (Colombo et al., 2018). We also co-cultured DRG axons derived from E14.5 *DR6*$^{-/-}$ animals with p75NTR positive Schwann cells in microfluidic devices (Fig.3A). Consistent with the previous finding, we found that application of DR6 ectodomain in the co-cultures lead to aberrant myelination as indicated by the myelin ovoid in immunostaining (Fig. 3B). However, whether neuronal DR6 acts *in trans* on Schwann cells to regulate myelination during development via p75NTR dependent or independent pathway remains unclear.

In pathological condition, p75NTR not only mediates axon degeneration, but also plays important roles in demyelination and remyelination. The expression of p75NTR and NGF genes is upregulated after axotomy, which could lead to schwann cell death (Ferri and Bisby, 1999; Hall et al., 1997; Soilu-Hänninen et al., 1999; Syroid et al., 2000). And NGF accelerates Schwann cell autophagy-mediated myelin debris clearance via p75NTR/AMPK/mTOR signaling pathway to promote demyelination after injury (Li et al., 2020). In neurodegenerative diseases, expression of p75NTR is considered as a marker of demyelinating Schwann cells (Kim et al., 2019). The intracellular domain of p75NTR was shown to localize at nucleus in Schwann cells to promote proliferation, preparing for nerve remyelination and regeneration (Akassoglou et al., 2002; Provenzano et al., 2011; Scott and Ramer, 2010). Indeed, knockout of p75NTR impaired remyelination of injured sciatic nerves and showed decreases in myelin sheath thickness in regenerating nerves (Song et al., 2006; Tomita et al., 2007). However, previous work in our lab showed that *p75NTR*$^{-/-}$ did not suppress axon degeneration nor demyelination in sciatic nerves two weeks after transection (Gamage et al., 2017). This discrepancy is likely due to the different time windows after injury (4-10 weeks after transection in their studies). Because p75NTR is expressed in both axon and schwann cells, it's important to delineate the relative contributions of axonal and glial p75NTR in neurodegeneration by using conditional knockout animals in future studies. Unlike p75NTR, much less is known about the roles of DR6 in demyelination induced by injury. Our lab found that knockout of DR6 protected axons from degeneration in transected sciatic nerve, which had less or thinner myelin sheath than WD deficient mice (Gamage et al., 2017). The perseverance of axons and axo-glial contact in *DR6*$^{-/-}$ mice might contribute to incomplete myelin degradation after injury, but the specific mechanism is unknown. Interestingly, we found that double knockout of DR6 and p75NTR in female mice displayed significant protection against demyelination in sciatic nerves 1 week after transaction, maintaining about 35% of intact myelin sheath (Fig.3C,D). This result suggests potential functional interaction between DR6 and p75NTR in regulating demyelination during degeneration, at least in female animals. Additionally,

previous study showed that CRD in ectodomain of DR6 interacts with p75NTR *in cis* to promote cortical neuron death in response to Aβ (Hu et al., 2013). Based on our observation of axon and myelin degeneration in *DR6*$^{-/-}$, *p75NTR*$^{-/-}$, and *DR6*$^{-/-}$*; p75NTR*$^{-/-}$ animals, we propose that in response to injury, axonal DR6 might be cleaved by calcium sensitive protease like ADAM10 to release its ectodomain, which act as a de-myelin signal via p75NTR on Schwann cells to coordinate axon-myelin degeneration (Fig.3E). The working model, as well as the mechanisms underlying gender differences in axon degeneration and demyelination requires further investigation.

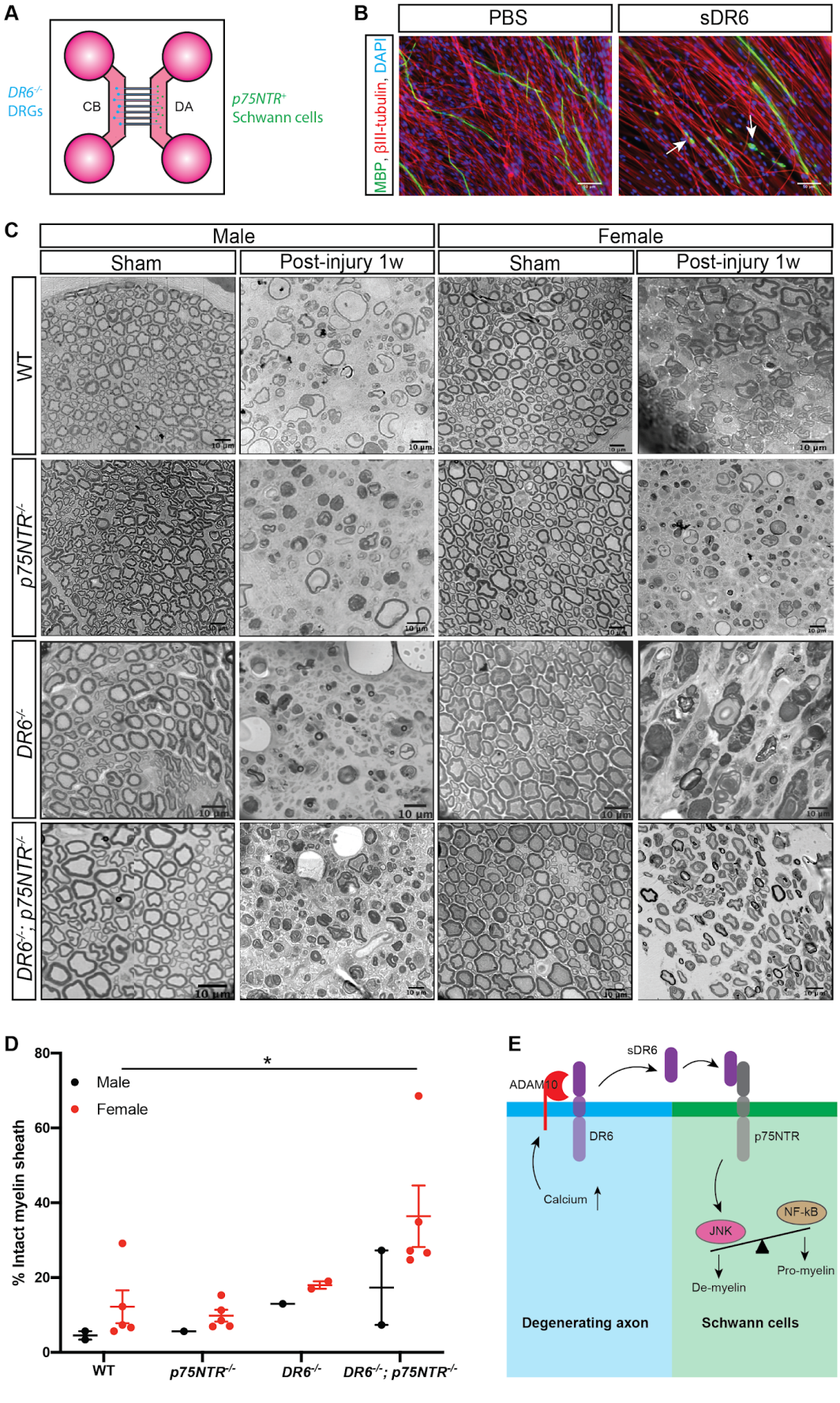
A
DR6-/- DRGs
CB
DA
p75NTR+ Schwann cells
B
PBS
sDR6
MBP, βIII-tubulin, DAPI
C
Male
Female
Sham
Post-injury 1w
WT
p75NTR-/-
DR6-/-
DR6-/-; p75NTR-/-
10 μm
D
% Intact myelin sheath
Male
Female
*
WT
p75NTR-/-
DR6-/-
DR6-/-; p75NTR-/-
E
sDR6
ADAM10
DR6
p75NTR
Calcium
JNK
NF-kB
Pro-myelin
De-myelin
Degenerating axon
Schwann cells

Appendix figure 3: Distinctive roles of DR6 and p75NTR in demyelination

(A) Schematic diagram of axon-Schwann cell co-culture in microfluidic device. DRGs from E14.5 *DR6*$^{-/-}$ embryos were plated in the cell body (CB) channel of the device. Schwann cells from P4 WT mice were harvested from sciatic nerves, purified via p75NTR positive magnetic cell sorting (MACS), and plated in the distal axonal (DA) channel of the device. (B) Representative images of axon-Schwann cell co-culture with or without the incubation of ectodomain of DR6 (sDR6) for 2 weeks. Scale bar = 50μm. (C) Representative images of toluidine blue staining of cross sections of sciatic nerves from male and female WT, *p75NTR*$^{-/-}$*, DR6*$^{-/-}$ and *DR6*$^{-/-}$*; p75NTR*$^{-/-}$ mice without or 1 week after injury, respectively. Scale bar = 10μm. (D) Quantification of percentages of intact myelin sheath in sciatic nerves from male and female WT, *p75NTR*$^{-/-}$*, DR6*$^{-/-}$ and *DR6*$^{-/-}$*; p75NTR*$^{-/-}$ mice 1 week after injury, respectively. Data are reported as mean±SEM, **p*<0.05, two-way ANOVA with Tukey's multiple comparison test. (E) Proposed model for the interaction of axonal DR6 and Schwann cell p75NTR in regulating demyelination in response to injury. Injury induced axonal calcium increase activates membrane bound secretase ADAM10, which cleaves and releases the ectodomain of DR6 (sDR6). sDR6 could interact with p75NTR CRDs *in trans* on Schwann cells to promote the transition from mature myelinating state into repair demyelinating state via JNK pathway.

Appendix 4

Transcriptional analysis of schwann cell plasticity in degeneration

During degeneration, mature Schwann cells dedifferentiate and migrate into the lesion site after injury, which then reacquire their maturity and remyelinate axons at a later stage (Nagoshi et al., 2011). Transcriptome and immunostaining analysis of transected nerves have revealed that myelinating and Remak Schwann cells activate a dedifferentiation program with dramatic downregulation of myelin genes and upregulation of markers of immature Schwann cells like c-jun, Sox2 and p75NTR (Boerboom et al., 2017; Wong et al., 2017). c-Jun dependent reprogramming converts these Schwann cells into “repair cell” state, activating trophic factors and surface proteins for support, forming regeneration tracks (Bungner bands) for axon guidance, and activating cytokines and autophagy for myelin breakdown (Brosius Lutz et al., 2017; Jessen and Mirsky, 2016, 2019). After axonal repair, these Schwann cells then re-differentiate into myelinating or mature Schwann cells by upregulating remyelination-related genes, such as Sox10, Krox20, NF-kB, and Ngr1/ErbB2 (Nocera and Jacob, 2020). Based on the plasticity of Schwann cell state in degeneration, we decide to use single-nuclei RNAseq (sNuc-Seq) on sham and injured sciatic nerve samples to determine the transcriptional changes in degeneration. We were able to identify four clusters of cells in unlabeled sham nerve samples, including adipocytes, fibroblasts, Schwann cells, and transcripts from axon fragments (Fig.4). To focus on the changes in Schwann cells, FACS incorporated with transgenic labelling of schwann cell nuclei will be used. And neuronal and glial conditional knockout of DR6 and p75NTR will be generated. Importantly, This provides a great platform to investigate the roles of DR6 and p75NTR in regulating Schwann cell transcriptome in response to injury, revealing downstream and potential therapeutic targets for neurodegenerative and demyelinating diseases.

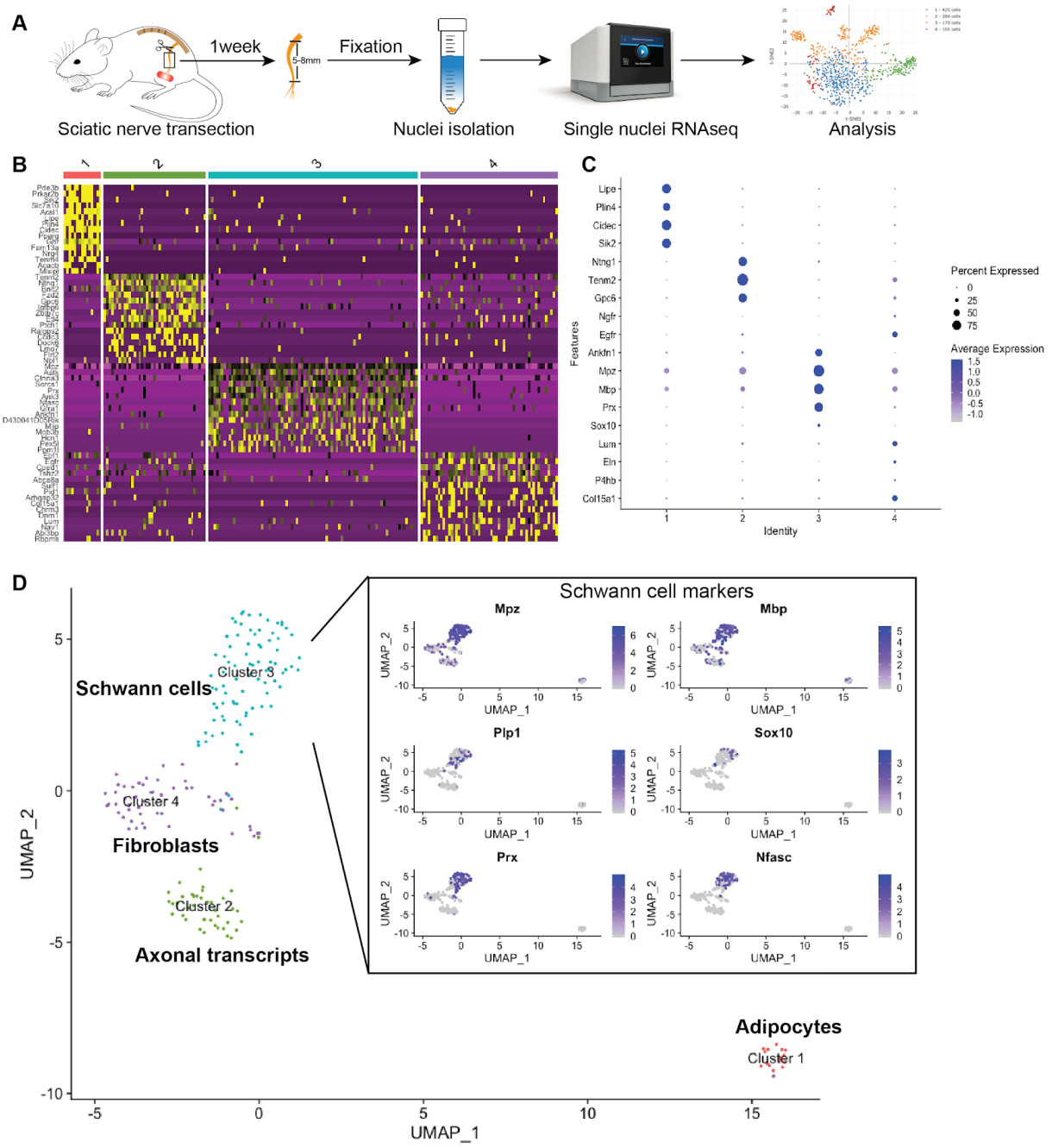

Appendix 4 figure: sNuc-Seq of sciatic nerves of WT mice

(A) Schematic diagram of process for sciatic nerve sNuc-Seq. (B) Heat map, (C) Feature plot and (D) Umap of WT uninjured sciatic nerve transcriptome analysis. Four clusters were identified, including adipocytes with high expression of lipid metabolism related genes, axonal transcripts

with neuronal markers, fibroblasts with high level of adhesion molecules and extracellular matrix related genes, and Schwann cells with high expressions of myelin proteins.

References

1. Abay, Z.C., Wong, M.Y.-Y., Teoh, J.-S., Vijayaraghavan, T., Hilliard, M.A., and Neumann, B. (2017). Phosphatidylserine save-me signals drive functional recovery of severed axons in Caenorhabditis elegans. Proc Natl Acad Sci USA *114*, E10196–E10205.

2. Adalbert, R., Nógrádi, A., Szabó, A., and Coleman, M.P. (2006). The slow Wallerian degeneration gene in vivo protects motor axons but not their cell bodies after avulsion and neonatal axotomy. Eur. J. Neurosci. *24*, 2163–2168.

3. Adalbert, R., Gilley, J., and Coleman, M.P. (2007). Abeta, tau and ApoE4 in Alzheimer's disease: the axonal connection. Trends Mol. Med. *13*, 135–142.

4. Adalbert, R., Morreale, G., Paizs, M., Conforti, L., Walker, S.A., Roderick, H.L., Bootman, M.D., Siklós, L., and Coleman, M.P. (2012). Intra-axonal calcium changes after axotomy in wild-type and slow Wallerian degeneration axons. Neuroscience *225*, 44–54.

5. Akassoglou, K., Yu, W.M., Akpinar, P., and Strickland, S. (2002). Fibrin inhibits peripheral nerve remyelination by regulating Schwann cell differentiation. Neuron *33*, 861–875.

6. Almasieh, M., Catrinescu, M.-M., Binan, L., Costantino, S., and Levin, L.A. (2017). Axonal Degeneration in Retinal Ganglion Cells Is Associated with a Membrane Polarity-Sensitive Redox Process. J. Neurosci. *37*, 3824–3839.

7. Arrázola, M.S., Saquel, C., Catalán, R.J., Barrientos, S.A., Hernandez, D.E., Martínez, N.W., Catenaccio, A., and Court, F.A. (2019). Axonal degeneration is mediated by necroptosis activation. J. Neurosci. *39*, 3832–3844.

8. Avery, M.A., Sheehan, A.E., Kerr, K.S., Wang, J., and Freeman, M.R. (2009). Wld S requires Nmnat1 enzymatic activity and N16-VCP interactions to suppress Wallerian degeneration. J. Cell Biol. *184*, 501–513.

9. Avery, M.A., Rooney, T.M., Pandya, J.D., Wishart, T.M., Gillingwater, T.H., Geddes, J.W., Sullivan, P.G., and Freeman, M.R. (2012). WldS prevents axon degeneration through increased mitochondrial flux and enhanced mitochondrial Ca2+ buffering. Curr. Biol. *22*, 596–600.

10. Azmitia, E.C. (2002). Chapter 8 Cajal's hypotheses on neurobiones and neurotropic factor match properties of microtubules and S-100β. In Changing Views of Cajal's Neuron, (Elsevier), pp. 87–100.

11. Babetto, E., Beirowski, B., Russler, E.V., Milbrandt, J., and DiAntonio, A. (2013). The Phr1 ubiquitin ligase promotes injury-induced axon self-destruction. Cell Rep. *3*, 1422–1429.

12. Bagur, R., and Hajnóczky, G. (2017). Intracellular ca2+ sensing: its role in calcium homeostasis and signaling. Mol. Cell *66*, 780–788.

13. Bamji, S.X., Majdan, M., Pozniak, C.D., Belliveau, D.J., Aloyz, R., Kohn, J., Causing, C.G., and Miller, F.D. (1998). The p75 neurotrophin receptor mediates neuronal apoptosis and is essential for naturally occurring sympathetic neuron death. J. Cell Biol. *140*, 911–923.

14. Bano, D., Munarriz, E., Chen, H.L., Ziviani, E., Lippi, G., Young, K.W., and Nicotera, P. (2007). The plasma membrane Na+/Ca2+ exchanger is cleaved by distinct protease families in neuronal cell death. Ann. N. Y. Acad. Sci. *1099*, 451–455.

15. Barker, V., Middleton, G., Davey, F., and Davies, A.M. (2001). TNFalpha contributes to the death of NGF-dependent neurons during development. Nat. Neurosci. *4*, 1194–1198.

16. Barsukova, A.G., Forte, M., and Bourdette, D. (2012). Focal increases of axoplasmic Ca2+, aggregation of sodium-calcium exchanger, N-type Ca2+ channel, and actin define the sites of spheroids in axons undergoing oxidative stress. J. Neurosci. *32*, 12028–12037.

17. Beirowski, B., Adalbert, R., Wagner, D., Grumme, D.S., Addicks, K., Ribchester, R.R., and Coleman, M.P. (2005). The progressive nature of Wallerian degeneration in wild-type and slow Wallerian degeneration (WldS) nerves. BMC Neurosci. *6*, 6.

18. Beirowski, B., Nógrádi, A., Babetto, E., Garcia-Alias, G., and Coleman, M.P. (2010). Mechanisms of axonal spheroid formation in central nervous system Wallerian degeneration. J. Neuropathol. Exp. Neurol. *69*, 455–472.

19. Benschop, R., Wei, T., and Na, S. (2009). Tumor necrosis factor receptor superfamily member 21: TNFR-related death receptor-6, DR6. Adv. Exp. Med. Biol. *647*, 186–194.

20. Bentley, C.A., and Lee, K.F. (2000). p75 is important for axon growth and schwann cell migration during development. J. Neurosci. *20*, 7706–7715.

21. Bleibaum, F., Sommer, A., Veit, M., Rabe, B., Andrä, J., Kunzelmann, K., Nehls, C., Correa, W., Gutsmann, T., Grötzinger, J., et al. (2019). ADAM10 sheddase activation is controlled by cell membrane asymmetry. J. Mol. Cell Biol. *11*, 979–993.

22. Boerboom, A., Dion, V., Chariot, A., and Franzen, R. (2017). Molecular mechanisms involved in schwann cell plasticity. Front. Mol. Neurosci. *10*, 38.

23. Bridge, K.E., Berg, N., Adalbert, R., Babetto, E., Dias, T., Spillantini, M.-G., Ribchester, R.R., and Coleman, M.P. (2009). Late onset distal axonal swelling in YFP-H transgenic mice. Neurobiol. Aging *30*, 309–321.

24. Brini, M., and Carafoli, E. (2011). The plasma membrane Ca^2+ ATPase and the plasma membrane sodium calcium exchanger cooperate in the regulation of cell calcium. Cold Spring Harb. Perspect. Biol. *3*.

25. Brosius Lutz, A., Chung, W.-S., Sloan, S.A., Carson, G.A., Zhou, L., Lovelett, E., Posada, S., Zuchero, J.B., and Barres, B.A. (2017). Schwann cells use TAM receptor-mediated phagocytosis in addition to autophagy to clear myelin in a mouse model of nerve injury. Proc Natl Acad Sci USA *114*, E8072–E8080.

26. Brown, M.C., Lunn, E.R., and Perry, V.H. (1992). Consequences of slow Wallerian degeneration for regenerating motor and sensory axons. J. Neurobiol. *23*, 521–536.

27. Budde, M.D., and Frank, J.A. (2010). Neurite beading is sufficient to decrease the apparent diffusion coefficient after ischemic stroke. Proc Natl Acad Sci USA *107*, 14472–14477.

28. Campenot, R.B. (1977). Local control of neurite development by nerve growth factor. Proc Natl Acad Sci USA *74*, 4516–4519.

29. Carpenter, S. (1968). Proximal axonal enlargement in motor neuron disease. Neurology *18*, 841–851.

30. Carty, M., and Bowie, A.G. (2019). SARM: From immune regulator to cell executioner. Biochem. Pharmacol. *161*, 52–62.

31. Chan, J.R., Jolicoeur, C., Yamauchi, J., Elliott, J., Fawcett, J.P., Ng, B.K., and Cayouette, M. (2006). The polarity protein Par-3 directly interacts with p75NTR to regulate myelination. Science *314*, 832–836.

32. Chao, M.V. (1994). The p75 neurotrophin receptor. J. Neurobiol. *25*, 1373–1385.

33. Chen, M., Maloney, J.A., Kallop, D.Y., Atwal, J.K., Tam, S.J., Baer, K., Kissel, H., Kaminker, J.S., Lewcock, J.W., Weimer, R.M., et al. (2012). Spatially coordinated kinase signaling regulates local axon degeneration. J. Neurosci. *32*, 13439–13453.

34. Clapham, D.E. (2007). Calcium signaling. Cell *131*, 1047–1058.

35. Coleman, M. (2005). Axon degeneration mechanisms: commonality amid diversity. Nat. Rev. Neurosci. *6*, 889–898.

36. Coleman, M.P., and Freeman, M.R. (2010). Wallerian degeneration, wld(s), and nmnat. Annu. Rev. Neurosci. *33*, 245–267.

37. Coleman, M.P., and Höke, A. (2020). Programmed axon degeneration: from mouse to mechanism to medicine. Nat. Rev. Neurosci. *21*, 183–196.

38. Coleman, M.L., Sahai, E.A., Yeo, M., Bosch, M., Dewar, A., and Olson, M.F. (2001).

Membrane blebbing during apoptosis results from caspase-mediated activation of ROCK I. Nat. Cell Biol. *3*, 339–345.

39. Coleman, M.P., Conforti, L., Buckmaster, E.A., Tarlton, A., Ewing, R.M., Brown, M.C., Lyon, M.F., and Perry, V.H. (1998). An 85-kb tandem triplication in the slow Wallerian degeneration (Wlds) mouse. Proc Natl Acad Sci USA *95*, 9985–9990.

40. Colombo, A., Hsia, H.-E., Wang, M., Kuhn, P.-H., Brill, M.S., Canevazzi, P., Feederle, R., Taveggia, C., Misgeld, T., and Lichtenthaler, S.F. (2018). Non-cell-autonomous function of DR6 in Schwann cell proliferation. EMBO J. *37*.

41. Conforti, L., Tarlton, A., Mack, T.G., Mi, W., Buckmaster, E.A., Wagner, D., Perry, V.H., and Coleman, M.P. (2000). A Ufd2/D4Cole1e chimeric protein and overexpression of Rbp7 in the slow Wallerian degeneration (WldS) mouse. Proc Natl Acad Sci USA *97*, 11377–11382.

42. Conforti, L., Fang, G., Beirowski, B., Wang, M.S., Sorci, L., Asress, S., Adalbert, R., Silva, A., Bridge, K., Huang, X.P., et al. (2007). NAD(+) and axon degeneration revisited: Nmnat1 cannot substitute for Wld(S) to delay Wallerian degeneration. Cell Death Differ. *14*, 116–127.

43. Conforti, L., Gilley, J., and Coleman, M.P. (2014). Wallerian degeneration: an emerging axon death pathway linking injury and disease. Nat. Rev. Neurosci. *15*, 394–409.

44. Cosgaya, J.M., Chan, J.R., and Shooter, E.M. (2002). The neurotrophin receptor p75NTR as a positive modulator of myelination. Science *298*, 1245–1248.

45. Costa, A.R., Pinto-Costa, R., Sousa, S.C., and Sousa, M.M. (2018). The Regulation of Axon Diameter: From Axonal Circumferential Contractility to Activity-Dependent Axon Swelling. Front. Mol. Neurosci. *11*, 319.

46. Cusack, C.L., Swahari, V., Hampton Henley, W., Michael Ramsey, J., and Deshmukh, M. (2013). Distinct pathways mediate axon degeneration during apoptosis and axon-specific pruning. Nat. Commun. *4*, 1876.

47. Czogalla, A., and Sikorski, A.F. (2005). Spectrin and calpain: a “target” and a “sniper” in the pathology of neuronal cells. Cell. Mol. Life Sci. *62*, 1913–1924.

48. Datar, A., Ameeramja, J., Bhat, A., Srivastava, R., Mishra, A., Bernal, R., Prost, J., Callan-Jones, A., and Pullarkat, P.A. (2019). The roles of microtubules and membrane tension in axonal beading, retraction, and atrophy. Biophys. J. *117*, 880–891.

49. Dawson, H.N., Cantillana, V., Jansen, M., Wang, H., Vitek, M.P., Wilcock, D.M., Lynch, J.R., and Laskowitz, D.T. (2010). Loss of tau elicits axonal degeneration in a mouse model of Alzheimer’s disease. Neuroscience *169*, 516–531.

50. Dechant, G., and Barde, Y.-A. (2002). The neurotrophin receptor p75(NTR): novel functions and implications for diseases of the nervous system. Nat. Neurosci. *5*, 1131–1136.

51. Deckwerth, T.L., and Johnson, E.M. (1993). Temporal analysis of events associated with programmed cell death (apoptosis) of sympathetic neurons deprived of nerve growth factor. J. Cell Biol. *123*, 1207–1222.

52. Delisle, M.B., and Carpenter, S. (1984). Neurofibrillary axonal swellings and amyotrophic lateral sclerosis. J. Neurol. Sci. *63*, 241–250.

53. Deppmann, C.D., Mihalas, S., Sharma, N., Lonze, B.E., Niebur, E., and Ginty, D.D. (2008). A model for neuronal competition during development. Science *320*, 369–373.

54. Ding, C., and Hammarlund, M. (2019). Mechanisms of injury-induced axon degeneration. Curr. Opin. Neurobiol. *57*, 171–178.

55. Di Stefano, M., and Conforti, L. (2013). Diversification of NAD biological role: the importance of location. FEBS J. *280*, 4711–4728.

56. Di Stefano, M., Nascimento-Ferreira, I., Orsomando, G., Mori, V., Gilley, J., Brown, R., Janeckova, L., Vargas, M.E., Worrell, L.A., Loreto, A., et al. (2015). A rise in NAD precursor nicotinamide mononucleotide (NMN) after injury promotes axon degeneration. Cell Death Differ.

22, 731–742.

57. Dombert, B., Balk, S., Lüningschrör, P., Moradi, M., Sivadasan, R., Saal-Bauernschubert, L., and Jablonka, S. (2017). BDNF/trkB Induction of Calcium Transients through Cav2.2 Calcium Channels in Motoneurons Corresponds to F-actin Assembly and Growth Cone Formation on β2-Chain Laminin (221). Front. Mol. Neurosci. *10*, 346.

58. Dubreuil, C.I., Winton, M.J., and McKerracher, L. (2003). Rho activation patterns after spinal cord injury and the role of activated Rho in apoptosis in the central nervous system. J. Cell Biol. *162*, 233–243.

59. Eddleman, C.S., Ballinger, M.L., Smyers, M.E., Fishman, H.M., and Bittner, G.D. (1998). Endocytotic formation of vesicles and other membranous structures induced by Ca2+ and axolemmal injury. J. Neurosci. *18*, 4029–4041.

60. Edwards, S.N., Buckmaster, A.E., and Tolkovsky, A.M. (1991). The death programme in cultured sympathetic neurones can be suppressed at the posttranslational level by nerve growth factor, cyclic AMP, and depolarization. J. Neurochem. *57*, 2140–2143.

61. Ehlers, M.D. (2004). Deconstructing the axon: Wallerian degeneration and the ubiquitin-proteasome system. Trends Neurosci. *27*, 3–6.

62. Endres, K., and Deller, T. (2017). Regulation of Alpha-Secretase ADAM10 In vitro and In vivo: Genetic, Epigenetic, and Protein-Based Mechanisms. Front. Mol. Neurosci. *10*, 56.

63. Essuman, K., Summers, D.W., Sasaki, Y., Mao, X., DiAntonio, A., and Milbrandt, J. (2017). The SARM1 Toll/Interleukin-1 Receptor Domain Possesses Intrinsic NAD+ Cleavage Activity that Promotes Pathological Axonal Degeneration. Neuron *93*, 1334-1343.e5.

64. Fernandes, K.A., Mitchell, K.L., Patel, A., Marola, O.J., Shrager, P., Zack, D.J., Libby, R.T., and Welsbie, D.S. (2018). Role of SARM1 and DR6 in retinal ganglion cell axonal and somal degeneration following axonal injury. Exp. Eye Res. *171*, 54–61.

65. Fernández, P., and Pullarkat, P.A. (2010). The role of the cytoskeleton in volume regulation and beading transitions in PC12 neurites. Biophys. J. *99*, 3571–3579.

66. Ferreirinha, F., Quattrini, A., Pirozzi, M., Valsecchi, V., Dina, G., Broccoli, V., Auricchio, A., Piemonte, F., Tozzi, G., Gaeta, L., et al. (2004). Axonal degeneration in paraplegin-deficient mice is associated with abnormal mitochondria and impairment of axonal transport. J. Clin. Invest. *113*, 231–242.

67. Ferri, C.C., and Bisby, M.A. (1999). Improved survival of injured sciatic nerve Schwann cells in mice lacking the p75 receptor. Neurosci. Lett. *272*, 191–194.

68. Figley, M.D., and DiAntonio, A. (2020). The SARM1 axon degeneration pathway: control of the NAD+ metabolome regulates axon survival in health and disease. Curr. Opin. Neurobiol. *63*, 59–66.

69. Finn, J.T., Weil, M., Archer, F., Siman, R., Srinivasan, A., and Raff, M.C. (2000). Evidence that Wallerian degeneration and localized axon degeneration induced by local neurotrophin deprivation do not involve caspases. J. Neurosci. *20*, 1333–1341.

70. Freeman, M.R. (2014). Signaling mechanisms regulating Wallerian degeneration. Curr. Opin. Neurobiol. *27*, 224–231.

71. Freeman, R.S., Burch, R.L., Crowder, R.J., Lomb, D.J., Schoell, M.C., Straub, J.A., and Xie, L. (2004). NGF deprivation-induced gene expression: after ten years, where do we stand? Prog. Brain Res. *146*, 111–126.

72. Fricker, M., Tolkovsky, A.M., Borutaite, V., Coleman, M., and Brown, G.C. (2018). Neuronal Cell Death. Physiol. Rev. *98*, 813–880.

73. Galindo, R., Banks Greenberg, M., Araki, T., Sasaki, Y., Mehta, N., Milbrandt, J., and Holtzman, D.M. (2017). NMNAT3 is protective against the effects of neonatal cerebral hypoxia-ischemia. Ann. Clin. Transl. Neurol. *4*, 722–738.

74. Gallo, G. (2006). RhoA-kinase coordinates F-actin organization and myosin II activity during semaphorin-3A-induced axon retraction. J. Cell Sci. *119*, 3413–3423.

75. Galvin, J.E., Uryu, K., Lee, V.M., and Trojanowski, J.Q. (1999). Axon pathology in Parkinson's disease and Lewy body dementia hippocampus contains alpha-, beta-, and gamma-synuclein. Proc Natl Acad Sci USA *96*, 13450–13455.

76. Gamage, K.K., Cheng, I., Park, R.E., Karim, M.S., Edamura, K., Hughes, C., Spano, A.J., Erisir, A., and Deppmann, C.D. (2017). Death receptor 6 promotes wallerian degeneration in peripheral axons. Curr. Biol. *27*, 890–896.

77. Geden, M.J., and Deshmukh, M. (2016). Axon degeneration: context defines distinct pathways. Curr. Opin. Neurobiol. *39*, 108–115.

78. Geden, M.J., Romero, S.E., and Deshmukh, M. (2019). Apoptosis versus axon pruning: Molecular intersection of two distinct pathways for axon degeneration. Neurosci. Res. *139*, 3–8.

79. Gehler, S., Gallo, G., Veien, E., and Letourneau, P.C. (2004). p75 neurotrophin receptor signaling regulates growth cone filopodial dynamics through modulating RhoA activity. J. Neurosci. *24*, 4363–4372.

80. Gentry, J.J., Barker, P.A., and Carter, B.D. (2004). The p75 neurotrophin receptor: multiple interactors and numerous functions. In NGF and Related Molecules in Health and Disease, (Elsevier), pp. 25–39.

81. George, E.B., Glass, J.D., and Griffin, J.W. (1995). Axotomy-induced axonal degeneration is mediated by calcium influx through ion-specific channels. J. Neurosci. *15*, 6445–6452.

82. Gerdts, J., Summers, D.W., Sasaki, Y., DiAntonio, A., and Milbrandt, J. (2013). Sarm1-mediated axon degeneration requires both SAM and TIR interactions. J. Neurosci. *33*, 13569–13580.

83. Gerdts, J., Brace, E.J., Sasaki, Y., DiAntonio, A., and Milbrandt, J. (2015). SARM1 activation

triggers axon degeneration locally via NAD^+ destruction. Science *348*, 453–457.

84. Gerdts, J., Summers, D.W., Milbrandt, J., and DiAntonio, A. (2016). Axon Self-Destruction: New Links among SARM1, MAPKs, and NAD+ Metabolism. Neuron *89*, 449–460.

85. Gershenbaum, M.R., and Roisen, F.J. (1978). A scanning electron microscopic study of peripheral nerve degeneration and regeneration. Neuroscience *3*, 1241–1250.

86. Gilley, J., and Coleman, M.P. (2010). Endogenous Nmnat2 is an essential survival factor for maintenance of healthy axons. PLoS Biol. *8*, e1000300.

87. Gilley, J., Orsomando, G., Nascimento-Ferreira, I., and Coleman, M.P. (2015). Absence of SARM1 rescues development and survival of NMNAT2-deficient axons. Cell Rep. *10*, 1974–1981.

88. Gilley, J., Ribchester, R.R., and Coleman, M.P. (2017). Sarm1 deletion, but not wlds, confers lifelong rescue in a mouse model of severe axonopathy. Cell Rep. *21*, 10–16.

89. Girouard, M.-P., Bueno, M., Julian, V., Drake, S., Byrne, A.B., and Fournier, A.E. (2018). The Molecular Interplay between Axon Degeneration and Regeneration. Dev. Neurobiol. *78*, 978–990.

90. Girouard, M.-P., Simas, T., Hua, L., Morquette, B., Khazaei, M.R., Unsain, N., Johnstone, A.D., Rambaldi, I., Sanz, R.L., Di Raddo, M.-E., et al. (2020). Collapsin response mediator protein 4 (CRMP4) facilitates Wallerian degeneration and axon regeneration following sciatic nerve injury. Eneuro.

91. Glass, J.D., Culver, D.G., Levey, A.I., and Nash, N.R. (2002). Very early activation of m-calpain in peripheral nerve during Wallerian degeneration. J. Neurol. Sci. *196*, 9–20.

92. Götz, J., Ittner, L.M., and Kins, S. (2006). Do axonal defects in tau and amyloid precursor protein transgenic animals model axonopathy in Alzheimer's disease? J. Neurochem. *98*, 993–1006.

93. Govek, E.-E., Newey, S.E., and Van Aelst, L. (2005). The role of the Rho GTPases in neuronal

development. Genes Dev. *19*, 1–49.

94. Griffin, J.W., and Watson, D.F. (1988). Axonal transport in neurological disease. Ann. Neurol. *23*, 3–13.

95. Griffiths, I., Klugmann, M., Anderson, T., Yool, D., Thomson, C., Schwab, M.H., Schneider, A., Zimmermann, F., McCulloch, M., Nadon, N., et al. (1998). Axonal swellings and degeneration in mice lacking the major proteolipid of myelin. Science *280*, 1610–1613.

96. de Groot, N.S., and Burgas, M.T. (2015). Is membrane homeostasis the missing link between inflammation and neurodegenerative diseases? Cell. Mol. Life Sci. *72*, 4795–4805.

97. Guedes-Dias, P., and Holzbaur, E.L.F. (2019). Axonal transport: Driving synaptic function. Science *366*.

98. Guse, A.H. (2015). Calcium mobilizing second messengers derived from NAD. Biochim. Biophys. Acta *1854*, 1132–1137.

99. Gu, Y., Jukkola, P., Wang, Q., Esparza, T., Zhao, Y., Brody, D., and Gu, C. (2017). Polarity of varicosity initiation in central neuron mechanosensation. J. Cell Biol. *216*, 2179–2199.

100. Haase, G., Pettmann, B., Raoul, C., and Henderson, C.E. (2008). Signaling by death receptors in the nervous system. Curr. Opin. Neurobiol. *18*, 284–291.

101. Hall, A. (1998). Rho GTPases and the Actin Cytoskeleton. Science (80-) *279*, 509–514.

102. Hall, S.M., Li, H., and Kent, A.P. (1997). Schwann cells responding to primary demyelination in vivo express p75NTR and c-erbB receptors: a light and electron immunohistochemical study. J. Neurocytol. *26*, 679–690.

103. Hamburger, V., and Oppenheim, R.W. (1990). Naturally occurring neuronal death in vertebrates. In Neuroembryology, (Boston, MA: Birkhäuser Boston), pp. 126–142.

104. Heckmann, B.L., Tummers, B., and Green, D.R. (2019). Crashing the computer: apoptosis

vs. necroptosis in neuroinflammation. Cell Death Differ. *26*, 41–52.

105. Hendry, I.A., and Campbell, J. (1976). Morphometric analysis of rat superior cervical ganglion after axotomy and nerve growth factor treatment. J. Neurocytol. *5*, 351–360.

106. Heo, J., and Campbell, S.L. (2005). Mechanism of redox-mediated guanine nucleotide exchange on redox-active Rho GTPases. J. Biol. Chem. *280*, 31003–31010.

107. Hollenbeck, P.J., and Saxton, W.M. (2005). The axonal transport of mitochondria. J. Cell Sci. *118*, 5411–5419.

108. Hoopfer, E.D., McLaughlin, T., Watts, R.J., Schuldiner, O., O'Leary, D.D.M., and Luo, L. (2006). Wlds protection distinguishes axon degeneration following injury from naturally occurring developmental pruning. Neuron *50*, 883–895.

109. Howell, G.R., Libby, R.T., Jakobs, T.C., Smith, R.S., Phalan, F.C., Barter, J.W., Barbay, J.M., Marchant, J.K., Mahesh, N., Porciatti, V., et al. (2007). Axons of retinal ganglion cells are insulted in the optic nerve early in DBA/2J glaucoma. J. Cell Biol. *179*, 1523–1537.

110. Hu, R., Du, Q., Yin, X., Li, J., Wang, T., and Zhang, L. (2014). Agonist antibody activates death receptor 6 downstream signaling involving TRADD recruitment. FEBS Lett. *588*, 401–407.

111. Hu, Y., Lee, X., Shao, Z., Apicco, D., Huang, G., Gong, B.J., Pepinsky, R.B., and Mi, S. (2013). A DR6/p75(NTR) complex is responsible for β-amyloid-induced cortical neuron death. Cell Death Dis. *4*, e579.

112. Ibáñez, C.F., and Simi, A. (2012). p75 neurotrophin receptor signaling in nervous system injury and degeneration: paradox and opportunity. Trends Neurosci. *35*, 431–440.

113. Jessen, K.R., and Mirsky, R. (2016). The repair Schwann cell and its function in regenerating nerves. J Physiol (Lond) *594*, 3521–3531.

114. Jessen, K.R., and Mirsky, R. (2019). The success and failure of the schwann cell response

to nerve injury. Front. Cell. Neurosci. *13*, 33.

115. Johnson, V.E., Stewart, W., and Smith, D.H. (2013). Axonal pathology in traumatic brain injury. Exp. Neurol. *246*, 35–43.

116. Johnstone, A.D., de Léon, A., Unsain, N., Gibon, J., and Barker, P.A. (2019). Developmental Axon Degeneration Requires TRPV1-Dependent Ca2+ Influx. Eneuro *6*.

117. Kallop, D.Y., Meilandt, W.J., Gogineni, A., Easley-Neal, C., Wu, T., Jubb, A.M., Yaylaoglu, M., Shamloo, M., Tessier-Lavigne, M., Scearce-Levie, K., et al. (2014). A death receptor 6-amyloid precursor protein pathway regulates synapse density in the mature CNS but does not contribute to Alzheimer's disease-related pathophysiology in murine models. J. Neurosci. *34*, 6425–6437.

118. Kanaan, N.M., Pigino, G.F., Brady, S.T., Lazarov, O., Binder, L.I., and Morfini, G.A. (2013). Axonal degeneration in Alzheimer's disease: when signaling abnormalities meet the axonal transport system. Exp. Neurol. *246*, 44–53.

119. Kanamori, T., Kanai, M.I., Dairyo, Y., Yasunaga, K., Morikawa, R.K., and Emoto, K. (2013). Compartmentalized calcium transients trigger dendrite pruning in Drosophila sensory neurons. Science *340*, 1475–1478.

120. Kantor, D.B., and Kolodkin, A.L. (2003). Curbing the excesses of youth. Neuron *38*, 849–852.

121. Kasof, G.M., Lu, J.J., Liu, D., Speer, B., Mongan, K.N., Gomes, B.C., and Lorenzi, M.V. (2001). Tumor necrosis factor-alpha induces the expression of DR6, a member of the TNF receptor family, through activation of NF-kappaB. Oncogene *20*, 7965–7975.

122. Kenchappa, R.S., Tep, C., Korade, Z., Urra, S., Bronfman, F.C., Yoon, S.O., and Carter, B.D. (2010). p75 neurotrophin receptor-mediated apoptosis in sympathetic neurons involves a biphasic activation of JNK and up-regulation of tumor necrosis factor-alpha-converting

enzyme/ADAM17. J. Biol. Chem. *285*, 20358–20368.

123. Kerschensteiner, M., Schwab, M.E., Lichtman, J.W., and Misgeld, T. (2005). In vivo imaging of axonal degeneration and regeneration in the injured spinal cord. Nat. Med. *11*, 572–577.

124. Kikuchi, T., Mukoyama, M., Yamazaki, K., and Moriya, H. (1990). Axonal degeneration of ascending sensory neurons in gracile axonal dystrophy mutant mouse. Acta Neuropathol. *80*, 145–151.

125. Kilinc, D., Gallo, G., and Barbee, K.A. (2008). Mechanically-induced membrane poration causes axonal beading and localized cytoskeletal damage. Exp. Neurol. *212*, 422–430.

126. Kim, Y.H., Kim, Y.H., Shin, Y.K., Jo, Y.R., Park, D.K., Song, M.-Y., Yoon, B.-A., Nam, S.H., Kim, J.H., Choi, B.-O., et al. (2019). p75 and neural cell adhesion molecule 1 can identify pathologic Schwann cells in peripheral neuropathies. Ann. Clin. Transl. Neurol. *6*, 1292–1301.

127. Kim, Y., Zhou, P., Qian, L., Chuang, J.-Z., Lee, J., Li, C., Iadecola, C., Nathan, C., and Ding, A. (2007). MyD88-5 links mitochondria, microtubules, and JNK3 in neurons and regulates neuronal survival. J. Exp. Med. *204*, 2063–2074.

128. Knowles, J.K., Simmons, D.A., Nguyen, T.-V.V., Vander Griend, L., Xie, Y., Zhang, H., Yang, T., Pollak, J., Chang, T., Arancio, O., et al. (2013). Small molecule p75NTR ligand prevents cognitive deficits and neurite degeneration in an Alzheimer's mouse model. Neurobiol. Aging *34*, 2052–2063.

129. Koch, J.C., Tönges, L., Barski, E., Michel, U., Bähr, M., and Lingor, P. (2014). ROCK2 is a major regulator of axonal degeneration, neuronal death and axonal regeneration in the CNS. Cell Death Dis. *5*, e1225.

130. Kohn, J., Aloyz, R.S., Toma, J.G., Haak-Frendscho, M., and Miller, F.D. (1999). Functionally antagonistic interactions between the TrkA and p75 neurotrophin receptors regulate sympathetic neuron growth and target innervation. J. Neurosci. *19*, 5393–5408.

131. Ko, K.W., Milbrandt, J., and DiAntonio, A. (2020). SARM1 acts downstream of neuroinflammatory and necroptotic signaling to induce axon degeneration. J. Cell Biol. *219*.

132. Kraemer, B.R., Snow, J.P., Vollbrecht, P., Pathak, A., Valentine, W.M., Deutch, A.Y., and Carter, B.D. (2014). A role for the p75 neurotrophin receptor in axonal degeneration and apoptosis induced by oxidative stress. J. Biol. Chem. *289*, 21205–21216.

133. Krauss, R., Bosanac, T., Devraj, R., Engber, T., and Hughes, R.O. (2020). Axons Matter: The Promise of Treating Neurodegenerative Disorders by Targeting SARM1-Mediated Axonal Degeneration. Trends Pharmacol. Sci. *41*, 281–293.

134. Kristiansen, M., and Ham, J. (2014). Programmed cell death during neuronal development: the sympathetic neuron model. Cell Death Differ. *21*, 1025–1035.

135. Kuester, M., Kemmerzehl, S., Dahms, S.O., Roeser, D., and Than, M.E. (2011). The crystal structure of death receptor 6 (DR6): a potential receptor of the amyloid precursor protein (APP). J. Mol. Biol. *409*, 189–201.

136. LaFerla, F.M. (2002). Calcium dyshomeostasis and intracellular signalling in Alzheimer's disease. Nat. Rev. Neurosci. *3*, 862–872.

137. Larhammar, M., Huntwork-Rodriguez, S., Jiang, Z., Solanoy, H., Sengupta Ghosh, A., Wang, B., Kaminker, J.S., Huang, K., Eastham-Anderson, J., Siu, M., et al. (2017). Dual leucine zipper kinase-dependent PERK activation contributes to neuronal degeneration following insult. Elife *6*.

138. Laser, H., Conforti, L., Morreale, G., Mack, T.G.M., Heyer, M., Haley, J.E., Wishart, T.M., Beirowski, B., Walker, S.A., Haase, G., et al. (2006). The slow Wallerian degeneration protein, WldS, binds directly to VCP/p97 and partially redistributes it within the nucleus. Mol. Biol. Cell *17*, 1075–1084.

139. Lauria, G., Morbin, M., Lombardi, R., Borgna, M., Mazzoleni, G., Sghirlanzoni, A., and Pareyson, D. (2003). Axonal swellings predict the degeneration of epidermal nerve fibers in

painful neuropathies. Neurology *61*, 631–636.

140. Lee, K.-S., Huh, S., Lee, S., Wu, Z., Kim, A.-K., Kang, H.-Y., and Lu, B. (2018). Altered ER-mitochondria contact impacts mitochondria calcium homeostasis and contributes to neurodegeneration in vivo in disease models. Proc Natl Acad Sci USA *115*, E8844–E8853.

141. Lin, Z., Tann, J.Y., Goh, E.T.H., Kelly, C., Lim, K.B., Gao, J.F., and Ibanez, C.F. (2015). Structural basis of death domain signaling in the p75 neurotrophin receptor. Elife *4*, e11692.

142. Li, R., Li, D., Wu, C., Ye, L., Wu, Y., Yuan, Y., Yang, S., Xie, L., Mao, Y., Jiang, T., et al. (2020). Nerve growth factor activates autophagy in Schwann cells to enhance myelin debris clearance and to expedite nerve regeneration. Theranostics *10*, 1649–1677.

143. Llobet Rosell, A., and Neukomm, L.J. (2019). Axon death signalling in Wallerian degeneration among species and in disease. Open Biol. *9*, 190118.

144. LoPachin, R.M., and Lehning, E.J. (1997). Mechanism of calcium entry during axon injury and degeneration. Toxicol. Appl. Pharmacol. *143*, 233–244.

145. Lorenzo, D.N., Badea, A., Zhou, R., Mohler, P.J., Zhuang, X., and Bennett, V. (2019). βII-spectrin promotes mouse brain connectivity through stabilizing axonal plasma membranes and enabling axonal organelle transport. Proc Natl Acad Sci USA *116*, 15686–15695.

146. Loreto, A., Di Stefano, M., Gering, M., and Conforti, L. (2015). Wallerian Degeneration Is Executed by an NMN-SARM1-Dependent Late Ca(2+) Influx but Only Modestly Influenced by Mitochondria. Cell Rep. *13*, 2539–2552.

147. Loreto, A., Hill, C.S., Hewitt, V.L., Orsomando, G., Angeletti, C., Gilley, J., Lucci, C., Sanchez-Martinez, A., Whitworth, A.J., Conforti, L., et al. (2020). Mitochondrial impairment activates the Wallerian pathway through depletion of NMNAT2 leading to SARM1-dependent axon degeneration. Neurobiol. Dis. *134*, 104678.

148. Lunn, E.R., Perry, V.H., Brown, M.C., Rosen, H., and Gordon, S. (1989). Absence of

Wallerian Degeneration does not Hinder Regeneration in Peripheral Nerve. Eur. J. Neurosci. *1*, 27–33.

149. Luo, L., and O'Leary, D.D.M. (2005). Axon retraction and degeneration in development and disease. Annu. Rev. Neurosci. *28*, 127–156.

150. Mack, T.G., Reiner, M., Beirowski, B., Mi, W., Emanuelli, M., Wagner, D., Thomson, D., Gillingwater, T., Court, F., Conforti, L., et al. (2001). Wallerian degeneration of injured axons and synapses is delayed by a Ube4b/Nmnat chimeric gene. Nat. Neurosci. *4*, 1199–1206.

151. Magni, G., Amici, A., Emanuelli, M., Orsomando, G., Raffaelli, N., and Ruggieri, S. (2004). Enzymology of NAD+ homeostasis in man. Cell. Mol. Life Sci. *61*, 19–34.

152. Malhotra, J.D., and Kaufman, R.J. (2011). ER stress and its functional link to mitochondria: role in cell survival and death. Cold Spring Harb. Perspect. Biol. *3*, a004424.

153. Maor-Nof, M., Romi, E., Sar Shalom, H., Ulisse, V., Raanan, C., Nof, A., Leshkowitz, D., Lang, R., and Yaron, A. (2016). Axonal Degeneration Is Regulated by a Transcriptional Program that Coordinates Expression of Pro- and Anti-degenerative Factors. Neuron *92*, 991–1006.

154. Maravall, M., Mainen, Z.F., Sabatini, B.L., and Svoboda, K. (2000). Estimating intracellular calcium concentrations and buffering without wavelength ratioing. Biophys. J. *78*, 2655–2667.

155. Martin, D.P., Schmidt, R.E., DiStefano, P.S., Lowry, O.H., Carter, J.G., and Johnson, E.M. (1988). Inhibitors of protein synthesis and RNA synthesis prevent neuronal death caused by nerve growth factor deprivation. J. Cell Biol. *106*, 829–844.

156. Martin, D.P., Ito, A., Horigome, K., Lampe, P.A., and Johnson, E.M. (1992). Biochemical characterization of programmed cell death in NGF-deprived sympathetic neurons. J. Neurobiol. *23*, 1205–1220.

157. Martin, L.J., Pan, Y., Price, A.C., Sterling, W., Copeland, N.G., Jenkins, N.A., Price, D.L., and Lee, M.K. (2006). Parkinson's disease alpha-synuclein transgenic mice develop neuronal

mitochondrial degeneration and cell death. J. Neurosci. *26*, 41–50.

158. Massa, S.M., Xie, Y., Yang, T., Harrington, A.W., Kim, M.L., Yoon, S.O., Kraemer, R., Moore, L.A., Hempstead, B.L., and Longo, F.M. (2006). Small, nonpeptide p75NTR ligands induce survival signaling and inhibit proNGF-induced death. J. Neurosci. *26*, 5288–5300.

159. Mathew, S.J., Haubert, D., Krönke, M., and Leptin, M. (2009). Looking beyond death: a morphogenetic role for the TNF signalling pathway. J. Cell Sci. *122*, 1939–1946.

160. Mattson, M.P. (2007). Calcium and neurodegeneration. Aging Cell *6*, 337–350.

161. Ma, M., Ferguson, T.A., Schoch, K.M., Li, J., Qian, Y., Shofer, F.S., Saatman, K.E., and Neumar, R.W. (2013). Calpains mediate axonal cytoskeleton disintegration during Wallerian degeneration. Neurobiol. Dis. *56*, 34–46.

162. McKenzie, B.A., Mamik, M.K., Saito, L.B., Boghozian, R., Monaco, M.C., Major, E.O., Lu, J.-Q., Branton, W.G., and Power, C. (2018). Caspase-1 inhibition prevents glial inflammasome activation and pyroptosis in models of multiple sclerosis. Proc Natl Acad Sci USA *115*, E6065–E6074.

163. McKenzie, B.A., Dixit, V.M., and Power, C. (2020). Fiery cell death: pyroptosis in the central nervous system. Trends Neurosci. *43*, 55–73.

164. McNeil, P.L., and Kirchhausen, T. (2005). An emergency response team for membrane repair. Nat. Rev. Mol. Cell Biol. *6*, 499–505.

165. Mc Guire, C., Beyaert, R., and van Loo, G. (2011). Death receptor signalling in central nervous system inflammation and demyelination. Trends Neurosci. *34*, 619–628.

166. Meeker, R.B., and Williams, K.S. (2015). The p75 neurotrophin receptor: at the crossroad of neural repair and death. Neural Regen. Res. *10*, 721–725.

167. Meeker, R., and Williams, K. (2014). Dynamic nature of the p75 neurotrophin receptor in

response to injury and disease. J. Neuroimmune Pharmacol. *9*, 615–628.

168. Meeker, R.B., Poulton, W., Clary, G., Schriver, M., and Longo, F.M. (2016). Novel p75 neurotrophin receptor ligand stabilizes neuronal calcium, preserves mitochondrial movement and protects against HIV associated neuropathogenesis. Exp. Neurol. *275 Pt 1*, 182–198.

169. Mejia Maza, A.J., Carmen-Orozco, R.P., Carter, E., Dávila, D.G., Castillo, G., Morales, J.D., Mamani, J., Gavídia, C., Alroy, J., Sterling, C.R., et al. (2018). Axonal swellings and spheroids: a new insight into the pathology of neurocysticercosis. Brain Pathol. *29*, 425–436.

170. Milde, S., Gilley, J., and Coleman, M.P. (2013). Subcellular localization determines the stability and axon protective capacity of axon survival factor Nmnat2. PLoS Biol. *11*, e1001539.

171. Miller, B.R., Press, C., Daniels, R.W., Sasaki, Y., Milbrandt, J., and DiAntonio, A. (2009). A dual leucine kinase-dependent axon self-destruction program promotes Wallerian degeneration. Nat. Neurosci. *12*, 387–389.

172. Mitchell, L., Hobbs, G.A., Aghajanian, A., and Campbell, S.L. (2013). Redox regulation of Ras and Rho GTPases: mechanism and function. Antioxid. Redox Signal. *18*, 250–258.

173. Mitrophanov, A.Y., and Groisman, E.A. (2008). Positive feedback in cellular control systems. Bioessays *30*, 542–555.

174. Mi, S., Lee, X., Hu, Y., Ji, B., Shao, Z., Yang, W., Huang, G., Walus, L., Rhodes, K., Gong, B.J., et al. (2011). Death receptor 6 negatively regulates oligodendrocyte survival, maturation and myelination. Nat. Med. *17*, 816–821.

175. Mi, W., Beirowski, B., Gillingwater, T.H., Adalbert, R., Wagner, D., Grumme, D., Osaka, H., Conforti, L., Arnhold, S., Addicks, K., et al. (2005). The slow Wallerian degeneration gene, WldS, inhibits axonal spheroid pathology in gracile axonal dystrophy mice. Brain *128*, 405–416.

176. Mok, S.-A., Lund, K., and Campenot, R.B. (2009). A retrograde apoptotic signal originating in NGF-deprived distal axons of rat sympathetic neurons in compartmented cultures. Cell Res.

19, 546–560.

177. Müller, M., Ahumada-Castro, U., Sanhueza, M., Gonzalez-Billault, C., Court, F.A., and Cárdenas, C. (2018). Mitochondria and calcium regulation as basis of neurodegeneration associated with aging. Front. Neurosci. *12*, 470.

178. Murata, H., Khine, C.C., Nishikawa, A., Yamamoto, K.-I., Kinoshita, R., and Sakaguchi, M. (2018). c-Jun N-terminal kinase (JNK)-mediated phosphorylation of SARM1 regulates NAD+ cleavage activity to inhibit mitochondrial respiration. J. Biol. Chem. *293*, 18933–18943.

179. Nagata, S., Suzuki, J., Segawa, K., and Fujii, T. (2016). Exposure of phosphatidylserine on the cell surface. Cell Death Differ. *23*, 952–961.

180. Nagoshi, N., Shibata, S., Hamanoue, M., Mabuchi, Y., Matsuzaki, Y., Toyama, Y., Nakamura, M., and Okano, H. (2011). Schwann cell plasticity after spinal cord injury shown by neural crest lineage tracing. Glia *59*, 771–784.

181. Neukomm, L.J., and Freeman, M.R. (2014). Diverse cellular and molecular modes of axon degeneration. Trends Cell Biol. *24*, 515–523.

182. Neukomm, L.J., Burdett, T.C., Seeds, A.M., Hampel, S., Coutinho-Budd, J.C., Farley, J.E., Wong, J., Karadeniz, Y.B., Osterloh, J.M., Sheehan, A.E., et al. (2017). Axon death pathways converge on axundead to promote functional and structural axon disassembly. Neuron *95*, 78-91.e5.

183. Newell, K.L., Boyer, P., Gomez-Tortosa, E., Hobbs, W., Hedley-Whyte, E.T., Vonsattel, J.P., and Hyman, B.T. (1999). Alpha-synuclein immunoreactivity is present in axonal swellings in neuroaxonal dystrophy and acute traumatic brain injury. J. Neuropathol. Exp. Neurol. *58*, 1263–1268.

184. Nikiforov, A., Kulikova, V., and Ziegler, M. (2015). The human NAD metabolome: Functions, metabolism and compartmentalization. Crit. Rev. Biochem. Mol. Biol. *50*, 284–297.

185. Nikolaev, A., McLaughlin, T., O'Leary, D.D.M., and Tessier-Lavigne, M. (2009). APP binds DR6 to trigger axon pruning and neuron death via distinct caspases. Nature *457*, 981–989.

186. Nocera, G., and Jacob, C. (2020). Mechanisms of Schwann cell plasticity involved in peripheral nerve repair after injury. Cell. Mol. Life Sci.

187. Ochs, S., Pourmand, R., Jersild, R.A., and Friedman, R.N. (1997). The origin and nature of beading: A reversible transformation of the shape of nerve fibers. Prog. Neurobiol. *52*, 391–426.

188. Ohgami, T., Kitamoto, T., and Tateishi, J. (1992). Alzheimer's amyloid precursor protein accumulates within axonal swellings in human brain lesions. Neurosci. Lett. *136*, 75–78.

189. Olsen, O., Kallop, D.Y., McLaughlin, T., Huntwork-Rodriguez, S., Wu, Z., Duggan, C.D., Simon, D.J., Lu, Y., Easley-Neal, C., Takeda, K., et al. (2014). Genetic analysis reveals that amyloid precursor protein and death receptor 6 function in the same pathway to control axonal pruning independent of β-secretase. J. Neurosci. *34*, 6438–6447.

190. Orem, B.C., Pelisch, N., Williams, J., Nally, J.M., and Stirling, D.P. (2017). Intracellular calcium release through IP3R or RyR contributes to secondary axonal degeneration. Neurobiol. Dis. *106*, 235–243.

191. Orem, B.C., Partain, S.B., and Stirling, D.P. (2020). Inhibiting store-operated calcium entry attenuates white matter secondary degeneration following SCI. Neurobiol. Dis. *136*, 104718.

192. Osterloh, J.M., Yang, J., Rooney, T.M., Fox, A.N., Adalbert, R., Powell, E.H., Sheehan, A.E., Avery, M.A., Hackett, R., Logan, M.A., et al. (2012). dSarm/Sarm1 is required for activation of an injury-induced axon death pathway. Science *337*, 481–484.

193. Panneerselvam, P., Singh, L.P., Ho, B., Chen, J., and Ding, J.L. (2012). Targeting of pro-apoptotic TLR adaptor SARM to mitochondria: definition of the critical region and residues in the signal sequence. Biochem. J. *442*, 263–271.

194. Pan, G., Bauer, J.H., Haridas, V., Wang, S., Liu, D., Yu, G., Vincenz, C., Aggarwal, B.B., Ni,

J., and Dixit, V.M. (1998). Identification and functional characterization of DR6, a novel death domain-containing TNF receptor. FEBS Lett. *431*, 351–356.

195. Papahadjopoulos, D., Nir, S., and Düzgünes, N. (1990). Molecular mechanisms of calcium-induced membrane fusion. J. Bioenerg. Biomembr. *22*, 157–179.

196. Park, J.W., Vahidi, B., Taylor, A.M., Rhee, S.W., and Jeon, N.L. (2006). Microfluidic culture platform for neuroscience research. Nat. Protoc. *1*, 2128–2136.

197. Park, K.J., Grosso, C.A., Aubert, I., Kaplan, D.R., and Miller, F.D. (2010). p75NTR-dependent, myelin-mediated axonal degeneration regulates neural connectivity in the adult brain. Nat. Neurosci. *13*, 559–566.

198. Pathak, A., and Carter, B.D. (2017). Retrograde apoptotic signaling by the p75 neurotrophin receptor. Neuronal Signal. *1*, NS20160007.

199. Pathak, A., Stanley, E.M., Hickman, F.E., Wallace, N., Brewer, B., Li, D., Gluska, S., Perlson, E., Fuhrmann, S., Akassoglou, K., et al. (2018). Retrograde Degenerative Signaling Mediated by the p75 Neurotrophin Receptor Requires p150Glued Deacetylation by Axonal HDAC1. Dev. Cell *46*, 376-387.e7.

200. Poon, I.K.H., Lucas, C.D., Rossi, A.G., and Ravichandran, K.S. (2014). Apoptotic cell clearance: basic biology and therapeutic potential. Nat. Rev. Immunol. *14*, 166–180.

Popko, B. (2011). Downregulating DR6 to drive remyelination. Nat. Med. *17*, 779–780.

201. Prineas, J.W., Ouvrier, R.A., Wright, R.G., Walsh, J.C., and McLeod, J.G. (1976). Giant axonal neuropathy—a generalized disorder of cytoplasmic microfilament formation. J. Neuropathol. Exp. Neurol. *35*, 458–470.

202. Probst, A., Götz, J., Wiederhold, K.H., Tolnay, M., Mistl, C., Jaton, A.L., Hong, M., Ishihara, T., Lee, V.M., Trojanowski, J.Q., et al. (2000). Axonopathy and amyotrophy in mice transgenic for human four-repeat tau protein. Acta Neuropathol. *99*, 469–481.

203. Provenzano, M.J., Minner, S.A., Zander, K., Clark, J.J., Kane, C.J., Green, S.H., and Hansen, M.R. (2011). p75(NTR) expression and nuclear localization of p75(NTR) intracellular domain in spiral ganglion Schwann cells following deafness correlate with cell proliferation. Mol. Cell. Neurosci. *47*, 306–315.

204. Pullarkat, P.A., Dommersnes, P., Fernández, P., Joanny, J.-F., and Ott, A. (2006). Osmotically driven shape transformations in axons. Phys. Rev. Lett. *96*, 048104.

205. Purves, D., and Lichtman, J.W. (1980). Elimination of synapses in the developing nervous system. Science *210*, 153–157.

206. Purves, D., Snider, W.D., and Voyvodic, J.T. (1988). Trophic regulation of nerve cell morphology and innervation in the autonomic nervous system. Nature *336*, 123–128.

207. Ramón y Cajal, S. (1928). Degeneration and regeneration of the nervous system.

208. Rao, S.N.R., and Pearse, D.D. (2016). Regulating Axonal Responses to Injury: The Intersection between Signaling Pathways Involved in Axon Myelination and The Inhibition of Axon Regeneration. Front. Mol. Neurosci. *9*, 33.

209. Ravichandran, K.S. (2010). Find-me and eat-me signals in apoptotic cell clearance: progress and conundrums. J. Exp. Med. *207*, 1807–1817.

210. Ribas, V.T., and Lingor, P. (2016). Calcium channel inhibition-mediated axonal stabilization improves axonal regeneration after optic nerve crush. Neural Regen. Res. *11*, 1245–1246.

211. Ribas, V.T., Koch, J.C., Michel, U., Bähr, M., and Lingor, P. (2017). Attenuation of axonal degeneration by calcium channel inhibitors improves retinal ganglion cell survival and regeneration after optic nerve crush. Mol. Neurobiol. *54*, 72–86.

212. Ridley, A.J. (2001). Rho family proteins: coordinating cell responses. Trends Cell Biol. *11*, 471–477.

213. Rosenberg, A.F., Wolman, M.A., Franzini-Armstrong, C., and Granato, M. (2012). In vivo nerve-macrophage interactions following peripheral nerve injury. J. Neurosci. *32*, 3898–3909.

214. Ros, U., Peña-Blanco, A., Hänggi, K., Kunzendorf, U., Krautwald, S., Wong, W.W.-L., and García-Sáez, A.J. (2017). Necroptosis execution is mediated by plasma membrane nanopores independent of calcium. Cell Rep. *19*, 175–187.

215. Roy, S., Zhang, B., Lee, V.M.-Y., and Trojanowski, J.Q. (2005). Axonal transport defects: a common theme in neurodegenerative diseases. Acta Neuropathol. *109*, 5–13.

216. Salvadores, N., Sanhueza, M., Manque, P., and Court, F.A. (2017). Axonal Degeneration during Aging and Its Functional Role in Neurodegenerative Disorders. Front. Neurosci. *11*, 451.

217. Santos, S.D.M., and Ferrell, J.E. (2008). Systems biology: On the cell cycle and its switches. Nature *454*, 288–289.

218. Sapar, M.L., Ji, H., Wang, B., Poe, A.R., Dubey, K., Ren, X., Ni, J.-Q., and Han, C. (2018). Phosphatidylserine Externalization Results from and Causes Neurite Degeneration in Drosophila. Cell Rep. *24*, 2273–2286.

219. Sasaki, S., Maruyama, S., Yamane, K., Sakuma, H., and Takeishi, M. (1989). Swellings of proximal axons in a case of motor neuron disease. Ann. Neurol. *25*, 520–522.

220. Sasaki, S., Warita, H., Abe, K., and Iwata, M. (2005). Impairment of axonal transport in the axon hillock and the initial segment of anterior horn neurons in transgenic mice with a G93A mutant SOD1 gene. Acta Neuropathol. *110*, 48–56.

221. Sasaki, Y., Araki, T., and Milbrandt, J. (2006). Stimulation of nicotinamide adenine dinucleotide biosynthetic pathways delays axonal degeneration after axotomy. J. Neurosci. *26*, 8484–8491.

222. Sasaki, Y., Nakagawa, T., Mao, X., DiAntonio, A., and Milbrandt, J. (2016). NMNAT1 inhibits axon degeneration via blockade of SARM1-mediated NAD+ depletion. Elife *5*.

223. Sasaki, Y., Engber, T.M., Hughes, R.O., Figley, M.D., Wu, T., Bosanac, T., Devraj, R., Milbrandt, J., Krauss, R., and DiAntonio, A. (2020). cADPR is a gene dosage-sensitive biomarker of SARM1 activity in healthy, compromised, and degenerating axons. Exp. Neurol. 113252.

224. Saxena, S., and Caroni, P. (2007). Mechanisms of axon degeneration: from development to disease. Prog. Neurobiol. *83*, 174–191.

225. Schindelin, J., Arganda-Carreras, I., Frise, E., Kaynig, V., Longair, M., Pietzsch, T., Preibisch, S., Rueden, C., Saalfeld, S., Schmid, B., et al. (2012). Fiji: an open-source platform for biological-image analysis. Nat. Methods *9*, 676–682.

226. Scott-Hewitt, N., Perrucci, F., Morini, R., Erreni, M., Mahoney, M., Witkowska, A., Carey, A., Faggiani, E., Schuetz, L.T., Mason, S., et al. (2020). Local externalization of phosphatidylserine mediates developmental synaptic pruning by microglia. EMBO J. *39*, e105380.

227. Scott, A.L.M., and Ramer, M.S. (2010). Schwann cell p75NTR prevents spontaneous sensory reinnervation of the adult spinal cord. Brain *133*, 421–432.

228. Sebbagh, M., Renvoizé, C., Hamelin, J., Riché, N., Bertoglio, J., and Bréard, J. (2001). Caspase-3-mediated cleavage of ROCK I induces MLC phosphorylation and apoptotic membrane blebbing. Nat. Cell Biol. *3*, 346–352.

229. Segawa, K., Kurata, S., Yanagihashi, Y., Brummelkamp, T.R., Matsuda, F., and Nagata, S. (2014). Caspase-mediated cleavage of phospholipid flippase for apoptotic phosphatidylserine exposure. Science *344*, 1164–1168.

230. Shacham-Silverberg, V., Sar Shalom, H., Goldner, R., Golan-Vaishenker, Y., Gurwicz, N., Gokhman, I., and Yaron, A. (2018). Phosphatidylserine is a marker for axonal debris engulfment but its exposure can be decoupled from degeneration. Cell Death Dis. *9*, 1116.

231. Shao, X., Sørensen, M.H., Xia, X., Fang, C., Hui, T.H., Chang, R.C.C., Chu, Z., and Lin, Y. (2020). Beading of injured axons driven by tension- and adhesion-regulated membrane shape

instability. Journal of The Royal Society Interface *17*, 20200331.

232. Shen, L.-L., Li, W.-W., Xu, Y.-L., Gao, S.-H., Xu, M.-Y., Bu, X.-L., Liu, Y.-H., Wang, J., Zhu, J., Zeng, F., et al. (2019). Neurotrophin receptor p75 mediates amyloid β-induced tau pathology. Neurobiol. Dis. *132*, 104567.

233. Sherman, D.L., and Brophy, P.J. (2005). Mechanisms of axon ensheathment and myelin growth. Nat. Rev. Neurosci. *6*, 683–690.

234. Shinzawa, K., Sumi, H., Ikawa, M., Matsuoka, Y., Okabe, M., Sakoda, S., and Tsujimoto, Y. (2008). Neuroaxonal dystrophy caused by group VIA phospholipase A2 deficiency in mice: a model of human neurodegenerative disease. J. Neurosci. *28*, 2212–2220.

235. Shin, J.E., Miller, B.R., Babetto, E., Cho, Y., Sasaki, Y., Qayum, S., Russler, E.V., Cavalli, V., Milbrandt, J., and DiAntonio, A. (2012). SCG10 is a JNK target in the axonal degeneration pathway. Proc Natl Acad Sci USA *109*, E3696-705.

236. Shlomovitz, I., Speir, M., and Gerlic, M. (2019). Flipping the dogma - phosphatidylserine in non-apoptotic cell death. Cell Commun. Signal. *17*, 139.

237. Simmons, D.A., Knowles, J.K., Belichenko, N.P., Banerjee, G., Finkle, C., Massa, S.M., and Longo, F.M. (2014). A small molecule p75NTR ligand, LM11A-31, reverses cholinergic neurite dystrophy in Alzheimer's disease mouse models with mid- to late-stage disease progression. PLoS ONE *9*, e102136.

238. Simon, D.J., Weimer, R.M., McLaughlin, T., Kallop, D., Stanger, K., Yang, J., O'Leary, D.D.M., Hannoush, R.N., and Tessier-Lavigne, M. (2012). A caspase cascade regulating developmental axon degeneration. J. Neurosci. *32*, 17540–17553.

239. Simon, D.J., Pitts, J., Hertz, N.T., Yang, J., Yamagishi, Y., Olsen, O., Tešić Mark, M., Molina, H., and Tessier-Lavigne, M. (2016). Axon Degeneration Gated by Retrograde Activation of Somatic Pro-apoptotic Signaling. Cell *164*, 1031–1045.

240. Singh, K.K., and Miller, F.D. (2005). Activity regulates positive and negative neurotrophin-derived signals to determine axon competition. Neuron *45*, 837–845.

241. Singh, K.K., Park, K.J., Hong, E.J., Kramer, B.M., Greenberg, M.E., Kaplan, D.R., and Miller, F.D. (2008). Developmental axon pruning mediated by BDNF-p75NTR-dependent axon degeneration. Nat. Neurosci. *11*, 649–658.

242. Sleigh, J.N., Rossor, A.M., Fellows, A.D., Tosolini, A.P., and Schiavo, G. (2019). Axonal transport and neurological disease. Nat. Rev. Neurol. *15*, 691–703.

243. Soilu-Hänninen, M., Ekert, P., Bucci, T., Syroid, D., Bartlett, P.F., and Kilpatrick, T.J. (1999). Nerve growth factor signaling through p75 induces apoptosis in Schwann cells via a Bcl-2-independent pathway. J. Neurosci. *19*, 4828–4838.

244. Song, X.-Y., Zhou, F.H.-H., Zhong, J.-H., Wu, L.L.Y., and Zhou, X.-F. (2006). Knockout of p75(NTR) impairs re-myelination of injured sciatic nerve in mice. J. Neurochem. *96*, 833–842.

245. Staal, J.A., Dickson, T.C., Gasperini, R., Liu, Y., Foa, L., and Vickers, J.C. (2010). Initial calcium release from intracellular stores followed by calcium dysregulation is linked to secondary axotomy following transient axonal stretch injury. J. Neurochem. *112*, 1147–1155.

246. Stankiewicz, T.R., and Linseman, D.A. (2014). Rho family GTPases: key players in neuronal development, neuronal survival, and neurodegeneration. Front. Cell. Neurosci. *8*, 314.

247. Stirling, D.P., and Stys, P.K. (2010). Mechanisms of axonal injury: internodal nanocomplexes and calcium deregulation. Trends Mol. Med. *16*, 160–170.

248. Stokin, G.B., Lillo, C., Falzone, T.L., Brusch, R.G., Rockenstein, E., Mount, S.L., Raman, R., Davies, P., Masliah, E., Williams, D.S., et al. (2005). Axonopathy and transport deficits early in the pathogenesis of Alzheimer's disease. Science *307*, 1282–1288.

249. Summers, D.W., DiAntonio, A., and Milbrandt, J. (2014). Mitochondrial dysfunction induces Sarm1-dependent cell death in sensory neurons. J. Neurosci. *34*, 9338–9350.

250. Summers, D.W., Gibson, D.A., DiAntonio, A., and Milbrandt, J. (2016). SARM1-specific motifs in the TIR domain enable NAD+ loss and regulate injury-induced SARM1 activation. Proc Natl Acad Sci USA *113*, E6271–E6280.

251. Summers, D.W., Milbrandt, J., and DiAntonio, A. (2018). Palmitoylation enables MAPK-dependent proteostasis of axon survival factors. Proc Natl Acad Sci USA *115*, E8746–E8754.

252. Summers, D.W., Frey, E., Walker, L.J., Milbrandt, J., and DiAntonio, A. (2020). DLK Activation Synergizes with Mitochondrial Dysfunction to Downregulate Axon Survival Factors and Promote SARM1-Dependent Axon Degeneration. Mol. Neurobiol. *57*, 1146–1158.

253. Sun, S.-C., Ma, D., Li, M.-Y., Zhang, R.-X., Huang, C., Huang, H.-J., Xie, Y.-Z., Wang, Z.-J., Liu, J., Cai, D.-C., et al. (2019). Mutations in C1orf194, encoding a calcium regulator, cause dominant Charcot-Marie-Tooth disease. Brain *142*, 2215–2229.

254. Surmeier, D.J., Halliday, G.M., and Simuni, T. (2017). Calcium, mitochondrial dysfunction and slowing the progression of Parkinson's disease. Exp. Neurol. *298*, 202–209.

255. Suzuki, K., and Koike, T. (2007). Mammalian Sir2-related protein (SIRT) 2-mediated modulation of resistance to axonal degeneration in slow Wallerian degeneration mice: a crucial role of tubulin deacetylation. Neuroscience *147*, 599–612.

256. Syroid, D.E., Maycox, P.J., Soilu-Hänninen, M., Petratos, S., Bucci, T., Burrola, P., Murray, S., Cheema, S., Lee, K.F., Lemke, G., et al. (2000). Induction of postnatal schwann cell death by the low-affinity neurotrophin receptor in vitro and after axotomy. J. Neurosci. *20*, 5741–5747.

257. Tabata, Y., Imaizumi, Y., Sugawara, M., Andoh-Noda, T., Banno, S., Chai, M., Sone, T., Yamazaki, K., Ito, M., Tsukahara, K., et al. (2018). T-type Calcium Channels Determine the Vulnerability of Dopaminergic Neurons to Mitochondrial Stress in Familial Parkinson Disease. Stem Cell Reports *11*, 1171–1184.

258. Takahashi, T., Yagishita, S., Amano, N., Yamaoka, K., and Kamei, T. (1997). Amyotrophic

lateral sclerosis with numerous axonal spheroids in the corticospinal tract and massive degeneration of the cortex. Acta Neuropathol. *94*, 294–299.

259. Tanaka, K., Kelly, C.E., Goh, K.Y., Lim, K.B., and Ibáñez, C.F. (2016). Death Domain Signaling by Disulfide-Linked Dimers of the p75 Neurotrophin Receptor Mediates Neuronal Death in the CNS. J. Neurosci. *36*, 5587–5595.

260. Tang-Schomer, M.D., Johnson, V.E., Baas, P.W., Stewart, W., and Smith, D.H. (2012). Partial interruption of axonal transport due to microtubule breakage accounts for the formation of periodic varicosities after traumatic axonal injury. Exp. Neurol. *233*, 364–372.

261. Tedeschi, A., Dupraz, S., Laskowski, C.J., Xue, J., Ulas, T., Beyer, M., Schultze, J.L., and Bradke, F. (2016). The calcium channel subunit alpha2delta2 suppresses axon regeneration in the adult CNS. Neuron *92*, 419–434.

262. Teng, K.K., Felice, S., Kim, T., and Hempstead, B.L. (2010). Understanding proneurotrophin actions: Recent advances and challenges. Dev. Neurobiol. *70*, 350–359.

263. Tian, N., Hanson, K.A., Canty, A.J., Vickers, J.C., and King, A.E. (2020a). Microtubule-dependent processes precede pathological calcium influx in excitotoxin-induced axon degeneration. J. Neurochem. *152*, 542–555.

264. Tian, W., Czopka, T., and López-Schier, H. (2020b). Systemic loss of Sarm1 protects Schwann cells from chemotoxicity by delaying axon degeneration. Commun. Biol. *3*, 49.

265. Tomita, K., Kubo, T., Matsuda, K., Fujiwara, T., Yano, K., Winograd, J.M., Tohyama, M., and Hosokawa, K. (2007). The neurotrophin receptor p75NTR in Schwann cells is implicated in remyelination and motor recovery after peripheral nerve injury. Glia *55*, 1199–1208.

266. Toyoshima, I., Yamamoto, A., Masamune, O., and Satake, M. (1989). Phosphorylation of neurofilament proteins and localization of axonal swellings in motor neuron disease. J. Neurol. Sci. *89*, 269–277.

267. Toyoshima, I., Sugawara, M., Kato, K., Wada, C., Hirota, K., Hasegawa, K., Kowa, H., Sheetz, M.P., and Masamune, O. (1998). Kinesin and cytoplasmic dynein in spinal spheroids with motor neuron disease. J. Neurol. Sci. *159*, 38–44.

268. Troy, C.M., Friedman, J.E., and Friedman, W.J. (2002). Mechanisms of p75-mediated death of hippocampal neurons. Role of caspases. J. Biol. Chem. *277*, 34295–34302.

269. Tsuchiya, K., Nakajima, S., Hosojima, S., Thi Nguyen, D., Hattori, T., Manh Le, T., Hori, O., Mahib, M.R., Yamaguchi, Y., Miura, M., et al. (2019). Caspase-1 initiates apoptosis in the absence of gasdermin D. Nat. Commun. *10*, 2091.

270. Twohig, J.P., Cuff, S.M., Yong, A.A., and Wang, E.C.Y. (2011). The role of tumor necrosis factor receptor superfamily members in mammalian brain development, function and homeostasis. Rev. Neurosci. *22*, 509–533.

271. Unsain, N., and Barker, P.A. (2015). New Views on the Misconstrued: Executioner Caspases and Their Diverse Non-apoptotic Roles. Neuron *88*, 461–474.

272. Unsain, N., Bordenave, M.D., Martinez, G.F., Jalil, S., von Bilderling, C., Barabas, F.M., Masullo, L.A., Johnstone, A.D., Barker, P.A., Bisbal, M., et al. (2018). Remodeling of the Actin/Spectrin Membrane-associated Periodic Skeleton, Growth Cone Collapse and F-Actin Decrease during Axonal Degeneration. Sci. Rep. *8*, 3007.

273. Vargas, M.E., and Barres, B.A. (2007). Why is Wallerian degeneration in the CNS so slow? Annu. Rev. Neurosci. *30*, 153–179.

274. Vargas, M.E., Yamagishi, Y., Tessier-Lavigne, M., and Sagasti, A. (2015). Live Imaging of Calcium Dynamics during Axon Degeneration Reveals Two Functionally Distinct Phases of Calcium Influx. J. Neurosci. *35*, 15026–15038.

275. Vial, J.D. (1958). The Early Changes in the Axoplasm during Wallerian Degeneration. J. Cell Biol. *4*, 551–556.

276. Vilar, M., Charalampopoulos, I., Kenchappa, R.S., Simi, A., Karaca, E., Reversi, A., Choi, S., Bothwell, M., Mingarro, I., Friedman, W.J., et al. (2009). Activation of the p75 neurotrophin receptor through conformational rearrangement of disulphide-linked receptor dimers. Neuron *62*, 72–83.

277. Villegas, R., Martinez, N.W., Lillo, J., Pihan, P., Hernandez, D., Twiss, J.L., and Court, F.A. (2014). Calcium release from intra-axonal endoplasmic reticulum leads to axon degeneration through mitochondrial dysfunction. J. Neurosci. *34*, 7179–7189.

278. Vohra, B.P.S., Sasaki, Y., Miller, B.R., Chang, J., DiAntonio, A., and Milbrandt, J. (2010). Amyloid precursor protein cleavage-dependent and -independent axonal degeneration programs share a common nicotinamide mononucleotide adenylyltransferase 1-sensitive pathway. J. Neurosci. *30*, 13729–13738.

279. Wakatsuki, S., and Araki, T. (2017). Specific phospholipid scramblases are involved in exposure of phosphatidylserine, an “eat-me” signal for phagocytes, on degenerating axons. Commun. Integr. Biol. *10*, e1296615.

280. Wakatsuki, S., Saitoh, F., and Araki, T. (2011). ZNRF1 promotes Wallerian degeneration by degrading AKT to induce GSK3B-dependent CRMP2 phosphorylation. Nat. Cell Biol. *13*, 1415–1423.

281. Walczak, H. (2013). Death receptor-ligand systems in cancer, cell death, and inflammation. Cold Spring Harb. Perspect. Biol. *5*, a008698.

282. Walker, L.J., Summers, D.W., Sasaki, Y., Brace, E.J., Milbrandt, J., and DiAntonio, A. (2017). MAPK signaling promotes axonal degeneration by speeding the turnover of the axonal maintenance factor NMNAT2. Elife *6*.

283. Waller, A. (1851). Experiments on the Section of the Glosso-Pharyngeal and Hypoglossal Nerves of the Frog, and Observations of the Alterations Produced Thereby in the Structure of

Their Primitive Fibres. Edinb. Med. Surg. J. *76*, 369–376.

284. Wang, G., Simon, D.J., Wu, Z., Belsky, D.M., Heller, E., O'Rourke, M.K., Hertz, N.T., Molina, H., Zhong, G., Tessier-Lavigne, M., et al. (2019a). Structural plasticity of actin-spectrin membrane skeleton and functional role of actin and spectrin in axon degeneration. Elife *8*.

285. Wang, H., Wang, X., Zhang, K., Wang, Q., Cao, X., Wang, Z., Zhang, S., Li, A., Liu, K., and Fang, Y. (2019b). Rapid depletion of ESCRT protein Vps4 underlies injury-induced autophagic impediment and Wallerian degeneration. Sci. Adv. *5*, eaav4971.

286. Wang, J.T., Medress, Z.A., and Barres, B.A. (2012). Axon degeneration: molecular mechanisms of a self-destruction pathway. J. Cell Biol. *196*, 7–18.

287. Wang, J., Zhai, Q., Chen, Y., Lin, E., Gu, W., McBurney, M.W., and He, Z. (2005). A local mechanism mediates NAD-dependent protection of axon degeneration. J. Cell Biol. *170*, 349–355.

288. Wang, Q., Zhang, S., Liu, T., Wang, H., Liu, K., Wang, Q., and Zeng, W. (2018). Sarm1/Myd88-5 Regulates Neuronal Intrinsic Immune Response to Traumatic Axonal Injuries. Cell Rep. *23*, 716–724.

289. Wang, T., Perera, N.D., Chiam, M.D.F., Cuic, B., Wanniarachchillage, N., Tomas, D., Samson, A.L., Cawthorne, W., Valor, E.N., Murphy, J.M., et al. (2020). Necroptosis is dispensable for motor neuron degeneration in a mouse model of ALS. Cell Death Differ. *27*, 1728–1739.

290. Wang, Y., Zhao, D., Pan, B., Song, Z., Shah, S.Z.A., Yin, X., Zhou, X., and Yang, L. (2015). Death Receptor 6 and Caspase-6 Regulate Prion Peptide-Induced Axonal Degeneration in Rat Spinal Neurons. J. Mol. Neurosci. *56*, 966–976.

291. deF. Webster, H. (1962). Transient, focal accumulation of axonal mitochondria during the early stages of wallerian degeneration. J. Cell Biol. *12*, 361–383.

292. Wheeler, M.A., Heffner, D.L., Kim, S., Espy, S.M., Spano, A.J., Cleland, C.L., and

Deppmann, C.D. (2014). TNF-α/TNFR1 signaling is required for the development and function of primary nociceptors. Neuron *82*, 587–602.

293. Whitmore, A.V., Lindsten, T., Raff, M.C., and Thompson, C.B. (2003). The proapoptotic proteins Bax and Bak are not involved in Wallerian degeneration. Cell Death Differ. *10*, 260–261.

294. Wirths, O., Weis, J., Szczygielski, J., Multhaup, G., and Bayer, T.A. (2006). Axonopathy in an APP/PS1 transgenic mouse model of Alzheimer's disease. Acta Neuropathol. *111*, 312–319.

295. Witte, M.E., Schumacher, A.-M., Mahler, C.F., Bewersdorf, J.P., Lehmitz, J., Scheiter, A., Sánchez, P., Williams, P.R., Griesbeck, O., Naumann, R., et al. (2019). Calcium Influx through Plasma-Membrane Nanoruptures Drives Axon Degeneration in a Model of Multiple Sclerosis. Neuron *101*, 615-624.e5.

296. Wong, K.M., Babetto, E., and Beirowski, B. (2017). Axon degeneration: make the Schwann cell great again. Neural Regen. Res. *12*, 518–524.

297. Wu, Y., Whiteus, C., Xu, C.S., Hayworth, K.J., Weinberg, R.J., Hess, H.F., and De Camilli, P. (2017). Contacts between the endoplasmic reticulum and other membranes in neurons. Proc Natl Acad Sci USA *114*, E4859–E4867.

298. Xie, Y., Meeker, R.B., Massa, S.M., and Longo, F.M. (2019). Modulation of the p75 neurotrophin receptor suppresses age-related basal forebrain cholinergic neuron degeneration. Sci. Rep. *9*, 5273.

299. Xiong, X., Hao, Y., Sun, K., Li, J., Li, X., Mishra, B., Soppina, P., Wu, C., Hume, R.I., and Collins, C.A. (2012). The Highwire ubiquitin ligase promotes axonal degeneration by tuning levels of Nmnat protein. PLoS Biol. *10*, e1001440.

300. Xu, K., Olsen, O., Tzvetkova-Robev, D., Tessier-Lavigne, M., and Nikolov, D.B. (2015). The crystal structure of DR6 in complex with the amyloid precursor protein provides insight into death receptor activation. Genes Dev. *29*, 785–790.

301. Yahata, N., Yuasa, S., and Araki, T. (2009). Nicotinamide mononucleotide adenylyltransferase expression in mitochondrial matrix delays Wallerian degeneration. J. Neurosci. *29*, 6276–6284.

302. Yamagishi, S., Fujitani, M., Hata, K., Kitajo, K., Mimura, F., Abe, H., and Yamashita, T. (2005). Wallerian degeneration involves Rho/Rho-kinase signaling. J. Biol. Chem. *280*, 20384–20388.

303. Yamashita, T., and Tohyama, M. (2003). The p75 receptor acts as a displacement factor that releases Rho from Rho-GDI. Nat. Neurosci. *6*, 461–467.

304. Yamashita, T., Tucker, K.L., and Barde, Y.A. (1999). Neurotrophin binding to the p75 receptor modulates Rho activity and axonal outgrowth. Neuron *24*, 585–593.

305. Yamashita, T., Higuchi, H., and Tohyama, M. (2002). The p75 receptor transduces the signal from myelin-associated glycoprotein to Rho. J. Cell Biol. *157*, 565–570.

306. Yamashita, T., Fujitani, M., Hata, K., Mimura, F., and Yamagishi, S. (2005). Diverse functions of the p75 neurotrophin receptor. Anat. Sci. Int. *80*, 37–41.

307. Yamauchi, J., Chan, J.R., and Shooter, E.M. (2004). Neurotrophins regulate Schwann cell migration by activating divergent signaling pathways dependent on Rho GTPases. Proc Natl Acad Sci USA *101*, 8774–8779.

308. Yang, J., Weimer, R.M., Kallop, D., Olsen, O., Wu, Z., Renier, N., Uryu, K., and Tessier-Lavigne, M. (2013). Regulation of axon degeneration after injury and in development by the endogenous calpain inhibitor calpastatin. Neuron *80*, 1175–1189.

309. Yang, J., Wu, Z., Renier, N., Simon, D.J., Uryu, K., Park, D.S., Greer, P.A., Tournier, C., Davis, R.J., and Tessier-Lavigne, M. (2015). Pathological axonal death through a MAPK cascade that triggers a local energy deficit. Cell *160*, 161–176.

310. Yang, T., Knowles, J.K., Lu, Q., Zhang, H., Arancio, O., Moore, L.A., Chang, T., Wang, Q.,

Andreasson, K., Rajadas, J., et al. (2008). Small molecule, non-peptide p75 ligands inhibit Abeta-induced neurodegeneration and synaptic impairment. PLoS ONE *3*, e3604.

311. Yan, D., and Jin, Y. (2012). Regulation of DLK-1 kinase activity by calcium-mediated dissociation from an inhibitory isoform. Neuron *76*, 534–548.

312. Yan, T., Feng, Y., Zheng, J., Ge, X., Zhang, Y., Wu, D., Zhao, J., and Zhai, Q. (2010). Nmnat2 delays axon degeneration in superior cervical ganglia dependent on its NAD synthesis activity. Neurochem. Int. *56*, 101–106.

313. Yong, Y., Gamage, K., Cheng, I., Barford, K., Spano, A., Winckler, B., and Deppmann, C. (2019). p75NTR and DR6 Regulate Distinct Phases of Axon Degeneration Demarcated by Spheroid Rupture. J. Neurosci. *39*, 9503–9520.

314. Yong, Y., Gamage, K., Cushman, C., Spano, A., and Deppmann, C.D. (2020). Regulation of degenerative spheroids after injury.

315. Zeng, F., Lu, J.-J., Zhou, X.-F., and Wang, Y.-J. (2011). Roles of p75NTR in the pathogenesis of Alzheimer's disease: a novel therapeutic target. Biochem. Pharmacol. *82*, 1500–1509.

316. Zeng, L., Li, T., Xu, D.C., Liu, J., Mao, G., Cui, M.-Z., Fu, X., and Xu, X. (2012). Death receptor 6 induces apoptosis not through type I or type II pathways, but via a unique mitochondria-dependent pathway by interacting with Bax protein. J. Biol. Chem. *287*, 29125–29133.

317. Zhai, Q., Wang, J., Kim, A., Liu, Q., Watts, R., Hoopfer, E., Mitchison, T., Luo, L., and He, Z. (2003). Involvement of the ubiquitin-proteasome system in the early stages of wallerian degeneration. Neuron *39*, 217–225.

318. Zhang, Y., Chen, X., Gueydan, C., and Han, J. (2018). Plasma membrane changes during programmed cell deaths. Cell Res. *28*, 9–21.

319. Zhao, Z.Y., Xie, X.J., Li, W.H., Liu, J., Chen, Z., Zhang, B., Li, T., Li, S.L., Lu, J.G., Zhang,

L., et al. (2019). A Cell-Permeant Mimetic of NMN Activates SARM1 to Produce Cyclic ADP-Ribose and Induce Non-apoptotic Cell Death. IScience *15*, 452–466.

320. Zhong, G., He, J., Zhou, R., Lorenzo, D., Babcock, H.P., Bennett, V., and Zhuang, X. (2014). Developmental mechanism of the periodic membrane skeleton in axons. Elife *3*.

321. Zhou, R., Han, B., Xia, C., and Zhuang, X. (2019). Membrane-associated periodic skeleton is a signaling platform for RTK transactivation in neurons. Science *365*, 929–934.

322. Ziv, N.E., and Spira, M.E. (1995). Axotomy induces a transient and localized elevation of the free intracellular calcium concentration to the millimolar range. J. Neurophysiol. *74*, 2625–2637.